PB81-157935

Ultrastructured and X-ray Microanaylsis of Macrophages Exposed to Non-Criteria Pollutants, with Emphasis on Certain Metals

Duke Univ. Medical Center
Durham, NC

Prepared for

Health Effects Research Lab.
Research Triangle Park, NC

Feb 81

U.S. Department of Commerce
National Technical Information Service
NTIS

TECHNICAL REPORT DATA
(Please read Instructions on the reverse before completing)

1. REPORT NO. EPA-600/1-81-018	2.	3. RECIPIENT'S ACCESSION NO. PB81 157935
4. TITLE AND SUBTITLE Ultrastructure and X-ray Microanalysis of Macrophages Exposed to Non-criteria Pollutants with Emphasis on Certain Metals		5. REPORT DATE February 1981 Issuing Date. 6. PERFORMING ORGANIZATION CODE
7. AUTHOR(S) John D. Shelburne, Peter Ingram, Susan R. Walker, and Catherine R. de Vries		8. PERFORMING ORGANIZATION REPORT NO.
9. PERFORMING ORGANIZATION NAME AND ADDRESS Dept. of Path., Duke Univ., Durham, NC 27710 and Chem. and Life Sci. Div., Research Triangle Insti. Research Triangle Park, NC 27709		10. PROGRAM ELEMENT NO. 1AA817 11. CONTRACT/GRANT NO. R 805460
12. SPONSORING AGENCY NAME AND ADDRESS Health Effects Research Laboratory RTP, NC Office of Research and Development U.S. Environmental Protection Agency Research Triangle Park, NC 27711		13. TYPE OF REPORT AND PERIOD COVERED Final 14. SPONSORING AGENCY CODE EPA 600/11

15. SUPPLEMENTARY NOTES

Project Officer: Michael D. Waters

16. ABSTRACT

Rabbit alveolar macrophages (RAMs) and cultured Chinese hamster ovary cells (CHOs) were exposed in vitro to the noncriteria pollutants manganese, cadmium, vanadium, nickel, lead, copper and cobalt, in either soluble or particulate form. To prevent the redistribution of soluble ions which occurs during conventional chemical fixation, methods of fixation by ultra-rapid freezing were developed which were applicable both to cells in suspension and to cell monolayers. Using chemical and freeze fixation, cellular and subcellular reactions to toxic elements were defined by both scanning and transmission electron microscopy. By exposing RAMs to red lead (Pb_3O_4), which is insoluble at pH 7 in tissue culture medium, it was shown that lead enters the cells through thephagosomal system and from that acid micro-environment is redistributed throughout the cytoplasm and nucleus. This system can be used as a model to study the movement of a toxic material on the surface of a particle within a lysosome into the interior of the cell.

17. KEY WORDS AND DOCUMENT ANALYSIS

a. DESCRIPTORS	b. IDENTIFIERS/OPEN ENDED TERMS	c. COSATI Field/Group
Rabbit alveolar macrophages Chinese hamster ovary cells Lead		

18. DISTRIBUTION STATEMENT RELEASE TO PUBLIC	19. SECURITY CLASS *(This Report)* UNCLASSIFIED	21. NO. OF PAGES 162
	20. SECURITY CLASS *(This page)* UNCLASSIFIED	22. PRICE

EPA Form 2220-1 (9-73)

PB81-157935

EPA 600/1-81-018
February 1981

ULTRASTRUCTURED AND X-RAY MICROANALYSIS OF MACROPHAGES EXPOSED TO NON-CRITERIA POLLUTANTS, WITH EMPHASIS ON CERTAIN METALS

by

John D. Shelburne, M.D., Ph.D.
Department of Pathology
Duke University Medical Center
Durham, NC 27710 U.S.A.

R-805460

Project Officer

Michael D. Waters
Genetic Toxicology Division
Health Effects Research Laboratory
Research Triangle Park, NC 27711

HEALTH EFFECTS RESEARCH LABORATORY
OFFICE OF RESEARCH AND DEVELOPMENT
U.S. ENVIRONMENTAL PROTECTION AGENCY
RESEARCH TRIANGLE PARK, NORTH CAROLINA 27711

REPRODUCED BY
NATIONAL TECHNICAL
INFORMATION SERVICE
U.S. DEPARTMENT OF COMMERCE
SPRINGFIELD, VA 22161

BEGIN FIRST LINE OF TEXT HERE
TYPING GUIDE SHEET
CENTER OF PAGE
TOP OF IMAGE AREA
DROPPED HEAD BEGIN SECTIONS HERE

DISCLAIMER

This report has been reviewed by the Health Effects Research Laboratory, U.S. Environmental Protection Agency, and approved for publication. Approval does not signify that the contents necessarily reflect the views and policies of the U.S. Environmental Protection Agency, nor does mention of trade names or commercial products constitute endorsement or recommendation for use.

BEGIN LAST LINE OF TEXT
BOTTOM OF IMAGE AREA OUTSIDE DIMENSION FOR TABLES AND ILLUSTRATIONS
PAGE NUMBER

FOREWORD

The many benefits of our modern, developing, industrial society are accompanied by certain hazards. Careful assessment of the relative risk of existing and new man-made environmental hazards is necessary for the establishment of sound regulatory policy. These regulations serve to enhance the quality of our environment in order to promote the public health and welfare and the productive capacity of our nation's population.

The Health Effects Research Laboratory, Research Triangle Park, conducts a coordinated environmental health research program in toxicology, epidemiology, and clinical studies using human volunteer subjects. These studies address problems in air pollution, non-ionizing radiation, environmental carcinogenesis and the toxicology of pesticides as well as other chemical pollutants. The Laboratory participates in the development and revision of air quality criteria documents on pollutants for which national ambient air quality standards exist or are proposed, provides the data for registration of new pesticides or proposed suspension of those already in use, conducts research on hazardous and toxic materials, and is primarily responsible for providing the health basis for non-ionizing radiation standards. Direct support to the regulatory function of the Agency is provided in the form of expert testimony and preparation of affidavits as well as expert advice to the Administrator to assure the adequacy of health care and surveillance of persons having suffered imminent and substantial endangerment of their health.

This study presents a new model for the study of the movement of toxic material on the surface of a particle within a lysosome into the interior of the cells. The model should increase our understanding of the alveolar macrophage, one of the first lines of defense against inhaled environmental pollutants.

F. Gordon Hueter, Ph.D.
Director
Health Effects Research Laboratory

ABSTRACT

Rabbit alveolar macrophages (RAMs) and cultured Chinese hamster ovary cells (CHOs) were exposed *in vitro* to the noncriteria pollutants manganese, cadmiun, vanadium, nickel, lead, copper and cobalt, in either soluble or particulate form. To prevent the redistribution of soluble ions which occurs during conventional chemical fixation, methods of fixation by ultra-rapid freezing were developed which were applicable both to cells in suspension and to cell monolayers. Using chemical and freeze fixation, cellular and subcellular reactions to toxic elements were defined by both scanning and transmission electron microscopy. The intracellular distribution of the toxic elements was determined by energy dispersive X-ray microanalysis (EDX) and secondary ion mass spectroscopy (SIMS). Soluble cadmium, nickel and copper salts, nickel oxide particles, and nickel oxide coated fly ash induced distinctive lamellar nuclear inclusions in RAMs but not CHOs. Cadmium also induced mitochondrial inclusions in both RAMs and CHO cells. Membrane-bound crystalline lead inclusions were seen in RAMs exposed to lead oxide coated fly ash or lead oxide (PbO). Free crystalline inclusions were seen in RAMs that had phagocytosed lead oxide coated fly ash and in cells exposed to soluble lead ($PbNO_2$). By exposing RAMs to red lead (Pb_3O_4), which is insoluble at pH 7 in tissue culture medium, it was shown that lead enters the cells through the phagosomal system and from that acid micro-environment is redistributed throughout the cytoplasm and nucleus. This system can be used as a model to study the movement of a toxic material on the surface of a particle within a lysosome into the interior of the cell.

TYPING GUIDE SHEET
BEGIN FIRST LINE OF TEXT HERE
CENTER OF PAGE
TOP OF IMAGE AREA
DROPPED HEAD. BEGIN SECTIONS HERE

CONTENTS

Foreword iii
Abstract iv

1. Introduction 1

2. Conclusions and Recommendations 3

3. Experiments with Cadmium 4
   CHO cells 4
   RAMs 4
   Mutant cells 5

4. Cell Particle Interactions 6
   Introduction 6
   Experiments on PbO 9
   Studies on Pb_3O_4 particles and RAMs 40
   Studies on NiO toxicity 75
   Summaries 136

5. Experiments With Other Metals and Solutions 138

6. Experiments on Instrumentation 141
   Sensitivity 141
   Discovery of a new imaging technique 142
   Discovery of a new drying technique 142

Publications Supported in Part by This Grant 143

General References 145

BEGIN LAST LINE OF TEXT
BOTTOM OF IMAGE AREA, OUTSIDE DIMENSION FOR TABLES AND ILLUSTRATIONS
3/8"

PAGE NUMBER
EPA-287 (Cin.)
(4-76)

SECTION 1

INTRODUCTION

It is well known that the alveolar macrophage represents one of the most important first lines of defense of man and other species against inhaled environmental pollutants. Consequently, we elected to study the effects of a wide variety of environmental pollutants on alveolar macrophages in order to better understand the crucial interactions. Our original purposes were as follows:

1. To investigate the ultrastructural effects of certain soluble metals on alveolar macrophages.

2. To investigate the ultrastructural effects of realistic and quasirealistic airborne respirable particles on alveolar macrophages.

3. To develop new techniques not currently available in the literature that would permit us and other individuals to study the subcellular movement (metabolism) of ions which either enter cells from solution or which enter cells from particles surfaces be they outside cells or within phagolysosomes.

4. To use these new techniques to study as many soluble ions and respirable particles as possible.

As is detailed in the report which follows, we have achieved all of the goals. In brief, we have developed a variety of new techniques which permit investigators to freeze-fix alveolar macrophages and thus to trap normal ions and xenobiotics in their *in vivo* location. Using these techniques we have studied the subcellular metabolism of numerous soluble ons such as cadmium, nickel, vanadium, copper, cobalt, and maganese and have studied a number of particles including 2-5 micron coal fly ash particles with or without coatings of PbO or NiO, and particles of PbO, Pb_3O_4, and NiO. These studies have shown that this work is possible and have pointed clearly to future studies involving new, more sensitive imaging techniques such as secondary ion microscopy. We will explore these new techniques in the future.

The following review of our work is supplemented by reprints of the many articles we have written during this grant which go into all of these topics in great detail. This review will not repeat all of that information but instead is designed as a summary of this work and as a guide to those papers. In addition, this report will discuss in detail those studies which we have not yet published since we do not have reprints to attach. Needless to say, all of the work which we have done on this grant will be published. The following survey of this work is roughly arranged in chronological order beginning with the earliest work and ending with the latest studies.

Our interest in this area began with a series of experiments using NiO and MnO_2 particles. We allowed RAMs to phagocytize these particles and then fixed them with conventional techniques. These cells were then embedded in Epon and studied by SEM/EDX. In doing this work we developed several new mapping techniques which worked quite well in the STEM mode and which have permitted us to clearly illustrate the location of these particles within cells (this work was published in our first manuscript (1). After we had completed that work, we asked ourselves the question -can we demonstrate the location of a soluble metal within the cytoplasm of the cell that had been exposed in vitro, not to particles, but to a metal in solution. Consequently, we chose for the initial experiments manganese since there was absolutely no manganese in the background of our instrument and since Dr. Water's group had extensive experience with the cytotoxicity of manganese. We published the findings of these experiments in 1977 (2) and concluded that we could demonstrate manganese within the cytoplasm of cells but that it was only demonstrable in electron dense cytoplasmic precipitates. In addition, we described a wide variety of ultrastructural effects of manganese. During these studies, we noted that we could not detect manganese elsewhere in the cytoplasm of these cells even though they had been incubated with rather high levels. In addition, at this time we began preliminary experiments with soluble cadmium in vitro. Again, we described and published a large number of ultrastructural effects of cadmium using conventional chemical fixation with glutaraldehyde and conventional embedding in Epon. However, we found that even though a galaxy of ultrastructural changes were present, including fascinating nuclear inclusions not previously described in the literature, using this conventionally prepared material we were not able to detect the location of cadmiun even though we were convinced that it was present (since we had used high levels for the exposure and since the subcellular changes were so pronounced).

As a result of these and many other observations, we became convinced that the only way to study the subcellular metabolism of trace metals was to avoid the use (whenever possible) of conventional techniques and to develop freezing techniques. Physiologists have shown that physiologic ions such as sodium and potassium are redistributed tremendously during chemical fixation and that the only way to preserve their true in vivo location is to use freezing techniques. Our experiments with manganese and cadmium seem to support that observation for physiologic ions as well as xenobiotics. However, when we looked into the literature, we found no published papers describing how to snap-freeze mammalian cells in suspension so that they could be serially sectioned using cryoultramicrotomy. We felt that it was important to cut sections of these cells since this is the only way to get inside of them to map their ultrastructure.

Consequently, we spent approximately the first year of this grant working very hard to develop these new techniques and were successful as witnessed by our publication in 1979 (5) of techniques for the freezing of macrophages either in suspension or as monolayers. We have continued to use those techniques for as many of the studies which are listed below as possible.

SECTION 2

CONCLUSIONS AND RECOMMENDATIONS

The use of freezing techniques for the evaluation of the metabolism of xenobiotics by morphologic means is absolutely essential. It is only in this manner that one can be certain that movement of the xenobiotic in question has not occurred. We have also concluded that energy dispersive X-ray microanalysis is an extremely sensitive and powerful tool for the location of xenobiotic elements within cells. This technique does suffer form some limitations, however, most importantly one of sensitivity. We have found that the sensitivity of X-ray microanalysis is in the hundreds of parts per million range, whereas the sensitivity of SIMS microanalysis is in the parts per million to parts per billion range. Consequently, we intend to pursue future studies on cell-xenobiotic interactions using a combination of energy dispersive x-ray microanalysis with its advantages of resolution combined with SIMS microanalysis with its advantages of sensitivity. In this manner the advantages of the two techniques will be additive if not potentiating. We have already begun SIMS experiments and have published our results (17-19). We propose to use these techniques for studies on model particles such as Pb_3O_4, PbO, NiO, MnO, and PBBP coated particles, quasirealistic particles such as PbO and NiO coated fly ash particles, tritiated benzo(a)pyrene coated iron oxide particles, and certain realistic particles, most importantly true coal fly ash particles obtained from ambient sources. We feel that in this manner the movement of xenobiotics from particle surfaces to other sites within macrophages and eventually to other sites within whole animals can be directly assessed.

SECTION 3

EXPERIMENTS WITH CADMIUM

As described in the attached reprint of the paper by Bell, et. al. (6), we have shown that cadmium produces a lamellar nuclear inclusion which we have proven to contain cadmium by microprobe analysis. Interestingly, we have seen similar lamellar nuclear inclusions in RAMs exposed to nickel, either in soluble or particulate form, as discussed below and in RAMs exposed in vitro to soluble copper. We have not seen these inclusions in RAMs exposed to manganese, lead, cobalt, or iron. In addition to the experiments noted in this manuscript, we have also done a number of new experiments with cadmium which are as follows:

EFFECT OF CADIUM ON CHO CELLS

Since CHO cells possess fewer lysosomes and more mitochondria than do RAMs, these cells were exposed to soluble cadmium as had been done previously for RAMs. The results to date of this work are that cytoplasmic densities similar to those noted in RAMs are still present and these are positive by microprobe analysis for calcium, magnesium and cadmium. The presence of magnesium is strong evidence that these inclusions are in mitochondria. Freeze substituted images are consistent with but do not absolutely unambiguously prove that hypothesis since the mitochondria appeared damaged by the cadmium and thus are difficult to recognize as mitochondria. The striking finding was that cadmium did not produce nuclear inclusions in CHO cells even though it did at the same doses and times produce nuclear inclusions in RAMs. Thus CHO cells are not a suitable model for studying the pathophysiology of cadmium with respect to its effects on nuclei. Cadmium did produce clumping of heterochromatin in treated cells but this did not appear to be a specific finding in the same sense that cadmium nuclear inclusions are.

RAMS EXPOSED TO CADMIUM CHLORIDE IN MEDIUM DEVOID OF PHOSPHATE AND SULFATE

Since the cytoplasmic densities observed in previous experiments with RAMs exposed to cadmium also gave peaks for phosphorus when studied by EDX, and because of the presence of extracellular cadmium phosphate precipitates, these experiments were repeated using special phosphate and sulfate free medium. When compared to cells exposed to regular media, control cells exposed to this special media without cadmium exhibited more numerous homogeneous nuclear bodies at 4 hours, swelling of ER cisternae, and peculiar flocculant mitochondrial matrix densities. Cells in this special media treated with cadmium did exhibit characteristic lamellar nuclear inclusions but fewer than observed in previous experiments with regular medium. No cytoplasmic densities at all were observed. Homogeneous nuclear bodies were extremely common. No extracellular precipitation of any sort was seen in frozen sections. Thus this special media did prevent the problem of extracellular precipitation noted previously but the lack of phosphate (probably) seems to have blocked the formation of mitochondrial densities containing cadmium and blocked partially the formation of cadmium specific nuclear bodies.

Microprobe analysis of frozen sections revealed - in marked contrast to previous experiments with regular media - a surprising lack of detectable cadmium. Nuclear inclusions were magnesium, calcium and phosphorus positive, but only occasionally exhibited a trace of cadmium. No other cadmium localization was detected. Perhaps the absence of phosphate prevented cadmium transport into cells (phosphate is, in some instances, necessary for calcium transport). Or, perhaps the phagocytosis of cadmium phosphate precipitates is necessary to get large amounts of cadmium into cells in a hurry (4 hours), bypassing normal membrane barriers. Experiments to test these hypotheses are underway.

EFFECT OF CADMIUM ON MUTANT CELLS

We have done a series of experiments on a mutant strain of CHO cells developed by Dr. Ken McCarty, Sr., Department of Biochemistry, Duke University. These CHO cells are resistant to cadmium and can successfully bind large amounts of cadmium intracellularly without visible toxic effects. An induced matallothionein is responsible for the remarkable behavior of these cells. Four different variables were studied. "Wild" CHO cells with and without cadmium and mutant CHO cells with an without cadmium were incubated on glass and Thermonox coverslips for 4 hours (wild) and 48 hours (mutant) in 0.1 mM cadmium chloride. At the end of the incubation, these coverslips were snap frozen in liquid nitrogen and freeze-dried on an Edwards freeze-drying apparatus or in a rotary vacuum pump chamber. After a light carbon coating, these cells were studied by SEM-EDX. Some coverslips were rinsed in medium without cadmium before snap freezing. The principal findings to date are: 1) the glass coverslip is a poor substrate because it contributes to high background radiation and to numerous spurious peaks including silicon, zinc, titanium, chromium. On the other hand, Thermonox coverslips are an excellent substrate as there is no increased background radiation. 2) the mutant cells exposed to cadmium do exhibit cadmium peaks and there are differences between cells. No cadmium peaks were seen in "wild" cells with or without cadmium exposure. These studies were done using the spot probe mode since cell size varies significantly. 3) "Wild" cells teated with cadmium were rounded. "Wild" cells not treated with cadmium and most mutant cells with or without cadmium were relatively flat. 4) sulfur peaks were consistently higher in treated mutant cells than in any of these other groups, possibly due to the presence of the induced metallothionein. 5) the results with rinsed vs. unrinsed cells were the same.

In addition, perhaps the most interesting results of this work with CHO cells concerned viral particles. Our experiments with CHO cells in two different laboratories have shown that treatment with cadmium causes the production of a type RNA virus, probably a tumor virus. In view of the fact that cadmium is a carcinogen, we feel this hitherto unreported finding is a significant discovery.

SECTION 4

CELL PARTICLE INTERACTIONS

INTRODUCTION

The process of phagocytosis serves many purposes to many organisms. In protozoans, it makes potential food available to the cell. In metazooans, it serves both in ingestion of food and in sequestration of foreign noxious substances from the rest of the organism. Each of these processes requires that the phagocyte recognize, internalize, and digest or regurgitate the exogenous material.

Recognition of foreign substances relies on the presence of surface receptors on the plasmalemma which transmit the message to phagocytose to the contractile components of the cytosol. Ingestion also involves adherence of the cell to the particle. Pseudopodia are then mobilized first to extend to surround the material and then to contract following fusion of the surface membranes around the particle. The intricacies of recognition and engulfment will not be discussed here, and attention will be directed toward the process and pathology of digestion of endocytosed particles.

Alveolar macrophages function primarily to clear particulate debris from the air spaces in the lung, and they are especially well adapted for interacting with inorganic particles and resistent organisms such as fungus and tubercle bacilli. The extent to which a cell can sequester a xenobiotic particle without at the same time falling victim to its toxicity depends on (1) properties of the particle e.g. its size and shape, its solubility, and its surface-membrane bonding effects; (2) properties of the secondary lysosome, e.g. its organic and inorganic ionic constituents which may be products of fusion with primary lysosomes and; (3) its membrane defenses, transport systems, and phospholipid bilayer constituents.

Two notable examples where size and shape are thought to contribute to the toxic manifestations in phagocytosis are in asbestosis and in gout. The ionic microenvironment of the phagosome affects the solubility of metals such as lead oxide compounds and nickel oxides in macrophages. And finally, either the toxin, the lysosomal enzymes, or new combinations of both may adversely affect lysosomal membrane permeability and transport systems in as yet undetermined ways for the majority of other known toxic particulates.

Alveolar macrophages have been found to harbor a range of digestive enzymes, including cathepsins, acid and alkaline phosphates, B-glucuronidase, B-galactosidase, aryl sulfatase, acid ribonuclease and deoxyribonuclease, esterase, cytochrome oxidases, neutral proteases and peroxidase (Ericsson and Brunk, 1974; Cohn and Wiener, 1963a; deDuve and Wattiaux, 1966). Most of these enzymes are found in greater amounts and specific activity in alveolar macrophages than in peritoneal macrophages, and greater in BCG-activated macrophages than in resting alveolar macrophages. Many of the enzymes are localized to the membrane-bound granular fraction within the cytosol and are latent until activated by freezing, thawing, mechanical injury or fusion with a phagosome. When fused with a phagosome, the primary lysosome liberates enzymes in a soluble form by a process that can be monitored by neutral red, a basic dye which is taken up by pinocytosis and concentrated into lysosomes. Cohn and Wiener (1963b) followed the temporal relationship for solubility and activity of the lysosomal enzymes and found that not only do enzymes become active at different rates, but they are available in discrete and limited quantities within the cells.

Several possible mechanisms have been suggested to account for the phenomenon of digestion. pH changes might be mediated by intramembrane ionic pumps, redox pumps, or by other means such as an increase in lactic acid production with phagocytosis. (Jacques and Bainton, 1978). Enzymes may arrive within the vacuole by a) selective transport systems as suggested by Roth (1960); b) fusion with enzyme-bearing lysosomes (see DeDuve and Wattiaux, 1963, for review); and c) inclusion from the external milieu or outer cell membrane during invagination of the plasmalemma (Boxer et al 1979).

In order to protect the cell from lytic effects, the cell may dilute the contents of the vacuole and resorb them gradually by micropinocytosis (Roth, 1960) by osmosis (Mast, 1942) or by selective transport of macromolecules and ions. The hydrolytic enzymes may bear a short half-life, be limited by granule size, number of transport system dynamics, or be themselves subject to other proteolytic enzymes. The vacuolar membrane may be equipped with protective features such as a distinctive phospholipid bilayer high in cholesterol (Johnson, 1975) or other factors.

But there are times when the mechanism of particle sequestration and digestion short-circuits or backfires. In the case of active tuberculosis, the pathogeneic microorganisms may multiply intracellularly and overcome the macrophage. Or in the case of inorganic particulates, electrostatic interactions between the particle and the vacuolar membrane may render the phagosome leaky and allow the release hydrolytic enzymes into the cytoplasm with ultimate autolysis of the cell. A well documented example of such a sequence of events is in gout (Weissman, 1975) where monosodium urate crystals hydrogen-bond with the membrane phospholipids of polymorphonuclear leukocytes phagosomes. This is also thought to occur in the interactions between silica particles and macrophages (Nash et al 1966, Allison, 1974). DeDuve's initial "suicide bag" model, based on the idea that a particle physically punctures the phagosomal membrane appears to be no longer tenable in these disease states.

Particle surface solubility within the phagosomal vacuole may have a devastating effect on the phagocyte when dissolved toxic ions or complexes leach out into the cytosol and migrate to other target sites within the cell. Particle shape and solubility may act synergistically against the cell when large surface areas contact the vacuolar membrane and solubilized ions or complexes leak out of containment. There is good indication that both these effects occur in asbestos/macrophage interactions (Harington, 1975). Other particles may behave in similar fashion. Reprecipitation of metal ions within non-phagosomal lysosomes is known to occur with iron, copper, mercury and lead (Allison, 1968). Other metals under investigation in this laboratory may also reprecipitate within lysosomes. Ions solubilized from particulate nickel have been found to induce the formation of lamellar intranuclear inclusion (deVries, 1980).

It is conceivable also that electrostatic gradients could be generated around a metal particle in the microenvironment of the lysosome in such a way as to alter the configuration of a receptor "surface" protein or glycoprotein. Effector molecules within the cytoplasm, such as cAMP, might then receive new messages to alter the metabolism of the cell without the offending compound ever actually entering the cytosol.

Not all inorganic particles that damage or kill alveolar macrophages affect the microenvironment surrounding the cell in vivo identically. Compounds containing silica interact with macrophages in such a way as to induce granuloma formation and collagen synthesis in the surrounding tissue. However, other toxic particulates like lead, nickel and cobalt are not fibrogenic, but rather produce an acute inflammatory reaction at the site of injury (Allison, 1968). It may be that certain toxins damage lysosomal enzyme inactivators such that some enzymes remain destructive longer than normal. On the other hand, certain enzymes may be selectively activated by these metals. The tissue effects mentioned above are currently subject to intensive investigation in many laboratories.

In an effort to study the effects of environmentally significant particulates in an in vitro setting, we utilized two cell systems -- the rabbit alveolar macrophage (RAM) and the chinese hamster ovary (CHO) cell. The RAM was chosen because it provided a model for the types of cell-particle interactions that normally occur in pulmonary alveoli. And the CHO cell line was used because it has been developed as a model system for the short term toxicity and mutagenicity testing of many metal particulates.

The chinese hamster ovary (CHO) cell has been used in the cytotoxicity studies of Garrett et al 1979a, 1979b, 1979c, and Hsie et al 1978. Hsie et al described the attributes of the CHO line as follows: CHO cells grow well (100% colony-forming capacity) in a standard medium, either as monolayers or as suspensions. Their doubling time is known (12-14 hrs. at 37°) and they are amenable to mitotic synchronization. Their karyotype is stable over twenty years. And they are therefore useful for monitoring the effects of mutagnes and carcinogens. Garrett et al (1979a) have used the CHO cell to monitor the mutagenicity of coal fly ash by evaluating a point change at the hypoxanthine-guanine phosphoribosyl transferase (HGPRT) locus. CHO cells have also been used to screen for cytotoxicity of particulate xenobiotics (Garrett et al 1979b, Hsie et al 1978).

Although the CHO cell line has been utilized in the above mentioned biochemical screening studies, very little has been published concerning the normal morphology and the interactions between lysosomes and phagocytic vacuoles in this system. The pH range and enzyme contents of the CHO lysosome are not well understood, and the number of lysosomes per cell is far less than is found in macrophages. In experiments which analyse the effects of particulate compounds on the chromosomal dynamics of the CHO cell only slight attention has been paid to the interactions within the particle ingestion and digestion system which render the mutagenic assays significant.

In the experiments to be described below, two different non-fibrogenic metals were studied. On one set of experiments, lead monoxide (PbO) was introduced to CHO cells and RAMs in order to evaluate the differences in ultrastructural manifestations of lead toxicity in these different cell types. In another set of experiments, red lead

(Pb_3O_4) was studied specifically to determine the effect of pH changes on the lead oxide particle within the lysosome of the macrophages. Whereas PbO is slightly soluble in the medium and more soluble within the cell as determined by atomic absorption analysis and electron beam X-ray microanalysis, Pb_3O_4 is not soluble at neutral pH or in the medium but is soluble after ingestion by a cell. Therefore we were confident that whatever intracellular changes occurred were a result of particle solubilization within phagosomes. Lysed cells then released solublized lead into the medium, but since initial viability of macrophages were in all cases greater than 90% and control viability at the end of the experiment was no less than 80% it seemed reasonable that the solubilization of lead oxide was not initially the result of lactic acid leaking from dying cells. These experiments also will be described below.

Nickel monoxide (NiO) and nickel oxide-coated fly ash were introduced to RAM cultures to assess cellular ultrastructural changes in macrophages attributable to this carcinogenic metal. Although NiO is reported to be insoluble at neutral pH and soluble at an acid pH, we encountered problems in reproducing our experiments, probably because certain industrial manufacturing processes for NiO leave a thicker oxide coat on the particle surfaces than others, and therefore the length of exposure and dosage required to produce characteristic responses to the toxin varied widely. Reproducible experiments were obtainable, however, with soluble nickel salts, and these confirmed our findings with nickel oxide particles.

We have described all of the instrumental analytic techniques employed in these experiments in the literature and we will cite these where appropriate in the materials and methods sections of the sections that follow.

EXPERIMENTS ON PbO

Introduction

It is known that many different types of cells can phagocytose particles (Elsbach, 1974). In mammals, pulmonary alveolar macrophages are primarily responsible for internalizing and digesting inhaled foreign material such as inorganic particles. However, in the laboratory, other cell systems offer the advantages of better reproducibility of experiments and more rapid, controlled exposure conditions. Fibroblasts and chinese hamster ovary cells have been used as screening systems for assessing the cytotoxicity of lead oxides (Fischer, 1975; Garrett et al 1979a, 1970b). In the present study we have exposed chinese hamster ovary cells and rabbit alveolar macrophages to PbO-coated and uncoated fly ash and PbO particles to determine the differences in ultrastructural pathology exhibited by the two cell types under similar culture conditions.

Materials and Methods

Two model systems were designed to assess ultrastructural changes due to the toxicity of phagocytosed PbO and PbO-coated particles. Rabbit alveolar macrophages (RAMs) obtained by pulmonary lavage (Waters et al 1975) and chinese hamster ovary (CHO) cells (Garrett et al 1979) were maintained in standard medium 199 with Earles or Hanks salts respectively, 10% heat-inactivated fetal calf serum, and antibiotics. The cells either were allowed to attach to the surface of plastic culture dishes or were rocked continuously in plastic flasks during incubation to maintain the macrophages in suspension.

Both RAMs and CHO cells were exposed to size-fractionated (2-5 um) particles of fly ash or fly ash coated with PbO (Yamate and Ashley, 1975) in concentrations of 0, 10, 50, 100, 250, 500, 750, or 1000 µg particles per ml culture medium for 20 hours. RAMs were also incubated with 100 µg/ml PbO particles supplied by Fisher (Lot #780458) for 20 hours. Cell viabilities were assessed by trypan blue dye exclusion and by examination of cell morphology by light microscopy. Any cell with a pyknotic, karyolytic or karyorrhectic nucleus was deemed nonviable.

In control experiments, PbO and PbO-coated fly ash particles were incubated with, but separated from, RAMs in the same dishes by 0.22 micron membrane filters. The cells were harvested as monolayers and processed for TEM, and the supernatant was decanted, centrifuged to remove any floating cells or particles, and refiltered through a .22 membrane filter. The fluid was heated to dryness in concentrated HNO_3 and reconstituted in 1% HNO_3 for atomic absorption analysis. The analysis was performed on a Perkin-Elmer Model 603 furnace-type photometer. Six analyses were performed on each of the two to four dishes for each experiment.

Cells that had been allowed to attach to the culture dishes as monolayers were fixed in 0.15M sodium cacodylate buffered 3% glutaraldehyde. Some of these monolayers were also postfixed in 2% osmium tetroxide in the same buffer. All monolayers were then dehydrated in a graded series of ethanol and embedded in Epon 812.

Suspensions of macrophages were spun down in capillary tubes, extruded as cell pellets into 0.15M sodium cacodylate buffered 3% glutaraldehyde and processed routinely through alcohol into Epon 812 or were snap frozen in liquid nitrogen-cooled liquid propane, freeze-substituted in acetone-osmium, and processed into Epon 812 following the method of Masters, 1979.

Thick sections for light microscopy were cut at 0.5 um and stained with toluidine blue. Thin sections of 80-100 nm were cut onto formvar and carbon-coated copper grids. Monolayers were cut en face and pellets were cut in longitudinal or cross-section. Both were stained with uranyl acetate, or uranyl acetate and lead citrate or were left unstained for electron microprobe analysis.

The grids were examined and photographed on a JEOL 100B at 80KV. Additionally, sections to be analysed by X-ray microprobe were viewed on an ETEC scanning electron microscope equipped with a Kevex 5100 energy dispersive analyser with a 30 mm^2 SI (Li) detector. STEM images prior to and after analysis were compared to confirm the location of the probe by beam damage.

Results

CHO cells readily phagocytosed both lead coated and uncoated fly ash particles (Figure 1, 4, 5). The viability of the cells remained virtually constant at 99% after 20 hours incubation for control cells and for all CHO cells exposed to less than 1000 ug/ml PbO coated fly ash. Viability for uncoated fly ash treated cells has been previously determined to be 83% (Garrett et al 1979). For cells treated with 1000 ug/ml PbO coated fly ash, viability dropped to 72% as determined by trypan blue dye exclusion.

RAMs were treated with either 1000 ug/ml PbO coated or uncoated fly ash or PbO particles for 20 hours. Total viabilities after 20 hr. incubation were 97% for untreated control RAMs, 72% for RAMs with uncoated fly ash and 47% for RAMs exposed to PbO coated fly ash. For RAMs prevented from phagocytosing PbO coated fly ash by a membrane filter, the viability was 83%. RAMs exposed to PbO particles were 76% viable and RAMs prevented from phagocytosing PbO were 81% viable. (See Table 3).

The most important results from the atomic absorption analyses concerned the experiments in which RAMs had ingested PbO coated flyash. In these experiments the viability was the lowest and the lead concentration in the medium was the highest. When phagocytosis was blocked, the lead concentration in the medium remained below 1ppm --close to the control value. Thus, it is likely that Pb was solubilized within the cells and then released.

TEM micrographs examined for ultrastructural changes showed that in CHO cells that had ingested uncoated fly ash or PbO coated fly ash very little structural damage could be found in the organelles. The ingested particles displaced large areas of cytoplasm, but there was only slight evidence of such sublethal changes as swelling of the endoplasmic reticulum or mitochondria in viable CHO cells. Cytosegrosomes were uncommon, and no crystalline densities were observed in the cytoplasm or nucleus of the cells (Figure 4, 5).

In RAMs exposed to uncoated fly ash, mitochondria appeared by TEM to be of normal size and configuration and without flocculent matrix densities in contrast to RAMs exposed to PbO coated fly ash, which were swollen and commonly did contain flocculent densities in the mitochondria. In uncoated fly ash treated RAMs, there were no consistent ultrastructural changes in the ER or Golgi of viable cells, and the nuclei resembled those of control macrophages.

On the other hand, RAMs exposed to PbO coated fly ash exhibited swelling of the ER in almost every cell that had ingested a particle. Evidences of cell death i.e. pyknosis and karyolysis were more common in the RAMs cultured with coated particles than in RAMs cultured with uncoated particles. In both viable and non-viable RAMs that had been cultured with PbO coated particles, crystals of lead salts were found free in the cytosol and in membrane-bound vacuoles at a distance from the ingested coated fly ash particles. These crystals were not seen in RAMs incubated with uncoated fly ash or in CHO cells cultured with uncoated or coated fly ash particles.

In RAMs exposed to PbO particles, fine crystalline densities were found in the cytoplasm localized to membrane bound vesicles (Figure 9). These densities had a fine fibrillar quality and appeared to have precipitated in concentric zones. In these cells, the mitochondria and ER were both swollen, but the nuclei were fairly normal indicating that the precipitation was not a result of cell death. When the RAMs were prevented from phagocytosing PbO particles, no crystalline densities developed in the cells, but on the cell surface were small blebs or bubbles of membrane. That the blebs are a response of the cells to lead ion in the medium was confirmed by the fact that the only other time that we have seen surface blebs has been in experiments in which we exposed RAMs to a soluble salt of lead ($Pb(NO_3)_2$) in the medium (Plate 11) (de Vries et al unpublished). These surface blebs were not seen in cells that had ingested particles of PbO or PbO coated flyash. These cells tended to be very round and smooth, and possibly that particular surface configuration did not permit surface bleb formation.

In the snap-frozen, freeze-substituted lead-treated RAMs, membrane bound cytoplasmic densities and the surrounding cytoplasm and Epon were located with TEM and spot probed by EDX. Fly ash particles also were probed to delineate the differences in elemental composition between the phagocytosed fly ash particles and the reprecipitated crystals. Plate 10, c, d, shows the typical spectrum obtained by analysis of a membrane-bound density. Lead and phosphorus are the elements most consistently found in these densities although calcium is often present as well. Plate 10b demonstrates that fly ash particles coated with PbO also produce peaks for Al, Si, K, Fe, along with Pb. There are no conspicuous peaks for P or Ca in the coated fly ash particles.

Since we found no ultrastructural changes specifically attributable to lead in the CHO cells exposed to PbO coated fly ash, we did not study cells by X-ray microanalysis.

Discussion

It is well known that particulate lead compounds pose a serious environmental health hazard. Depending on the source of particulates, airborne lead compounds may range from lead oxides to lead halides and organic compounds (NAS report on airborne lead, 1972). From whole animal studies (Fairhall and Sayer, 1940) PbO has been found to be among the most toxic forms of lead when inhaled. The reasons for this are not entirely clear because the solubility of lead products in the alveolar microenviornment has not been well defined.

The present series of experiments sought to elucidate the function of phagocytosis in the toxicity of PbO and to describe the ultrastructural changes attributible to lead coated particles within two different types of phagocytic cells.

The CHO cell has been developed as a model system for screening the cytotoxicity of metal compounds in vitro (Garrett et al 1979 a,b). These cells are well maintained in culture, and therefore lend themselves to reproducible studies. Although not derived from a normally phagocytic cell type, we have shown that the CHO cell does phagocytose particles in vitro (Garrett et al 1979b). Since mitochondria are abundant in these cells and since lysosomes are few as determined by TEM, it was of interest to know whether the particles would produce toxic manifestations similar to those seen in RAMs subjected to similar experimental conditions. Examination of viable CHO cells after 20 hours of incubation with PbO coated fly ash at all dosages showed clearly that little recognizable organelle damage had occurred in CHO cells that had ingested particles. These cells resembled control CHO cells and CHO cells that had ingested uncoated fly ash, despite the fact that at 1000 ug/ml, viability had dropped to 72%. While we did observe some completely necrotic cells in these experiments, just what the early toxic effects of PbO on CHO cells are, however, is not precisely known. Garrett et al (1979) have used parameters such as ATP levels to determine the cytotoxicity of various particulates in the CHO cell system, but further work must be done to bring to light the details of lead toxicity in the CHO cell.

Rabbit alveolar macrophages also were studied for their susceptibility to lead intoxication via the phagosomal-lysosomal pathway. Since the alveolar macrophage is known to contain lysosomal proteolytic enzymes, peroxides, and superoxide ions in an acid environment, and since lysosomes are a major constituent of the macrophage organelle population in contrast with the CHO organelle population, we considered that the lead-lysosome interaction might account for damage to lead-exposed RAMs.

We found that at the lowest dosage where viability of CHO cells dropped slightly but significantly (1000 ug/ml), PbO coated fly ash was extremely destructive to RAMs. At this dosage, where as CHO viability was 72%, RAM viability was 49%. Viable RAMs that had ingested coated particles exhibited a range of manifestations of sublethal toxicity, and in addition, a very chracteristic pattern of recrystalization of Pb, P, and Ca containing crystals in the cytosol. Some of these specific and sublethal changes have been described previously. Lysosomal lead densities have been reported to occur in fibroblasts cultured with soluble lead (Brun and Brunk, 1971), and crystalline densities identified by EDX as compounds of Pb, P, and Ca have been found in the kidneys of whole animals treated with soluble lead in vivo (Carroll et al 1970). Goyer and Krall (1969) and Watrach (1964) have reported mitochondrial changes in various cell types of animals exposed to soluble lead salts in vivo.

Biochemical parameters for lead toxicity in RAMs have been studied by Aranyi et al (1976) who report that levels of acid phosphatase and LDH do change in RAMs exposed to PbO coated fly ash over a period of 21 hours. These authors propose that lead solubilization from the surface of PbO coated fly ash particle in standard culture medium is not significantly lethal to RAMs after 21 hours. In their experiments, the RAMs were exposed to medium previously incubated with PbO coated fly ash, cells were not incubated with coated fly ash. Our experiments confirmed their proposal by separating the RAMs from the coated fly ash in the same medium by a membrane filter, Pb solubilization from surface bound lead in the medium was not a major factor in cell toxicity. This was also true for PbO particles separated from the RAMs by a membrane filter. It is therefore probable that the process of phagocytosis accounts for most of the toxic effects of particulate lead seen in cells exposed to particles for 20 hours. In RAMs, these effects are visible by ultrastructural morphology as well as by a strikingly diminished viability. In CHO cells, the effects are more subtle and less well defined by changes in the cell's fine structure, and the cells are more resistant to damage as determined by viability data.

Conclusion

The effect of particulate lead monoxide on two phagocytic cell models has been studied in vitro. In the CHO cell, very little ultrastructural damage occurred despite extensive phagocytosis of PbO coated fly ash. This may be attributable to a paucity of lysosomes in this cell type or to a mechanism yet to be determined. In the RAM model, at concentrations of particles only slightly toxic to CHO cells, massive lytic change was evident as well as a characteristic reprecipitation of Pb, P, and Ca containing crystals. When phagocytosis was blocked, these changes were prevented. It is thought that the increased toxicity in RAMs is due to the potentiating effects of the lysosomal pH, proteolytic enzymes, peroxides, or superoxides on the lead particles in phagolysosomes. In other words, it is possible that in the lead-containing phagosome in the macrophage, the lysosomal microenviornment contributes to the increased solubility of the lead oxide. This lead may then damage the lysosomal membrane sufficiently to permit leakage of lead ion into the cytosol where it produces toxic effects and reprecipitates within other cytoplasmic organelles.

We propose, therefore, that because the RAM is a naturally phagocytic cell, and because it is more sensitive to the toxic effects of particulate lead monoxide than is the CHO cell, the RAM is a more accurate screening model for assessing the toxicity of respirable lead particles than is the CHO cell.

TABLE 1
RELATIVE TOXICITY OF LEAD PARTICULATES*

Inhaled	Ingested
Lead carbonate	Lead arsenate
Lead monoxide	Lead carbonate
Metallic lead	Lead monoxide
Lead arsenate	Lead sulfate
Lead chromate	Metallic lead
Red lead (Pb_3O_4)	Lead chromate
Lead dioxide	Red lead (Pb_3O_4)
Lead phosphate	Lead dioxide
Lead silicate	Lead phosphate
Lead sulfide	Lead sulfide

*From Fairhall and Sayers (1940). The toxicity data are based on whole animals studies in Waldron & Stofen (1974) p. 43. (Listed from most to least toxic).

TABLE 2
SOLUBILITIES OF SELECTED LEAD COMPOUNDS

Compound	In Cold H_20	In Acid
PbO	17 mg/100 ml	s. HNO_3
Pb carbonate (Pb (CO_3)	1.1 mg/100 ml	s. acid
Pb (metallic)	insoluble	s. HNO_3
Pb_3O_4	insoluble	s. ac. acid
Pb $(PO_4)_2$	.014 mg/100 ml	s. HNO_3
$PbSO_4$	42.5 mg/100 ml^{250}	s. conc H_2SO_4
PbS	124.4 mg/100 ml	s. acid
$PbBr_2$	very sol.	s. dilute HCl
$PbCl_2$	very sol.	-------------

From Waldron and Stofen (1974) p. 41; and Handbook of Chemistry and Physics (1972-1973) Chemical Rubber Company.

TABLE 3

CELL TYPE	EXPOSURE (20 HR.)	VIABILITY	LEAD IN MEDIUM*	TEM MORPHOLOGY
CHO	Control	99%		Normal for CHO
CHO	1000 ug/ml uncoated fly ash	83%		Normal for viable cells which had ingested fly ash
CHO	1000 ug/ml PbO coated fly ash	72%		Normal for viable cells which had ingested PbO coated fly ash
RAM	Control	97%	.28ppm	Normal for RAM
RAM	1000 ug/ml uncoated fly ash	72%		Nonspecific sublethal changes for viable cells which had ingested fly ash (some normal)
RAM	1000 ug/ml PbO coated fly ash, filter (phagocytosis blocked)	83%	.78ppm	Membrane surface blebs on plasmalemma. Otherwise normal
RAM	1000 ug/ml PbO coated fly ash, exposed	47%	8.8ppm	Extensive lysis of cells that had ingested particles. Crystals of Pb, P, and Ca.
RAM	1000 ug/ml PbO particles, filter (Phagocytosis blocked)	81%	.22ppm	Membrane blebs on plasmalemma. Otherwise normal
RAM	1000 ug/ml PbO particles, exposed	76%	.42ppm	Membrane-bound cytoplasmic crystalline densities

---

*Atomic absorption data ±5%

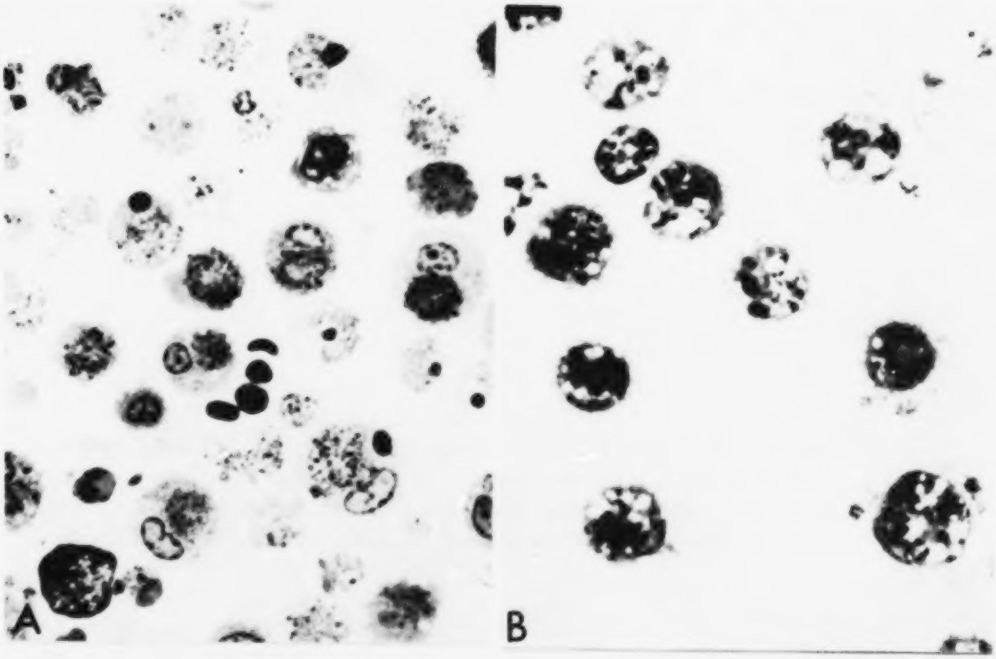

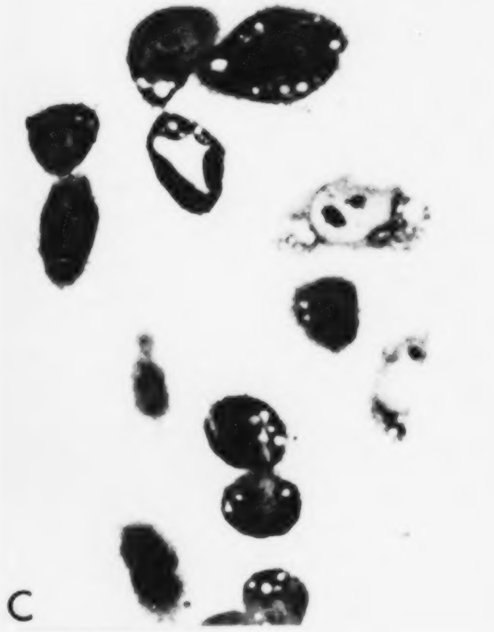

Plate I

Light micrographs of control RAMs and CHO cells exposed to fly ash particles. (X 1000)

A. Control RAMs. The nuclei and lysosomes concentrate in an area opposite the nucleus.

B. RAMs exposed to uncoated fly ash particles. The particles are represented as lucent areas.

C. CHO cells that have ingested uncoated fly ash. These cells accommodate the particles better than do RAMs.

FIGURE 2

Transmission electron micrograph of control CHO cells. Note the nuclei, prominent nucleoli, prominent mitochondria, and paucity of lysosomes. The cells were fixed in glutaraldehyde, embedded in Epon and double stained with lead nitrate and uranyl acetate.

A. X 17,100.

B. X 12,500

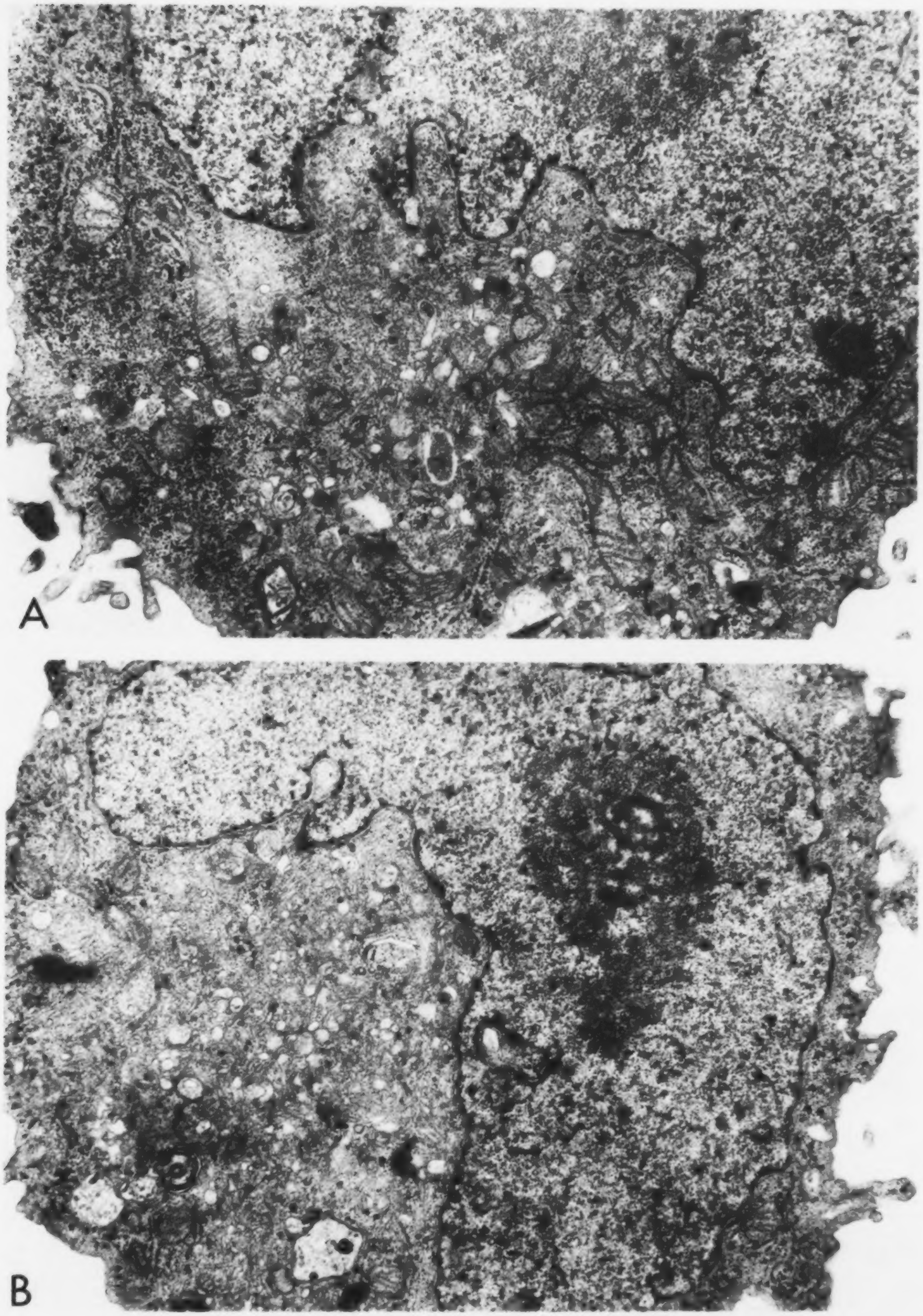
A
B

FIGURE 3

Control RAMs at low power to show typical normal morphology. The nuclei are eccentric, and there are many dense lysosomes. The cell boundaries are ruffled.

A. X 12,100

B. X 13,300

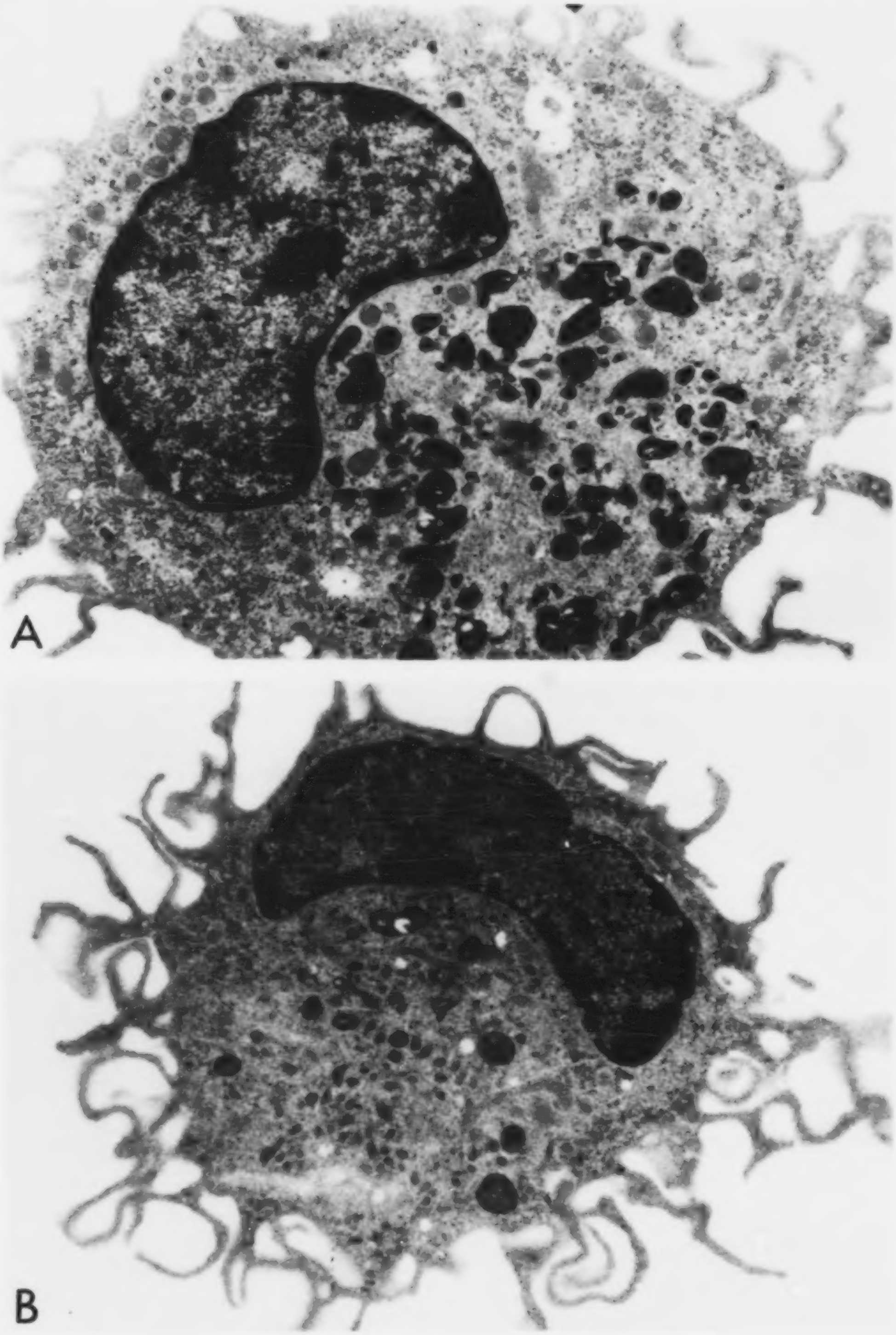
A
B

FIGURE 4

Transmission electron micrograph of a CHO cell which has ingested particles of uncoated fly ash (P). The nucleus surrounds a pseudo-inclusion of fly ash, but otherwise appears normal. The ER is not swollen, but some of the mitochondria appear distorted and more lucent.

X 12,500

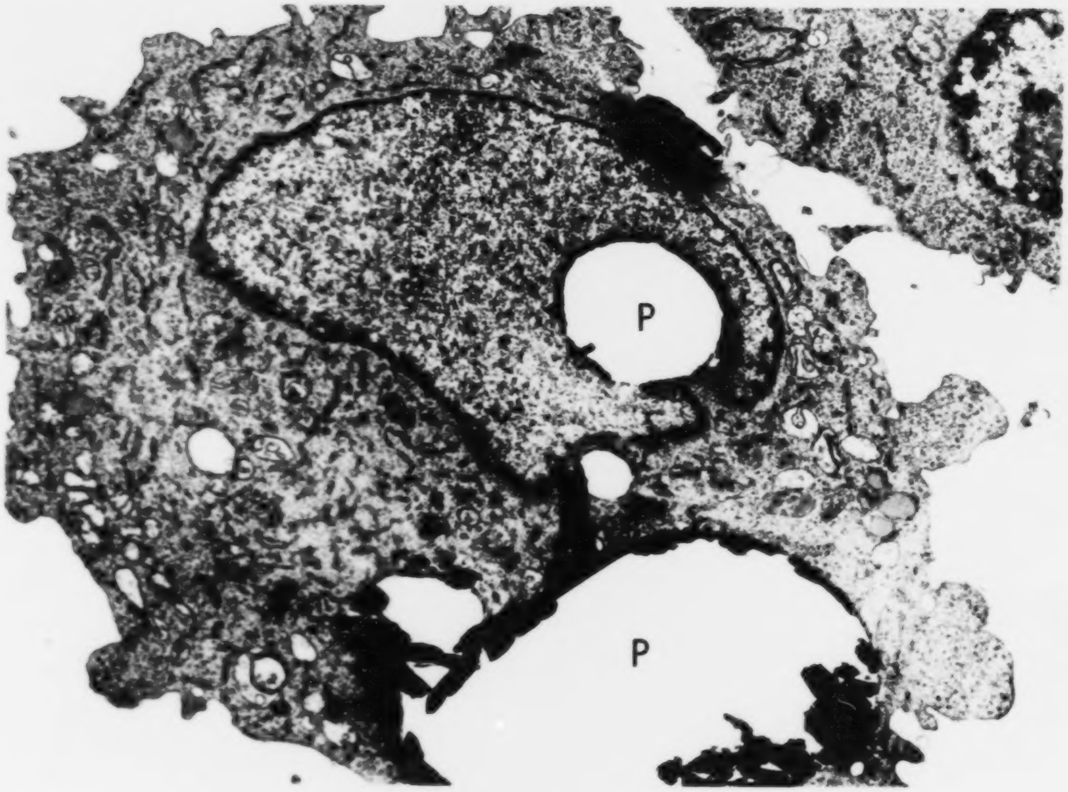
P
P

FIGURE 5

Transmission electron micrograph of CHO cells exposed to PbO-coated fly ash particles. Although the nucleus in A appears grossly distorted and contains pseudoinclusions and invaginations, pleomorphic nuclei are not unusual for control CHO cells.

A. Two cells which have ingested particles (P) are represented here. The mitochondria and Golgi apparatus remain intact as does most of the ER. Small vacuoles are apparent within the cytoplasm. (X 8,000)

B. A higher power view shows the cytoplasm to be fairly normal, with well developed Golgi apparatus and ER, several large, normal mitochondria, and an intact ER. (X 27,400)

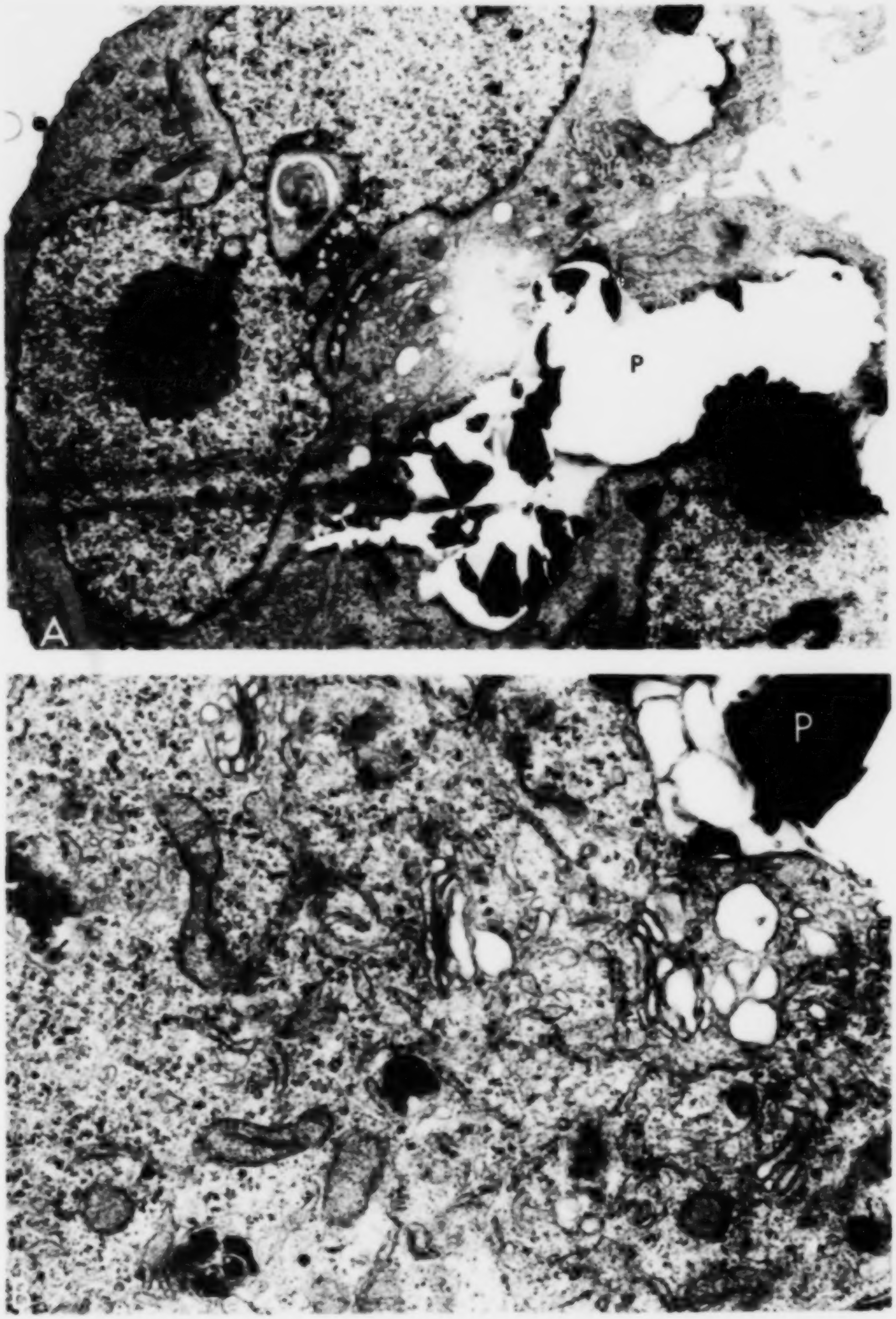
A
P
P

FIGURE 6

RAM with phagocytosed uncoated 2-5 um fly ash particles (P). Some of these shatter on sectioning. However, cytoplasmic organization and nuclear integrity remain intact.

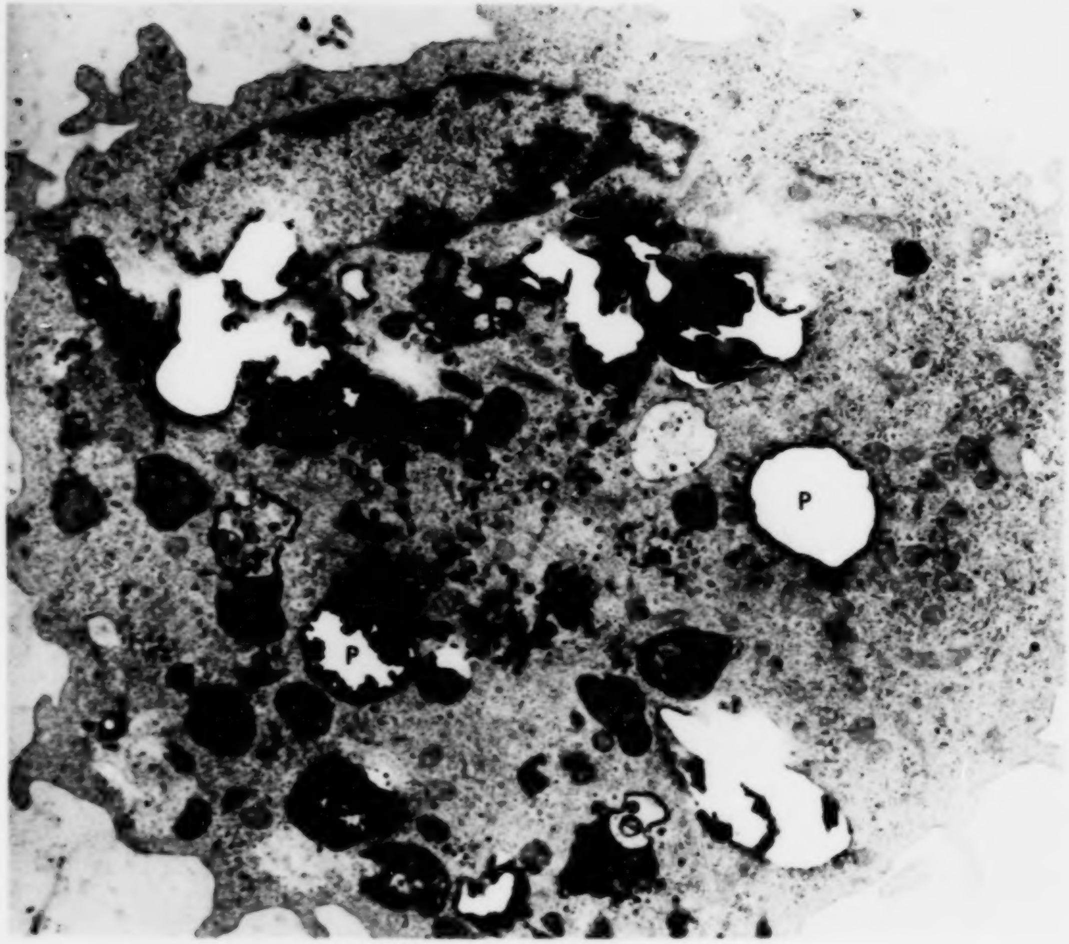
P
P

FIGURE 7

RAMs with phagocytosed PbO-coated fly ash particles (P). These cells develop cytoplasmic crystals (C) which contain Pb, P, and Ca.

A. One crystal is membrane bound whereas the other appears not to be. The cytoplasm of the cell is grossly disorganized and pale, and the few remaining mitochondria are swollen and contain flocculent matrix densities. (X 38,500)

B. In this area, only lysosomes remain of the cell's organelles, and the cytosol is pale and disintegrated. (X 58,600)

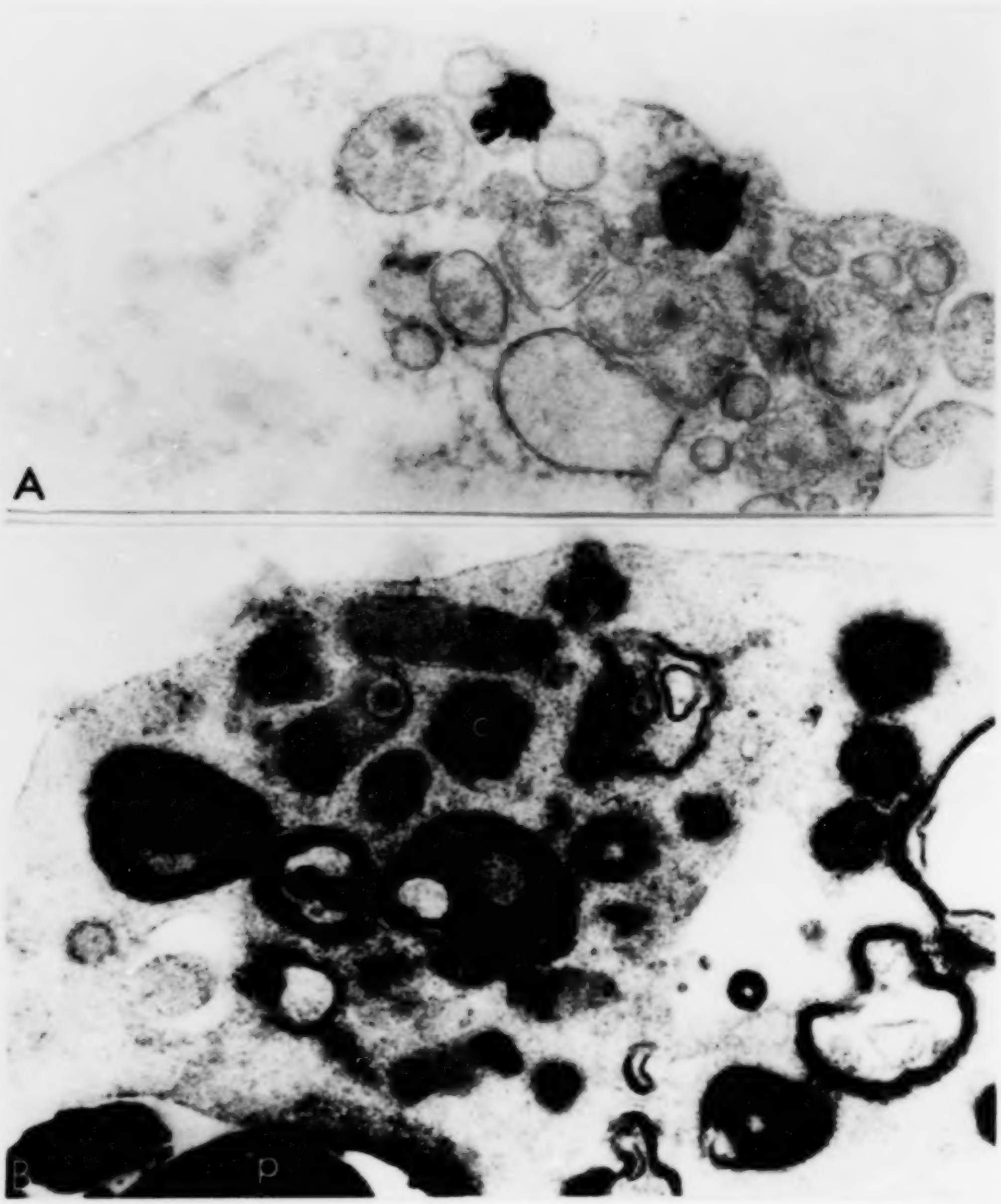
A
c
B
p

FIGURE 8

At higher magnification many inclusions are found to consist of dense spicular material crystalizing in a radiating pattern. (X 72,500)

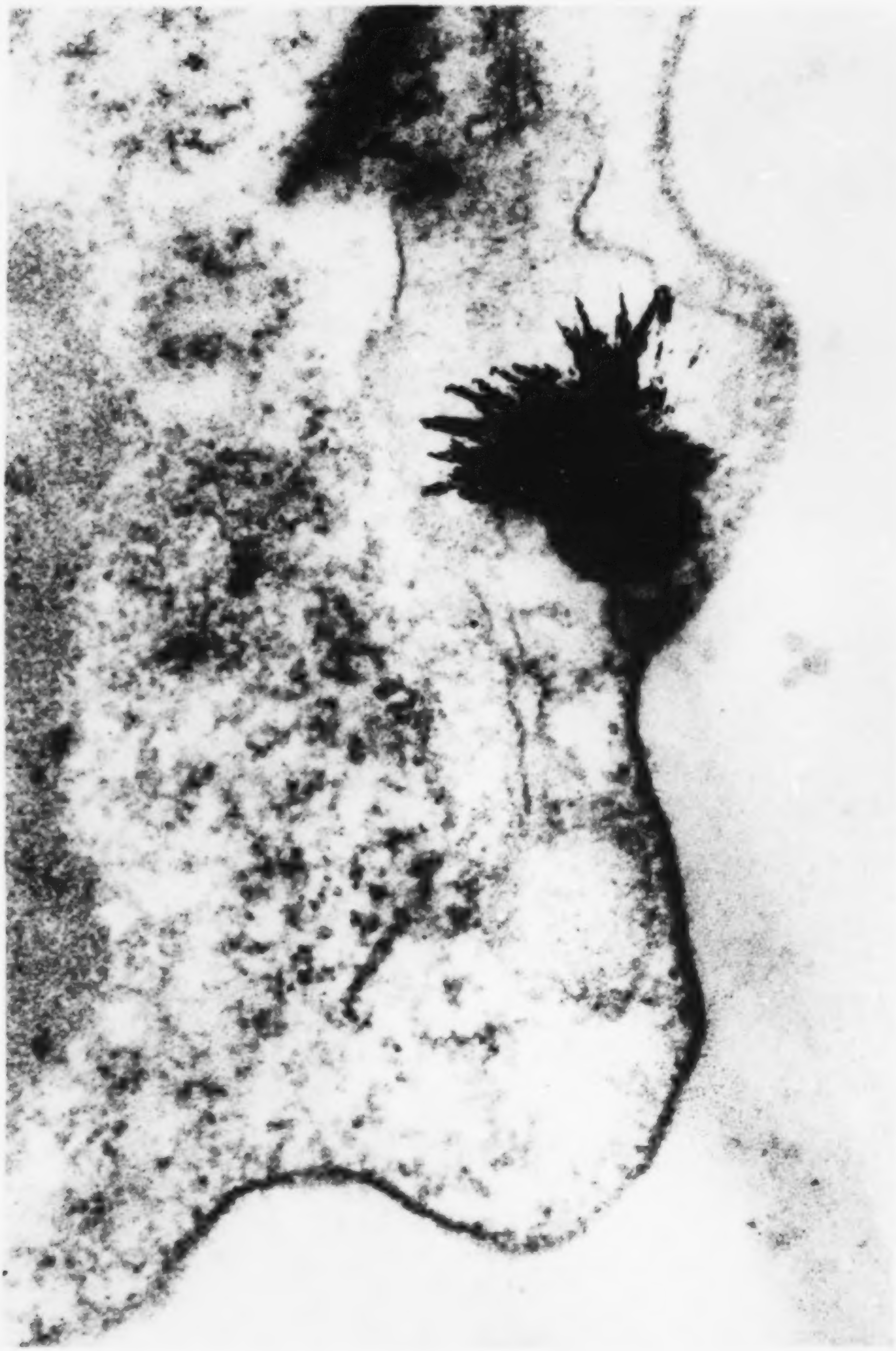

FIGURE 9

This RAM was exposed to PbO particles (P). Membrane bound densities, (presumably lysosomal) are seen at a distance from the ingested particle. In contrast to the inclusions produced by PbO-coated fly ash, these densities bear a resemblance to the intranuclear inclusions seen in kidney tubule cells after lead poisoning in vivo. The mitochondria here are swollen and there are numerous cytoplasmic vacuoles. (X 37,500)

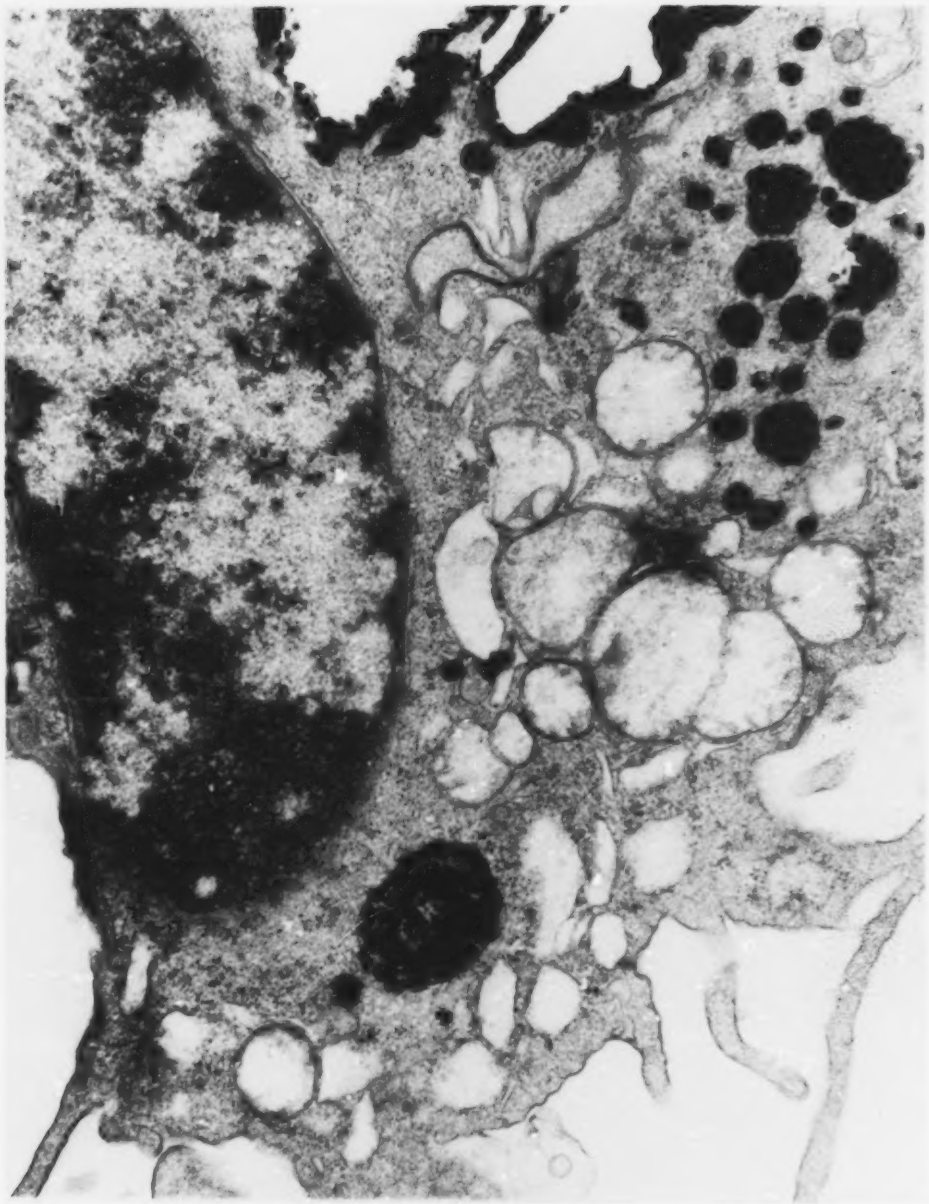

FIGURE 10

X-ray microprobe analysis of RAMs exposed to PbO coated fly ash. The cells were fixed with glutaraldehyde only, embedded in Epon and mounted on copper grids.

A. Background cytosol devoid of particles or crystals. Al and Si are instrument background, Cl is from the Epon, and P and S are from the cytosol.

B. Particles of PbO-coated fly ash. Lead M and L lines are present in addition to a multitude of peaks representing fly ash particle constituents and other background peaks mentioned above. Only a trace of phosphorus is present. (Cu is from the copper grid).

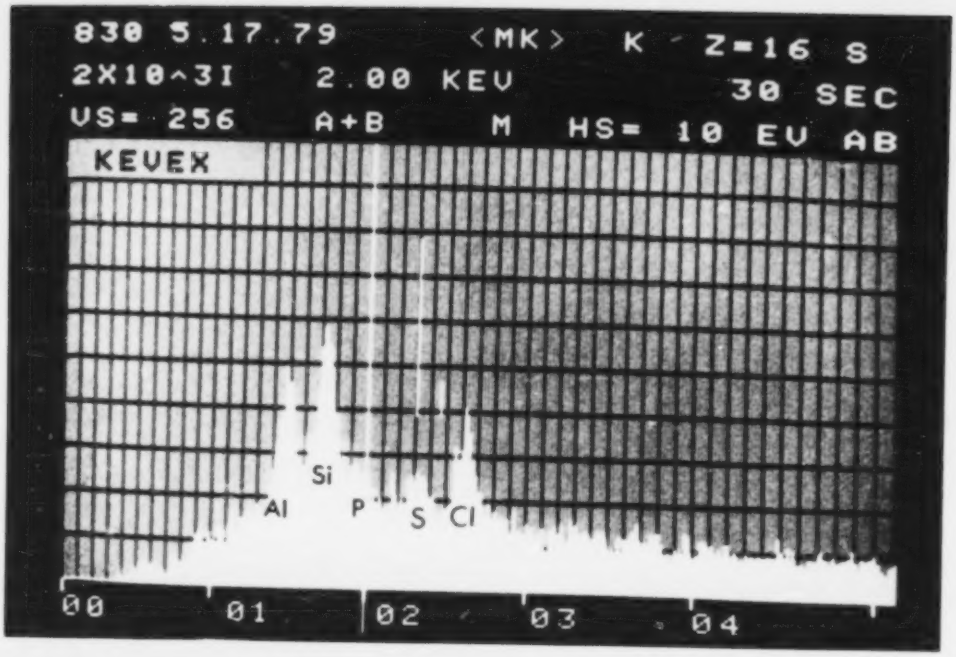
830 5.17.79
<MK>
K
Z=16 S
2X10^3I
2.00 KEV
30 SEC
VS= 256
A+B
M
HS= 10 EV
AB
KEVEX
Si
Al
P
S
Cl
00
01
02
03
04

A

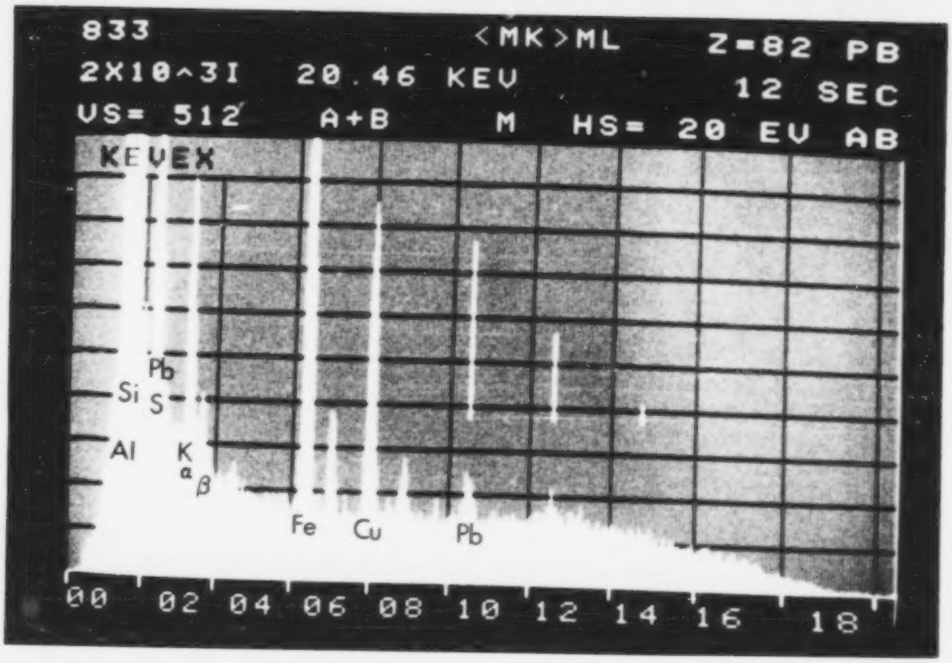
833
<MK>ML
Z=82 PB
2X10^3I
20.46 KEV
12 SEC
VS= 512
A+B
M
HS= 20 EV
AB
KEVEX
Pb
Si
S
Al
K
α
β
Fe
Cu
Pb
00
02
04
06
08
10
12
14
16
18

B

C. Crystalline cytoplasmic inclusion similar to those shown in Plates VII, VIII. In contrast to the previous spectrum, prominent peaks for phosphorus and calcium are present.

D. Different view of the same spectrum above showing lead M and L lines as well as the calcium and phosphorus peaks.

FIGURE 11

RAM exposed to soluble (Pb(NO_3)$_2$. There are many vacuoles at the periphery of this cell, and small blebs or bubbles of plasma membrane have formed at the surface of the cell.

X 30,000

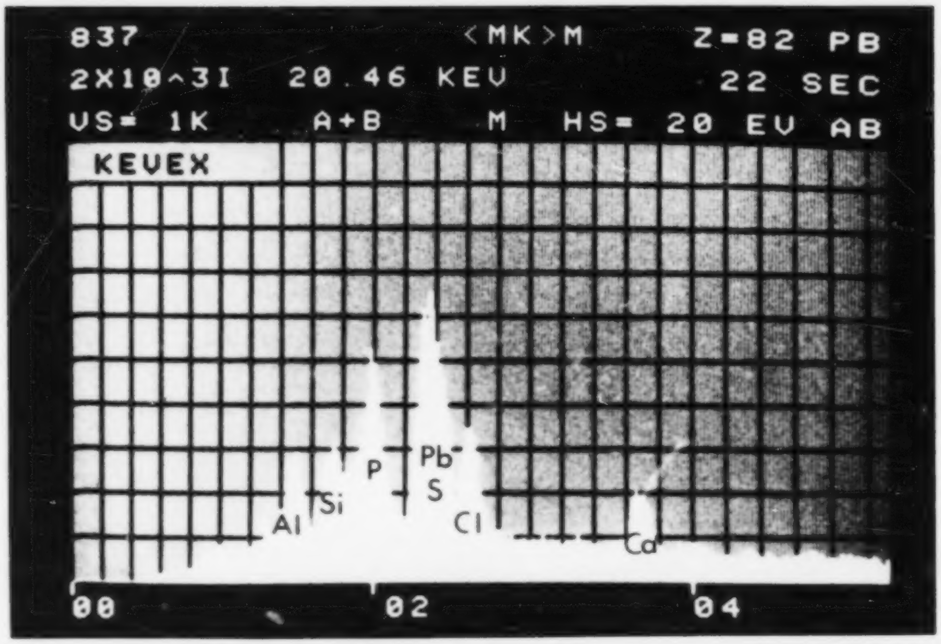
837
<MK>M
Z=82 PB
2X10^3I
20.46 KEV
22 SEC
VS= 1K
A+B
M
HS= 20 EV
AB
KEVEX
Al
Si
P
Pb
S
Cl
Ca
00
02
04

C

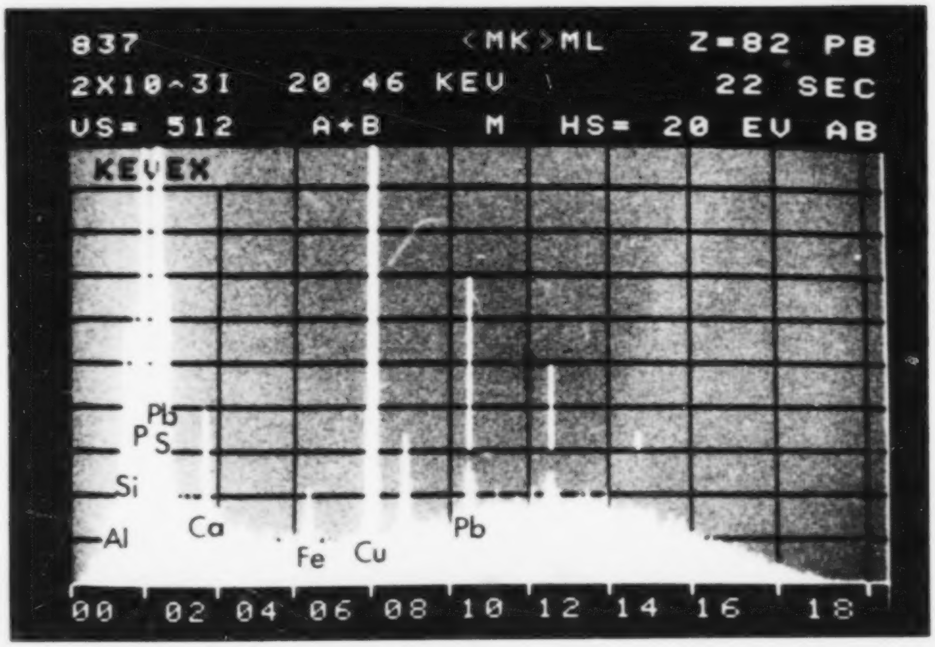
837
<MK>ML
Z=82 PB
2X10^3I
20.46 KEV
22 SEC
VS= 512
A+B
M
HS= 20 EV
AB
KEVEX
Pb
P
S
Si
Al
Ca
Fe
Cu
Pb
00
02
04
06
08
10
12
14
16
18

D

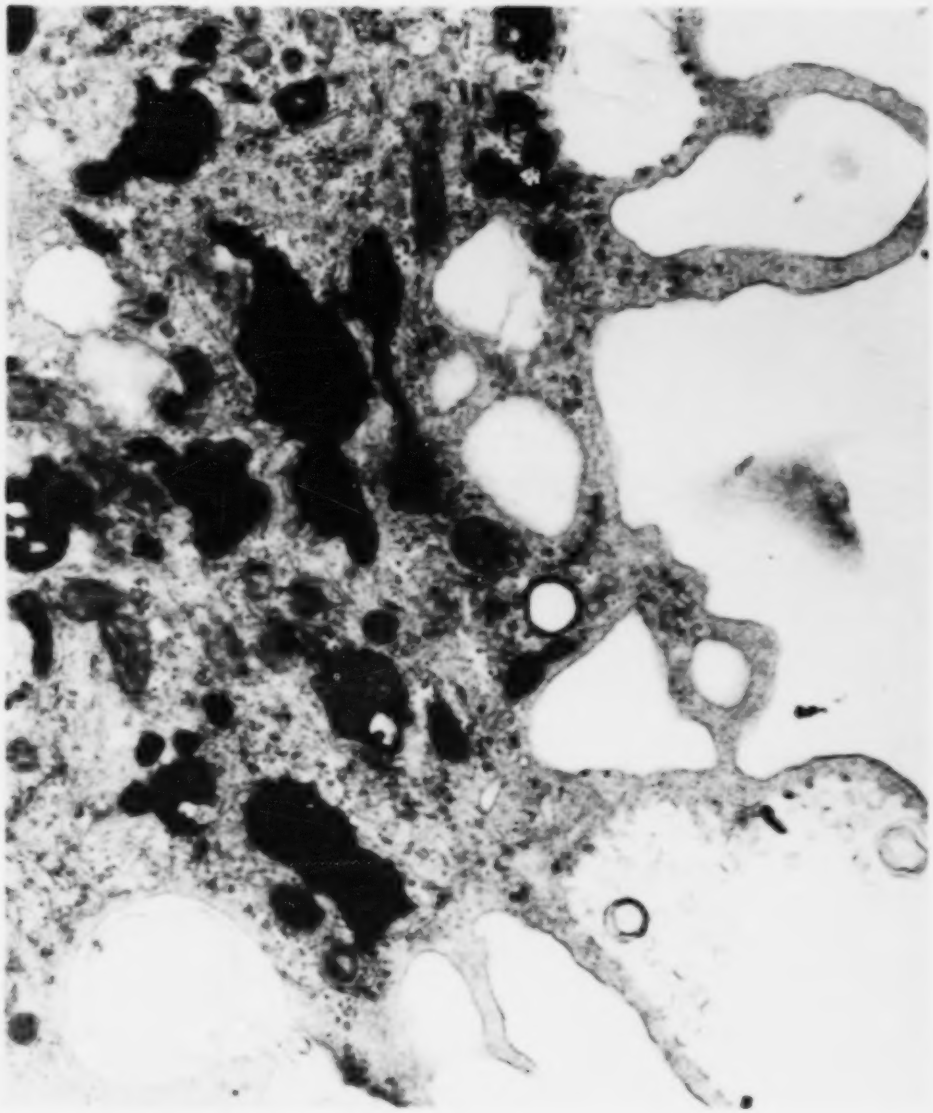

STUDIES ON Pb_3O_4 PARTICLES AND RAMS

Introduction

Red lead (Pb_3O_4) is a compound used commercially as an antirust additive for paints. When inhaled, it produces symptoms of lead toxicity similar to those found in other forms of lead exposure. Red lead is not soluble in neutral environments, but is soluble at weakly acidic pH. Therefore, it is probable that in alveolar macrophages which have ingested Pb_3O_4 particles, the decreased lysosomal pH enhances solubility and dispersion of lead ion within the microenvironment of the cell and the pulmonary alveolus. In an in vitro model, using rabbit alveolar macrophages exposed to particles of Pb_3O_4, we investigated the intracellular solubilization and redistribution of lead ions from ingested particle surfaces.

Materials and Methods

Rabbit alveolar macrophages were obtained by pulmonary lavage as previously described (Waters et al 1975), and were allowed to attach as monolayers in plastic culture dishes in medium 199 with fetal calf serum and antibiotics. In some of the culture dishes, small pieces of sterile aluminum foil or Thermanox cover slips were introduced and the RAM monolayers attached to them.

After two hours of incubation at 37° (to allow the cells to stabilize and adhere to the dishes), the cells were exposed to 100 ug/ml Pb_3O_4 (red lead) particles (Fisher Lot #781298, less than or equal to two microns in diameter) (Figure 6) in fresh medium for 4, 24, or 48 hours at 37°. Control dishes for each regimen were exposed to identical culture conditions but not to Pb_3O_4. In another control experiment Pb_3O_4 particles were incubated with but were separated from the cells by a 0.22 micron membrane filter (Millipore). These cells were incubated for 4 hours at 37°.

Cell viabilities were assessed by light microscopy at 1000X using toluidine glue stained 0.5 micron sections of Epon-embedded cells. Cells with pyknotic, karyolytic, or karyorrhectic nuclei were considered to be nonviable.

After incubation, the supernatants were decanted, centrifuged to remove suspended cells and particles, and filtered for atomic absorption analysis through a .22 membrane filter. The medium was heated to dryness in concentrated HNO_3 and reconstituted in 1% HNO_3. AA was performed on a Perkin-Elmer Model 603 furnace-type spectrometer. Concentration values for lead are expressed as an average of six determinations for each supernatant sample.

RAM monolayers were gently rinsed with serum-free medium and conventionally fixed in 3% Na-cacodylate buffered glutaraldehyde dehydrated in ethanol, and embedded in Epon 812 for transmission electron microscopy (TEM) or were snap-frozen in liquid nitrogen-cooled liquid propane and freeze-dried for scanning electron microscopy and electron microprobe analysis (SEM/EDX) or secondary ion mass spectroscopy (SIMS) (to be described below).

Thin sections of monolayers were cut en face at 80-100 nm, mounted on formvar and carbon-coated copper grids, and stained with lead citrate and uranyl acetate or were left unstained for EDX microanalysis. For TEM visualization and photography, a

JEOL 100B electron microscope was used at 80KV. Thick sections of 0.5 um were cut with a glass knife and stained with toluidine blue for light microscopy.

In preparation for SEM/EDX studies, Thermanox cover slips were rinsed in serum-free medium and blotted on the undersurface, glued to carbon stubs, and dropped rapidly into liquid nitrogen-cooled liquid propane. This entire process involved approximately 15-30 seconds. The monolayers were stored under liquid nitrogen for several minutes before being transferred under nitrogen to a forepump vacuum chamber. Vacuum was established and maintained for 20 hours, after which time the cells were assumed to be dry, and were transferred to vacuum dessicators for storage. The freeze dried monolayers were carbon-coated prior to visualization and analysis on an ETEC scanning electron microscope with EDX capabilities (2). Intracellular particles were localized by two methods; backscatter imaging, and TRIX (Total Rate Imaging with X-Rays) (Ingram and Shelburne, 1980).

Pieces of aluminum foil with monolayers of RAMs attached were rinsed gently with serum-free medium or left unrinsed, and blotted, snap-frozen and freeze-dried as in the above procedure for SEM/EDX. The cells were then coated with gold-palladium and stored in vacuum dessicators until analysed with the SIMS technique. Ion microanalysis was performed on a Cameca Instruments Model IMS 3F ion microanalyser (Linton et al 1980), using O_2^+ or Cs^- as primary ion sources. Control and lead-treated RAMs were imaged between 5 and 15 minutes of sputtering time (total sputtering time was 125 cycles X 20 sec/cycle or 42 min.). Sputtering rate was established to be 5-10 Å /sec through the cell monolayer. Relative concentrations of K, Ca, Mg, Cl, P, and Pb were compared for control vs. treated cells since quantitative measurement of absolute concentrations of elements in a given soft tissue sample is difficult by this technique. The $^{27}Al_2^+$ signal from the background substrate served as a normalizing factor to correct for differences in cell coverage of the surface areas analysed. In order to characterize the ion concentrations at various levels within the cells, three-dimensional portraits of relative ion concentrations were derived as a function of sputtering time.

Results

By light microscopy, RAMs treated with Pb_3O_4 for 4, 24, or 48 hours demonstrated a considerable pathologic reaction to the chemical. It was sometimes difficult to tell by LM whether the cells had phagocytosed particles or merely retained them adherent to the cell surface. Moreover, since ingested particles often produced lysis of the cell, thereby releasing solubilized lead ion into the medium, it was difficult to correlate cytotoxicity with phagocytosis of Pb_3O_4 particles by light microscopy. The general features of sublethal and lethal toxicity that were often present in the cells, however, were cytoplasmic vacuolization, clumping of chromatin, swelling of the endoplasmic reticulum and nuclear envelope; karyorrhexis, karyolysis, and pyknosis of the nuclei.

Viability for RAMs exposed to Pb_3O_4 for 4 hours was 74%; for 24 hours, 67%; and for 48 hours, 0.1%. Viability for control RAMs at 4 hours was 97%; for 24 hours, 90%; and for 48 hours, 85%. For cells that had been prevented from ingesting particles in the medium by a membrane filter, viability at 4 hours was 92% and at 24 hours, 86% (See Table 4).

Atomic absorption data for the various exposure regimens revealed lead concentrations in the medium as shown in Table 4. Note that no solubility of the Pb_3O_4 was detected in the experiments in which phagocytosis was blocked.

Examination of treated cells by transmission electron microscopy revealed widespread lytic damage to most of the RAMs that had ingested particles at all exposure times including the shortest time (4 hours) (Figures 14,15,16). Massive disorganization of the cytoplasm was the rule, and pyknosis and karyorrhexis were prominent features. The few relatively normal appearing viable cells containing intracellular Pb_3O_4 particles were considered to have ingested the particles quite recently. Spicules of electron-dense crystalline material were found within the cytoplasm and sometimes within the nucleus of both necrotic and apparently viable cells (Figures 15,16). In some cells, these densities were found within single-membrane limited organelles, possibly lysosomes, which were not, however, associated with the phagocytosed Pb_3O_4 particles. Other densities were free within the cytosol or associated with the heterochromatin of the nucleus. These nuclear densities did not resemble the protein-containing lead induced nuclear inclusions seen in the proximal renal tubule cells of animals treated with soluble lead salts.

The mitochondria of treated cells were usually swollen, and flocculent densities were commonly present within them. The endoplasmic reticulum generally was swollen too, but occasionally it formed whorls around areas of cytoplasm.

By SEM, after 24 and 48 hours of exposure to Pb_3O_4, treated cells were only sparsely attached to the Thermanox cover slips as compared to the control cells at the same exposure time. Also, they were more "rounded up" than control cells. Backscatter and TRIX imaging revealed the subsurface location of large phagocytosed particles in lead-treated cells. The lead oxide content of the ingested particles was confirmed by EDX microprobe, and maps for the diffuse intracellular redistribution of lead were obtained for treated cells (Figure 18c). As can be seen from the dot map, Pb localized most densely to the large ingested particles, but also seemed present in a more diffuse and widespread pattern. In Epon embedded, unstained, thin sections spot probed by EDX, the crystalline cytoplasmic and intranuclear densities observed previously with TEM were determined to consist of compounds of Pb, P, and Ca (Figure 21b). These results are similar to results obtained for RAMs exposed to the monoxide of lead.

The results of SIMS analysis of control RAMs and RAMs exposed to Pb_3O_4 have been published (Linton, Walker, deVries, and Shelburne, 1980) and will be summarized only briefly here. Control and treated cells were bombarded with ions of either O_2^+ (to enhance detection of positive secondary ions, such as Pb, Al, and other elements with low ionization potentials) or Cs^- (to enhance detection of elements with high electron affinities such as C, or H). Since the O_2^+ primary ion bombardment provided very sensitive conditions for the majority of ions of interest in this experiment, only the O_2^+ bombardment experiments will be considered here.

Secondary ion mass spectrometry as performed on a Cameca IMS-3F microanalyzer is somewhat analogous to the scanning electron microscope although a focused primary ion beam is rastered over the cell surface. This beam bombardment effects the release of secondary ions which are detected by a mass spectrometer programmed to differentiate between the ions of interest and other compounds or isotopes of comparable atomic mass. A two dimensional distribution of the ion is detected, multiplied, and imaged on a fluorescent screen. In this way, images for control and lead-treated cells were obtained (Figures 19, 20). By visual comparison, it will be noted that in a given cell (arrows) images for many different ions, e.g. Na, K, Mg, Ca, P, and Pb may be compared. However, because the ion spectrometer is more sensitive for some ions than for others, longer exposure times were required for certain elements in order to produce satisfactory photographs. Therefore, the relative intensity of the image only roughly correlated with the absolute concentration of the ion within the cell.

In control cells, all elements probed (Na, K, Mg, Ca, and P) were detected except Pb (Figure 19). Phosphorus maps were only weakly positive. In the Pb_3O_4 treated cells, note the bright spot for lead (Figure 9G) which is seen in a cell which is also strongly positive for P and Ca (Figure 20, F, E).

Even with SIMS, absolute concentrations of elements in cells are not reliably measurable at the present time. Therefore, relative concentrations of elements in treated and control cells were compared in order to establish the flux of labile ions in cells injured by exposure to particulate lead (Table 5). The values were expressed as a ratio between treated RAMs and control RAMs and were normalized for cell surface area by the Al (background substrate) signal. The most interesting finding was that Pb, P, and Ca were significantly increased within treated cells -- a finding which corresponds to EDX data. In addition, an elevated chlorine level within the cells reflects a typical response to injury (Trump et al 1979).

When ion concentrations were analysed as a function of depth within the cell (measured by sputtering time) it was found that at deeper levels lead treated cells retained greater quantities of ions than did control cells. The difference was thought to be a consequence of the morphological rounding up of injured RAMs. Control cells, because they retain a normal more flat morphology, are entirely etched to the substrate at a sputtering time (depth) when treated cells still project above the aluminum surface.

Discussion

Red lead is frequently used as a paint additive to retard rust formation on the underlying metal. Sandblasters removing this paint from bridges, or others involved in occupational exposure to its dust of aerosols may inhale particles of respirable size (2-5 um) which are phagocytosed by alveolar macrophages.

The tetroxide compound of lead, Pb_3O_4 is insoluble in cell culture medium as determined by atomic absorption analysis. This is in contrast to PbO which is soluble in medium. Pb_3O_4 is soluble in dilute acetic acid at a pH comparable to the lysosomal pH within a macrophage (Jacques & Bainton, 1978). Therefore, it was thought that Pb_3O_4 particles might be a sensitive model for investigating the effect of pH on cells exposed to cytotoxic particles. In an *in vivo* model using rabbit alveolar macrophages, we found by several different methods that we could detect intracellular redistribution of lead throughout the cell from the surface of an ingested particle.

By light and transmission electron microscopy, it was apparent that only cells which had ingested Pb_3O_4 particles developed ultrastructural evidence of cytotoxicity, e.g. crystalline densities, mitochondrial swelling, and endoplasmic reticulum disorganization. Cells prevented from phagocytosing particles by a membrane filter and control cells retained a normal fine structure consistent with many observations of normal RAMs. On the other hand, in lead treated cells, crystalline densities corresponding to Pb, P, and Ca were found throughout the cell -- both in the nucleus and in the cytosol within and outside of membrane limited organelles. Similar patterns of densities have been described previously in RAMs exposed to lead monoxide and in other cells exposed to soluble lead in vivo and in vitro (Brun and Brunk, 1971; Carroll et al, 1970).

By atomic absorption analysis, it was found that in experiments where cells had ingested Pb_3O_4 for 24 or 48 hours, a significant amount of Pb was released into the medium, whereas lead levels for supernatants of control cells, cells prevented from phagocytosing Pb_3O_4 by a membrane filter and Pb treated cells at 4 hours and 24 hours were comparable, and remained below 1 ppm. Comparing 24 and 48 hour experiments, we found that the lead released from the treated cells into the medium increased with time.

Three different methods of in situ analysis were employed both to determine the extent of lead redistributed within the RAM and to assess the changes in intracellular ion patterns of other ions within the cell. SEM/EDX offers the advantage of visualizing whole freeze-dried cells in their near-normal morphology while subsequently identifying subsurface particles and their elemental composition. In the SEM/EDX the x-y resolution is good (.1 um); however, the z axis resolution is poor (1 um), and elemental analysis is limited by a low sensitivity for elements of low atomic number. Using thin sections visualized by STEM/EDX, the same limitations of detection and x-y resolution hold true, but intracellular contents are better visualized because a cell section rather than a whole cell is analysed, and an electron beam can more accurately be centered on a small region of interest within a cell, for example, a single organelle. The z resolution is optimized by the thinness of the sample itself.

In SIMS analysis, the reverse of sensitivity and resolution limits for the EDX exists. That is, the x-y resolution is poor (1.0 um), whereas the z axis resolution is excellent (50 A), and the sensitivity for elements of low atomic number is also excellent. By combining the results of all three methods of in situ analysis, we have determined that lead solubilized from the surface of ingested Pb_3O_4 particles, diffused from the phagolysosomes of RAMs -- probably by increasing the lysosomal membrane permeability -- and gained access to the cytosol and nucleus where it reprecipitated as compounds of Pb, P, and Ca. Concurrent with these cytotoxic events, other ion migrations also took place, e.g. a Cl– influx. The combined approach to analysis of freeze-dried material both defined and localized several ionic changes within the cell.

Conclusion

RAMs were exposed to particles of Pb_3O_4, a lead oxide compound known to be soluble at a weakly acidic pH but insoluble in culture medium. By running parallel experiments in which RAMs were incubated with but prevented from phagocytosing these particles, we found that phagocytosis of the particles was necessary to produce toxicity. In cells which ingested particles, morphological manifestations of cell injury were apparent soon after phagocytosis, and in these cells, a common finding was the formation of Pb, P, and Ca precipitates within the cytosol and nuclei. We believe, therefore, that the solubilization and toxicity of Pb_3O_4 particles is a function of the decreased pH within the phagolysosome of RAMs and that this solubilization is responsible for the appearance of lead-containing dense crystals at sites distant from the internalized particles.

TABLE 4

EXPOSURE CONDITIONS	VIABILITY	LEAD IN MEDIUM*
Control RAM 4 hours	97%	1ppm (.26ppm)
RAM w/ Pb_3O_4, + filter 4 hrs. (phagocytosis blocked)	92%	1ppm (< .2ppm)
RAM w/ Pb_3O_4 particles, 4 hrs.	74%	1ppm (.85ppm)
Control RAM, 24 hrs.	90%	1ppm (.40ppm)
RAM w/ Pb_3O_4, + filter 24 hrs. (phagocytosis blocked)	86%	1ppm (< .2ppm)
RAM w/ Pb_3O_4 particles, 24 hrs.	67%	4.9ppm
Control RAM, 48 hrs.	85%	1ppm (.27ppm)
RAM w/ Pb_3O_4 particles, 48 hrs.	0.1%	44.0ppm

---

* Atomic absorption data obtained by averaging 2-4 experiments, with 6 AA determinations per experiment. ± 5%.

TABLE 5

Comparison of Relative Elemental Concentrations in Pb_3O_4 Treated vs. Control RAMs by SIMS

Element	1 min. Sputtering	20 min. Sputtering
$K \frac{\text{treated}}{\text{control}}$	0.84	1.4
$Ca \frac{\text{treated}}{\text{control}}$	0.84	2.5
$Mg \frac{\text{treated}}{\text{control}}$	1.5	0.53
$Cl \frac{\text{treated}}{\text{control}}$	0.67	2.9
$P \frac{\text{treated}}{\text{control}}$	1.0	3.1
$Pb \frac{\text{treated}}{\text{control}}$	120	260

FIGURE 12

Transmission electron micrograph of control RAMs. The nuclei are eccentric, and the cytosol is replete with lysosomes and rough endoplasmic reticulum. Mitochondria are also evident in smaller number (cell at top left).

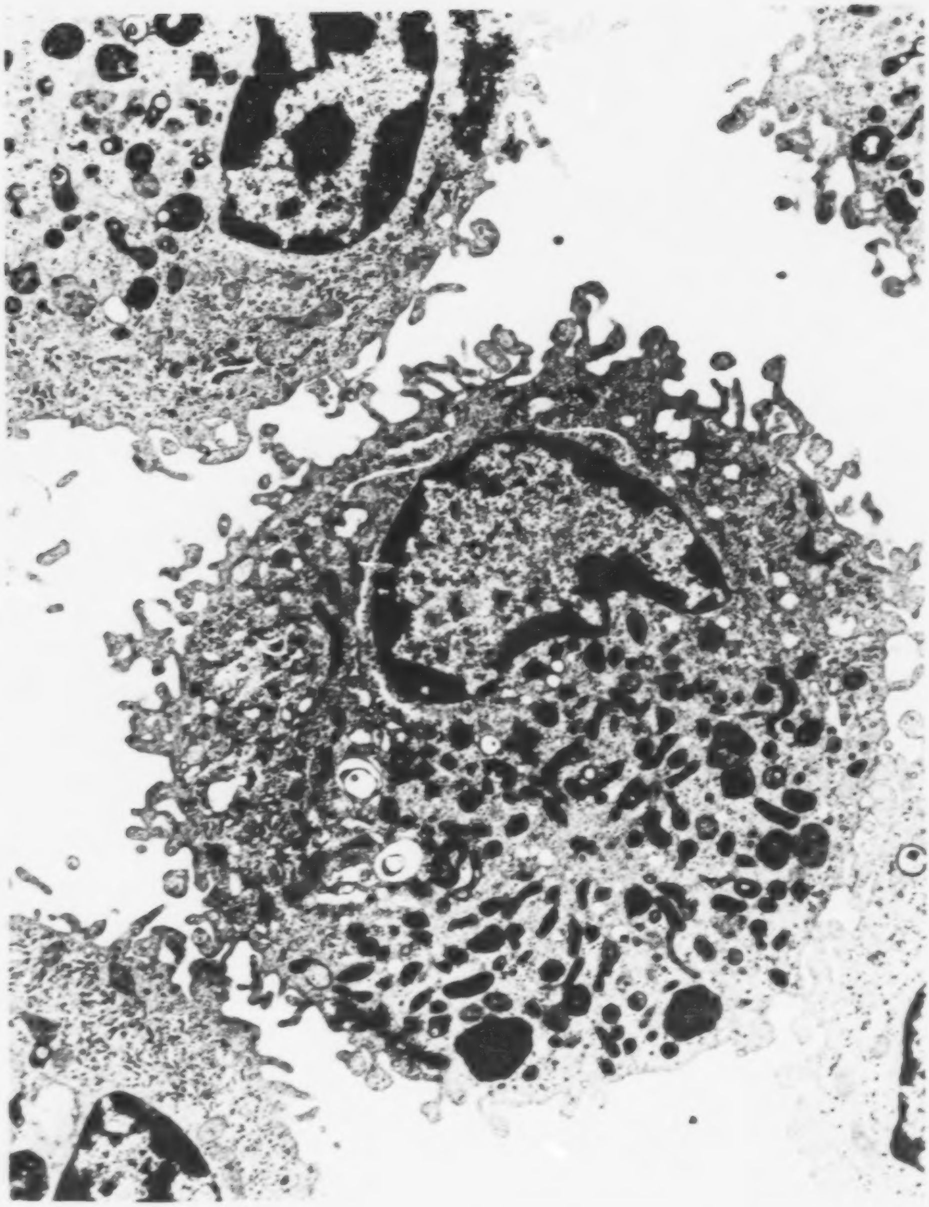

FIGURE 13

Control RAM fixed by snap-freezing only, freeze-dried and carbon coated. The cytoplasmic ruffles are intact, and the quality of freeze-fixation is excellent.

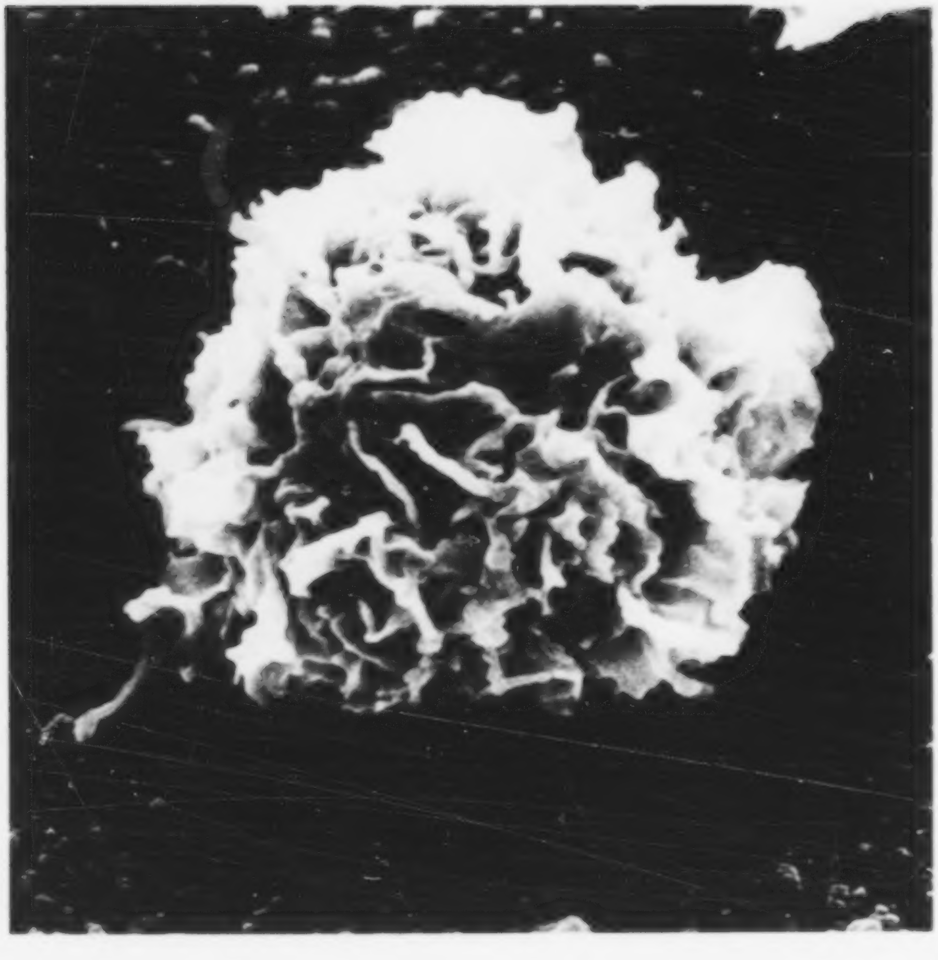

FIGURE 14

Transmission electron micrograph of a necrotic cell exposed to Pb_3O_4 with diffuse precipitates of lead/phosphorus/calcium (arrows). Much cytoplasmic detail has been lost, and the nuclear chromatin has condensed and fragmented. (X 12,750)

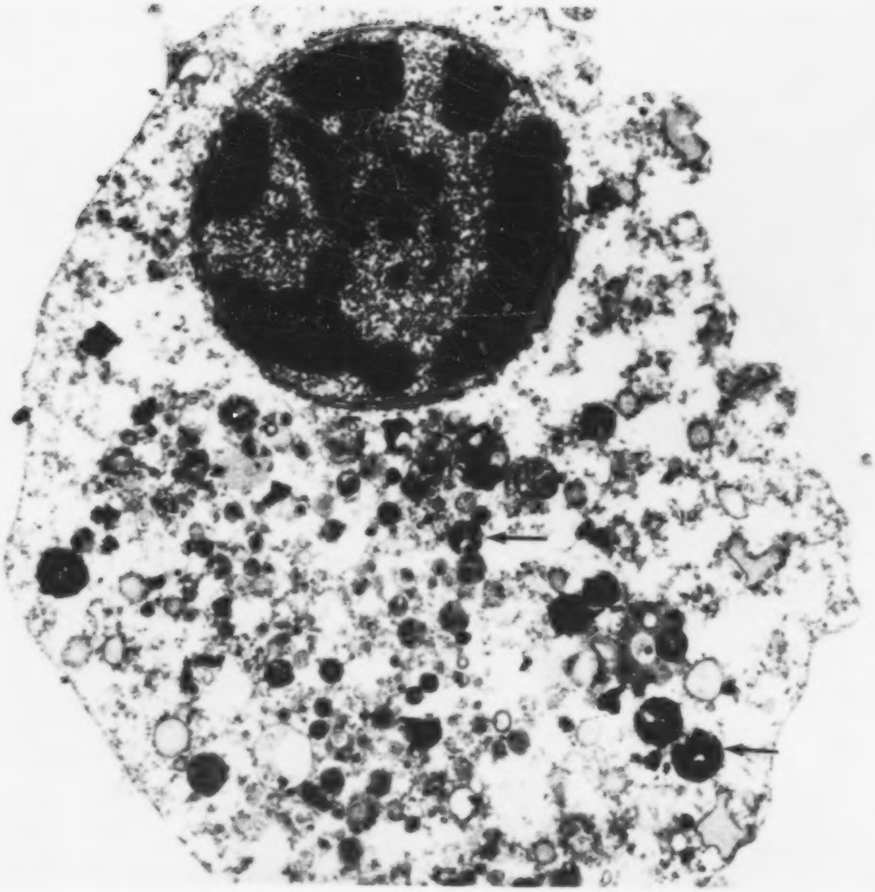

FIGURE 15

A. In a RAM which has ingested Pb_3O_4, the nuclear envelope has swollen (arrow). The cytoplasmic ruffles have retracted and the cytosol has become flocculent and cloudy. X 24,000

B. Crystals of Pb/P/Ca center over the heterochromatin in this cell exposed to Pb_3O_4. The euchromatin has cleared and now contains coarse aggregates of karyoplasm and dense heterochromatin. X 25,000

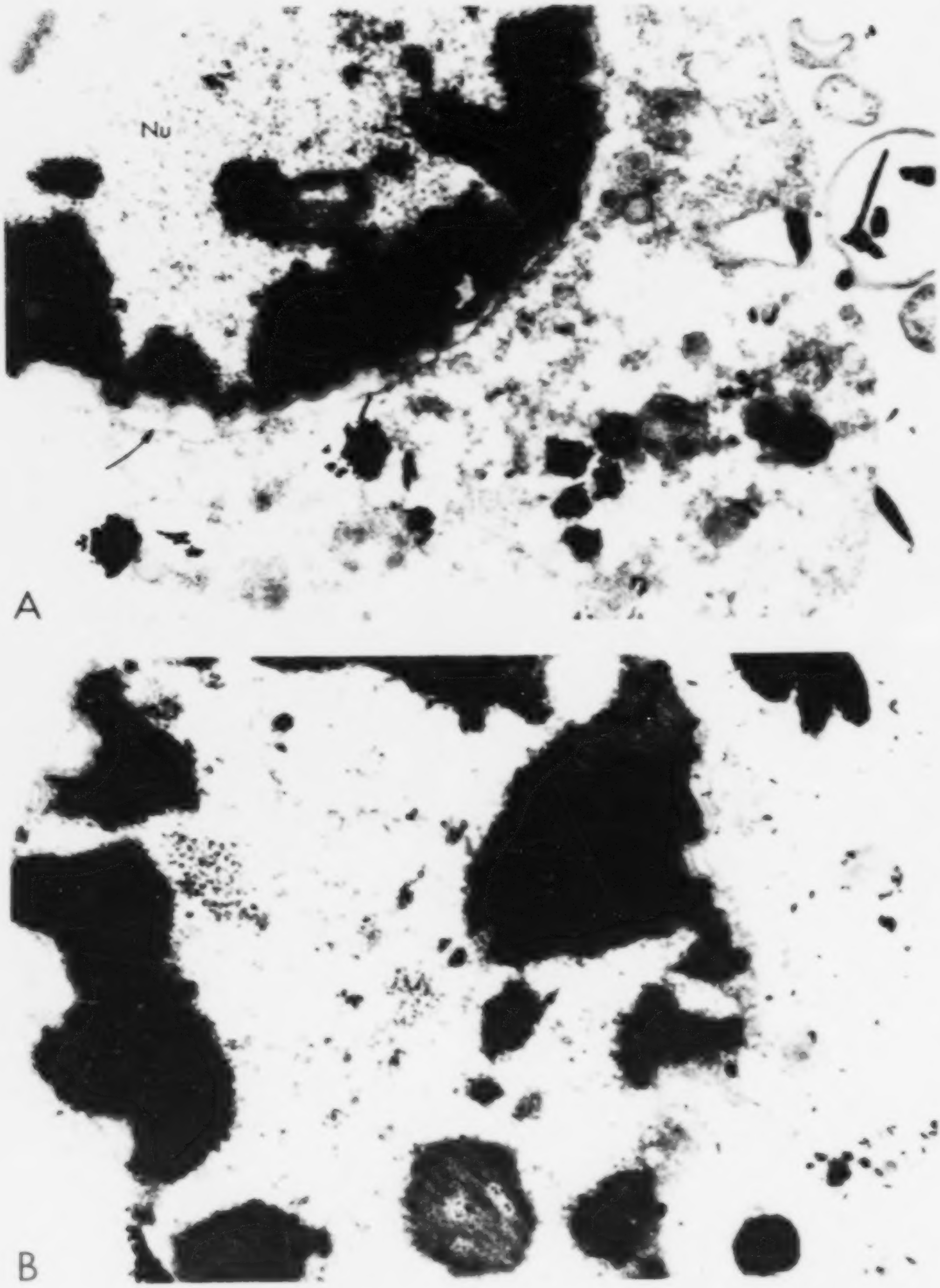
Nu
A
B

FIGURE 16

This cell has been exposed to particles of Pb_3O_4. It was only fixed with glutaraldehyde and is unstained. Besides the large dense particles of Pb_3O_4, there are circular aggregates of fine precipitates localized to denser areas within a pale cytoplasm. It is probable that these are similar to the densities produced in RAM's by ingestion of PbO particles (Plate IX in B).

A. X 11,000

B. X 60,000

C. X 70,000

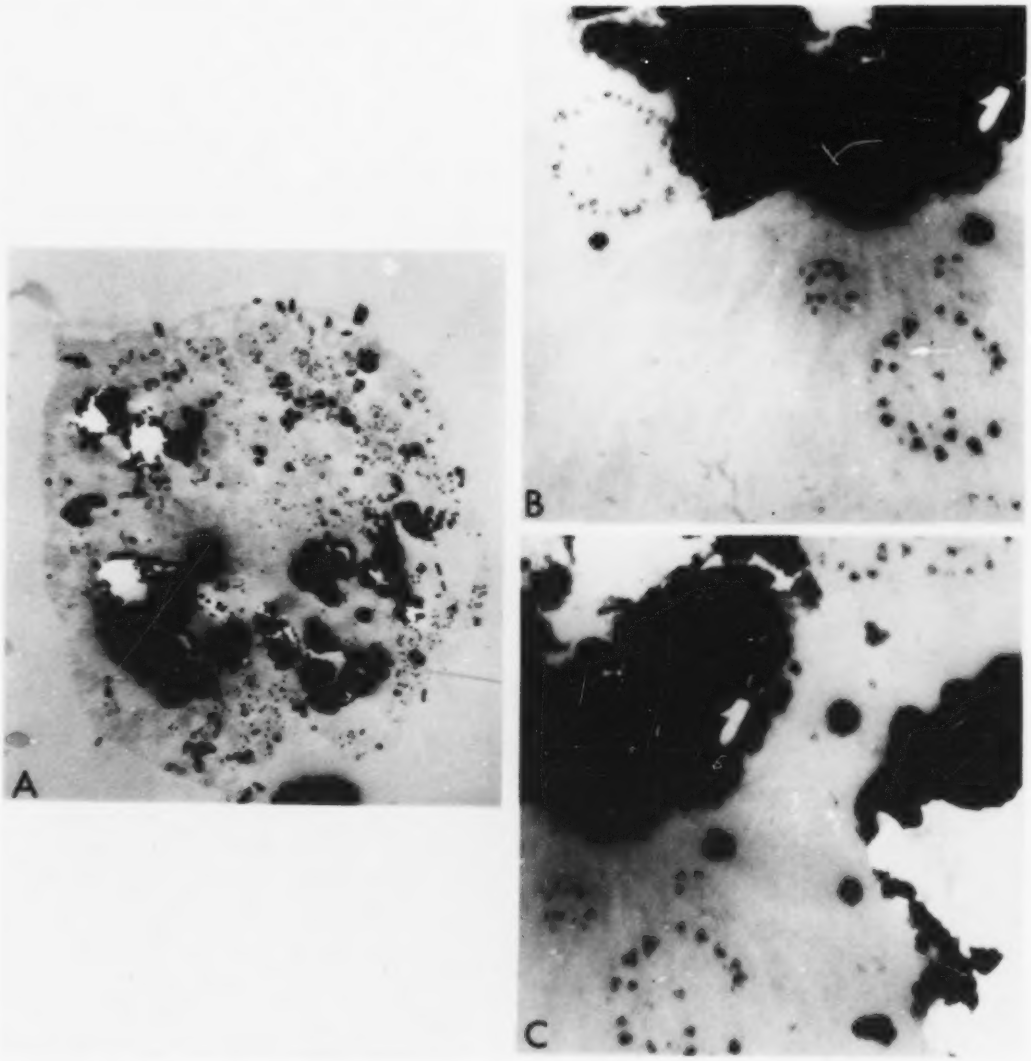
A
B
C

FIGURE 17

For comparison, recrystallization particles (A) are displayed above particles of Pb_3O_4 (B) which have been exposed to the same fixation and embedding conditions as have cells for TEM.

A. X 30,000

B. X 28,000

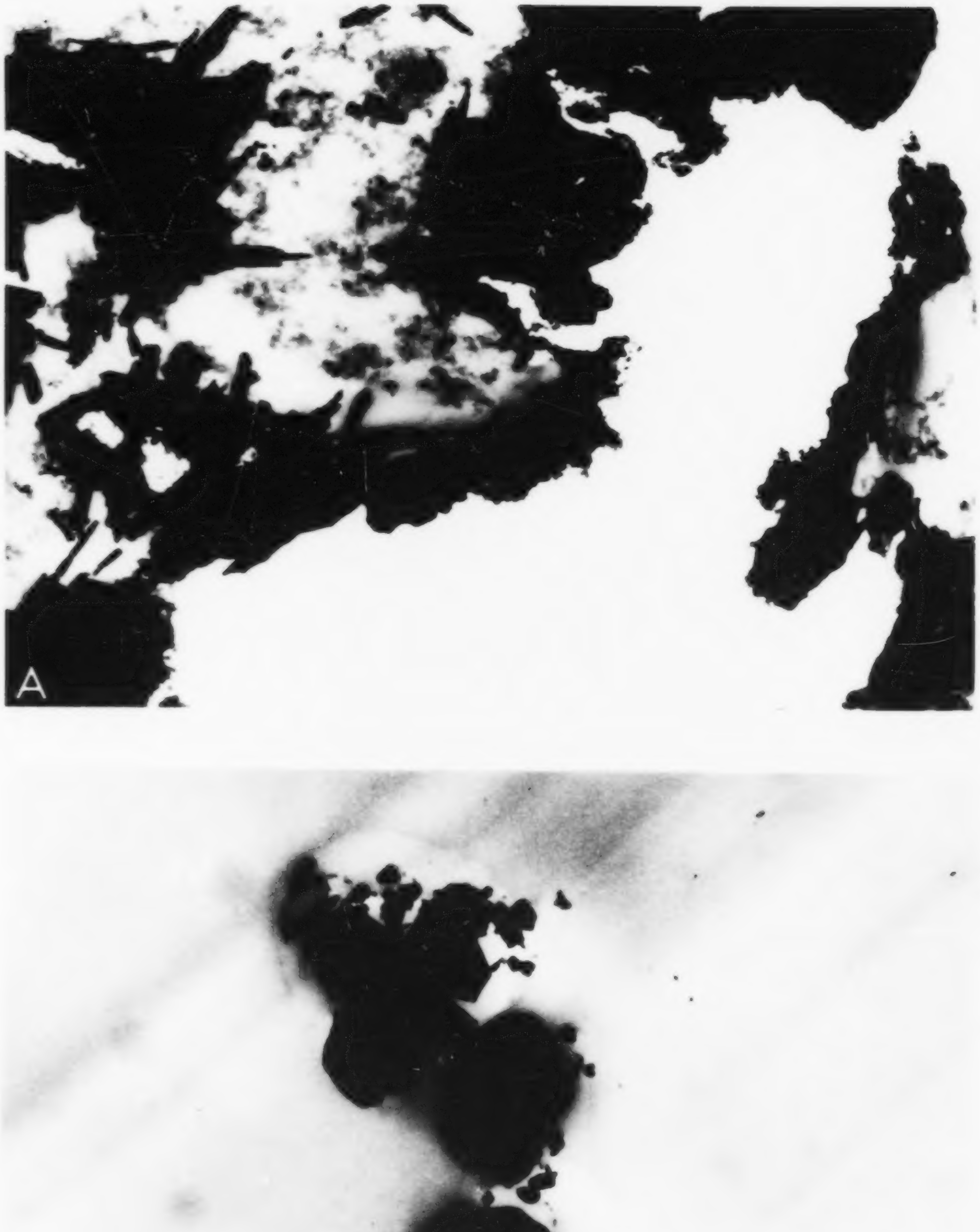
A
B

FIGURE 18a

SEM of a viable RAM (foreground) and a necrotic RAM (background). (X 7600).

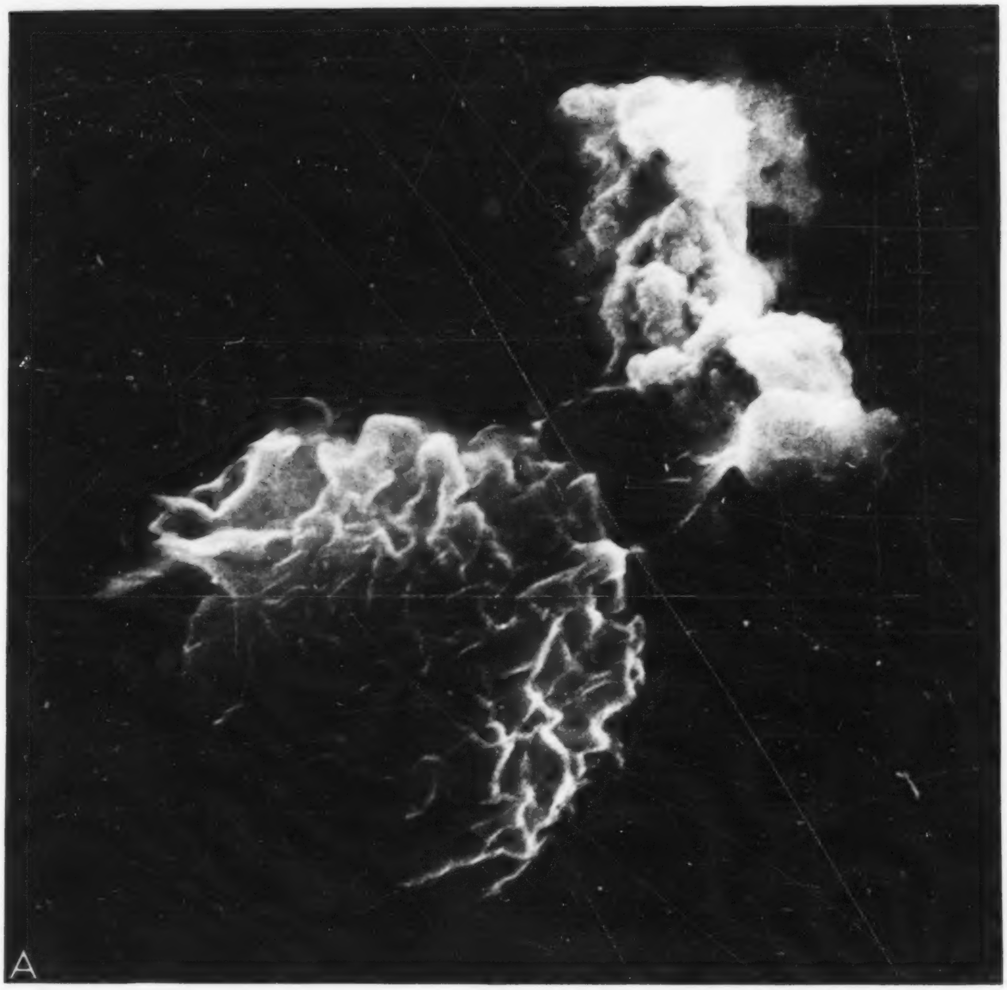
A

FIGURE 18b

SEM backscatter showing a lead particle within the cytoplasm of the viable cell and a diffuse dense area around it.

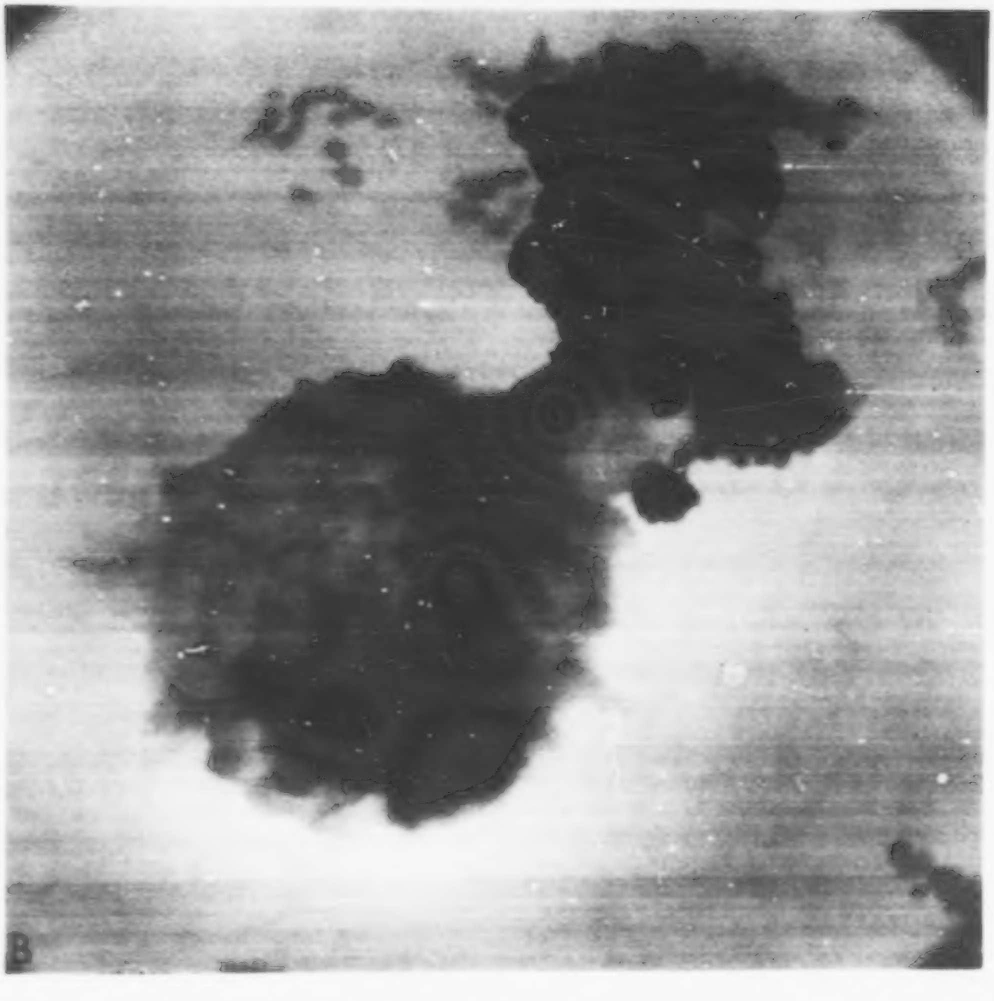
B

FIGURE 18c

X-ray map for the distribution of lead in this same field. Note the intense localization to the necrotic cell and to the ingested particle.

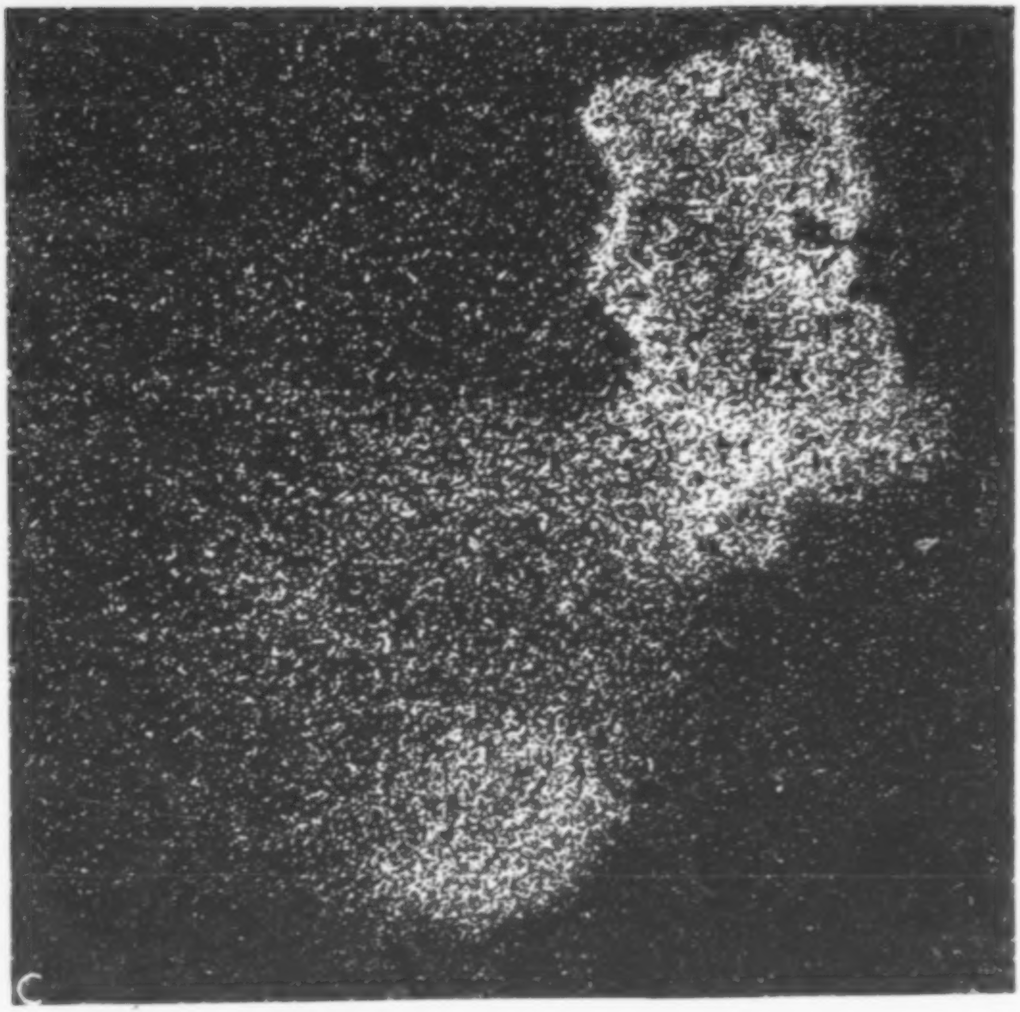
c

FIGURE 19

Ion micrographs of RAMs cell monolayers on Al foil are snap-frozen, freeze-dried and examined. Field width is 150 um. The primary ion conditions are: O_2^+ bombardment, 200 NAMP, and 12.3 KEV.

Control cells. Note the close similarity between the Na, K, and Ca maps. One cell is marked by an arrow. No lead was detected.

A. Al image ($^{27}Al_2^+$), exposure time = 1/15 sec.
B. Na image ($^{23}Na^+$), exposure time = 1/60 sec.
C. K image ($^{39}K^+$), exposure time = 1/16 sec.
D. Mg image ($^{24}Mg^+$), exposure time = 2 sec.
E. Ca image ($^{40}Ca^+$), exposure time = 1/8 sec.
F. P image ($^{31}P^+$), exposure time = 30 sec.
G. Pb image ($^{208}Pb^+$), exposure time = 30 sec.

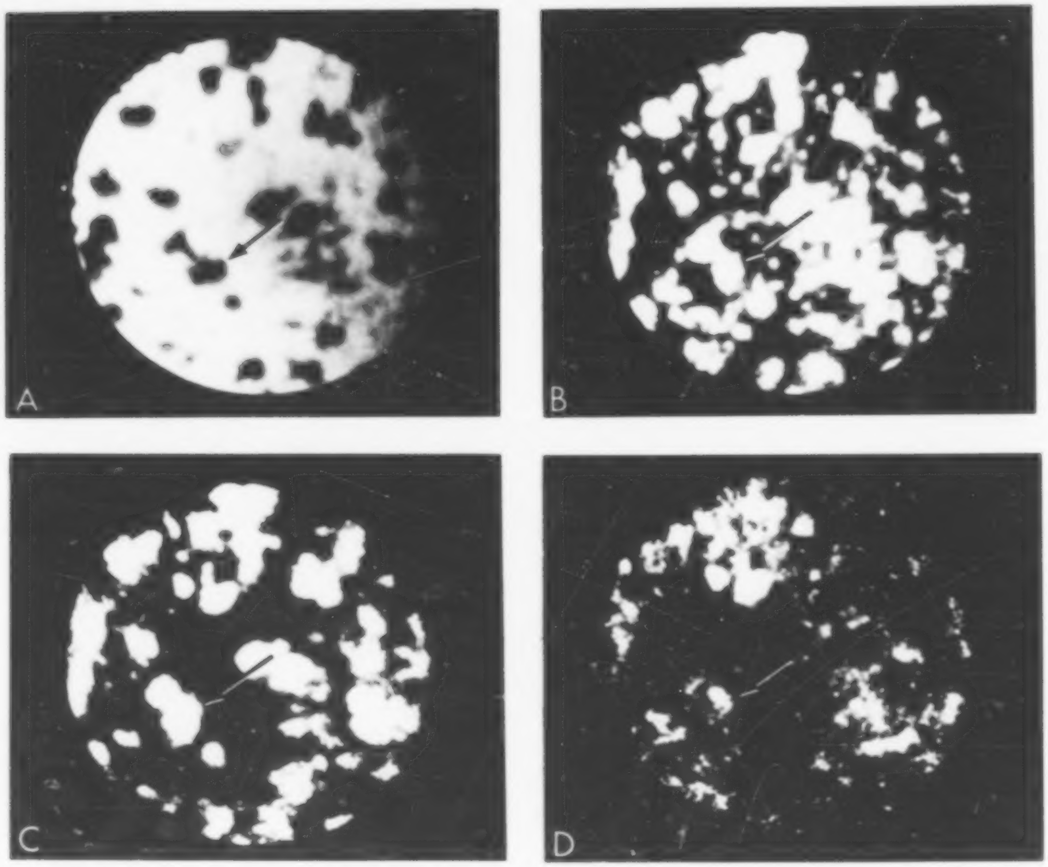
A
B
C
D

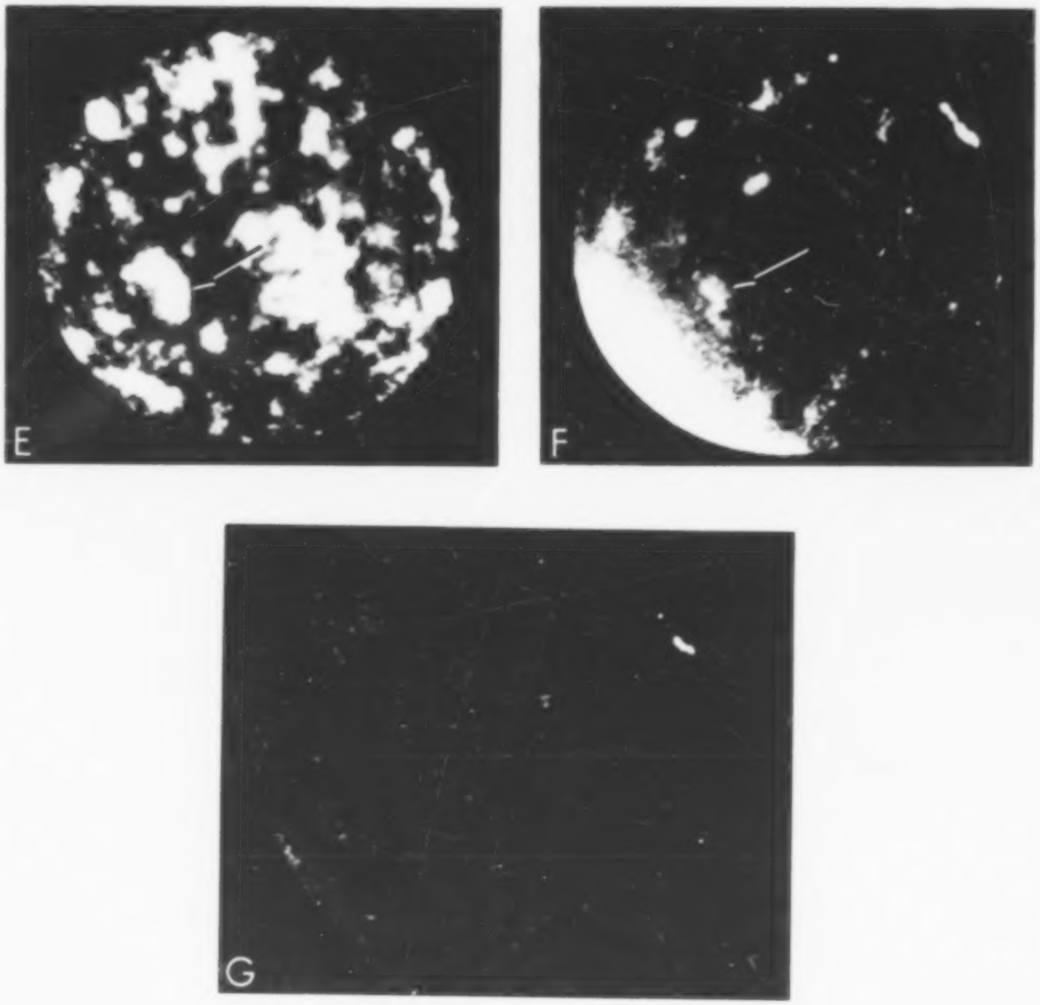
E
F
G

FIGURE 20

RAMs exposed to Pb_3O_4 particles for four hours. Width ~150 um. Cells monolayers were prepared as above for control cells. The cell shown at the arrow is necrotic. It has lost the normal intracellular levels of Na and K and has developed intracellular Pb/P/Ca precipitates. The cells map for Pb, P, Ca, and (weakly) Mg.

A. Al image ($^{27}Al_2^+$), exposure time = 1/125 sec.
B. Na image ($^{23}Na^+$), exposure time = 1/16 sec.
C. K image ($^{39}K^+$), exposure time = 1/16 sec.
D. Mg image ($^{24}Mb^+$), exposure time = 2 sec.
E. Ca image ($^{40}Ca^+$), exposure time = 1/8 sec.
F. P image ($^{31}P^+$), exposure time = 30 sec.
G. Pb image ($^{208}Pb^+$), exposure time = 30 sec.

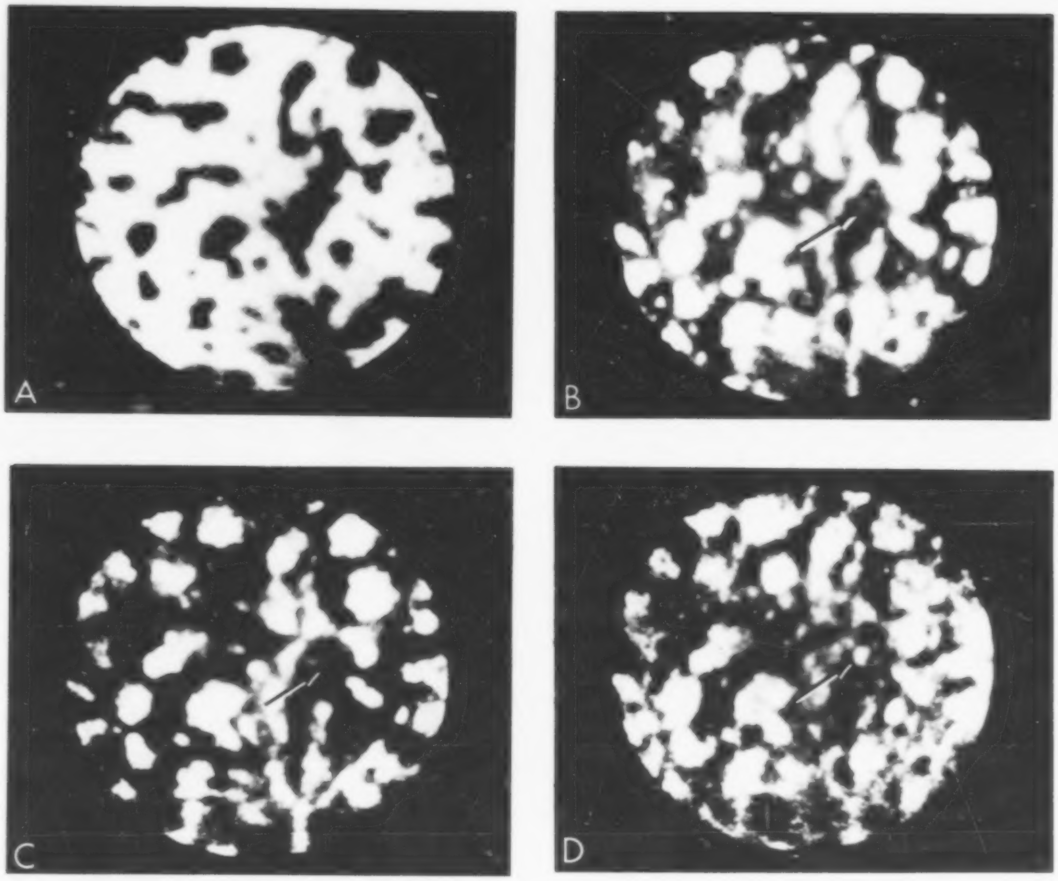
A
B
C
D

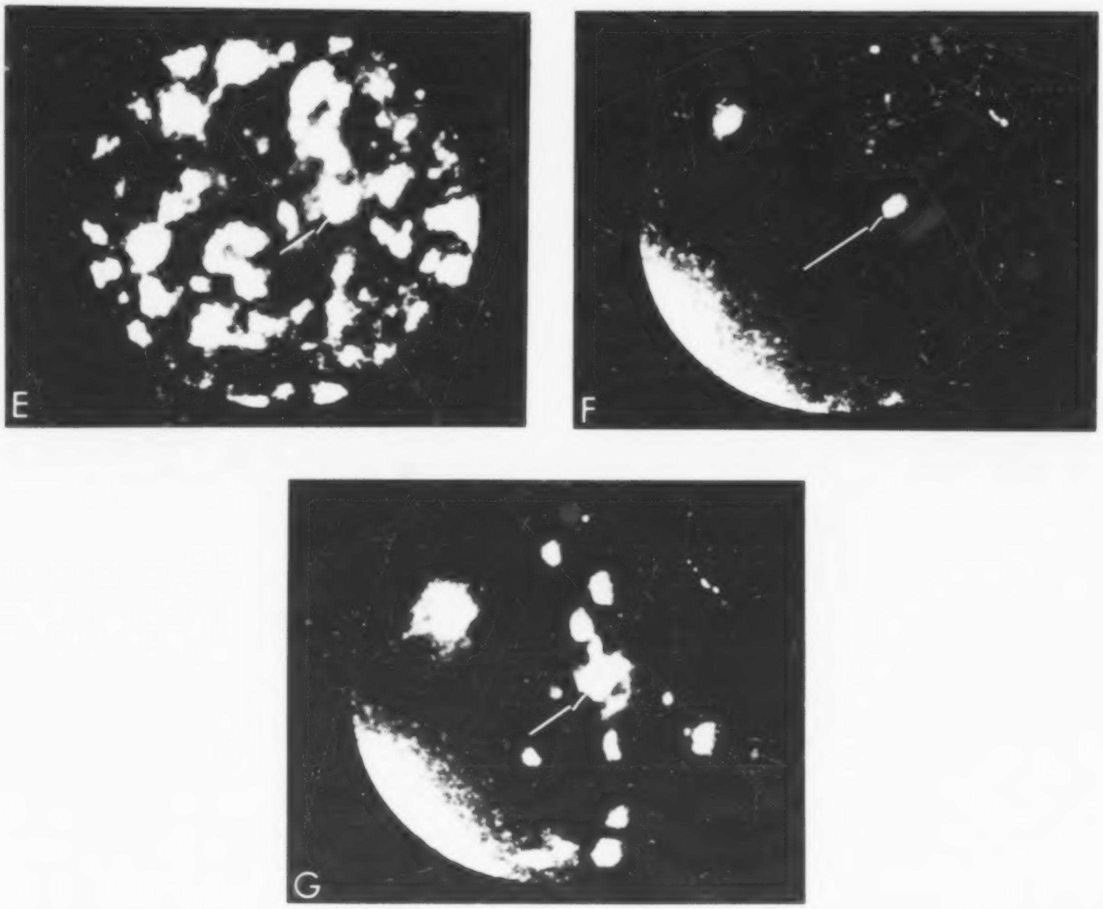
E
F
G

FIGURE 21

X-ray microprobe anlysis of RAMs exposed to Pb_3O_4

These cells were fixed with glutaraldehyde/osmium embedded in Epon and mounted on copper grids. They were not stained. In each spectrum, 2000 counts were accumulated in the 4.5-4.96 KEV window.

a. Empty Epon background peaks. The Cu is from the grid, the Cl from the Epon, and the Si and Al peaks are from the instrument.

b. Cytosol devoid of particles. Osmium is present and lead may be present. Other peaks are similar to those in empty epon.

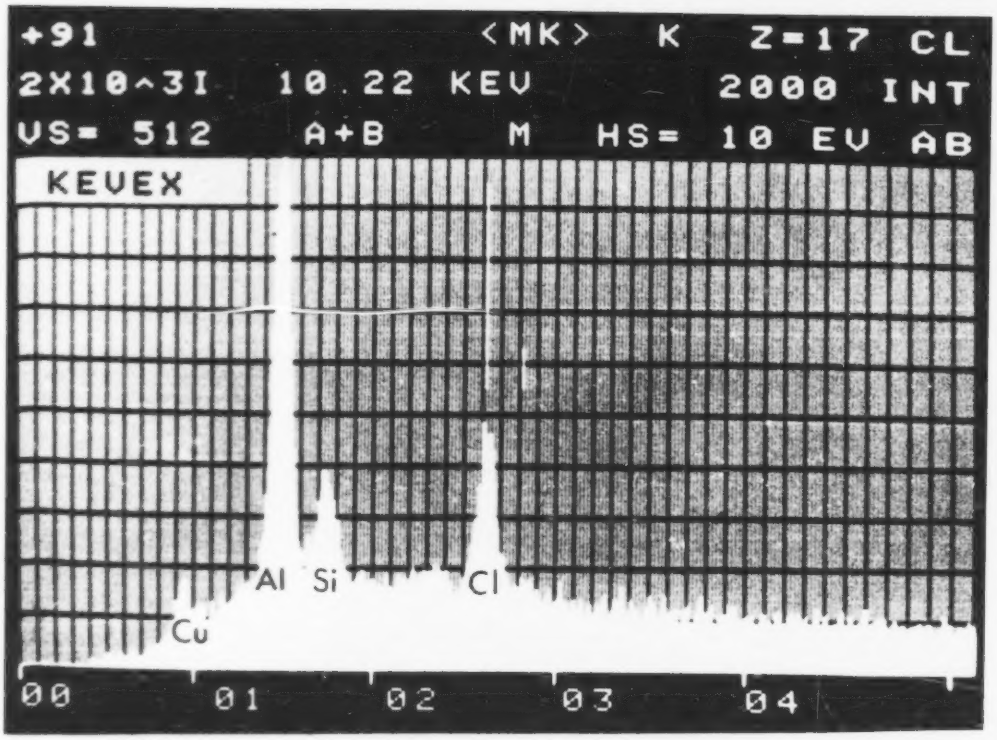
+91 <MK> K Z=17 CL
2X10^3I 10.22 KEV 2000 INT
VS= 512 A+B M HS= 10 EV AB
KEVEX
Al
Si
Cl
Cu
00
01
02
03
04

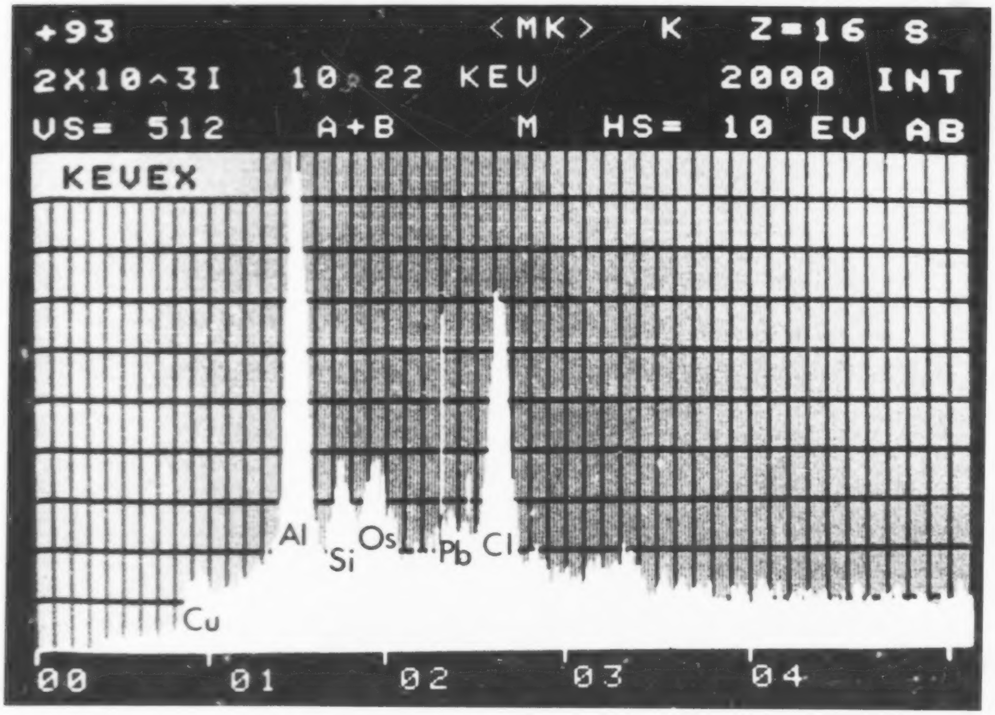
+93 <MK> K Z=16 S
2X10^3I 10.22 KEV 2000 INT
VS= 512 A+B M HS= 10 EV AB
KEVEX
Al
Si
Os
Pb
Cl
Cu
00
01
02
03
04

c. Pb_3O_4 particle exhibits a large Pb peak. Note that there is no peak for phosphorus when the particle is probed. (L,M lines for Pb were also detected as described above).

d. Crystalline cytoplasmic density similar to those illustrated in Figures 16-17. Many of these densities are membrane bound. There are now peaks for Pb, P, and Ca present.

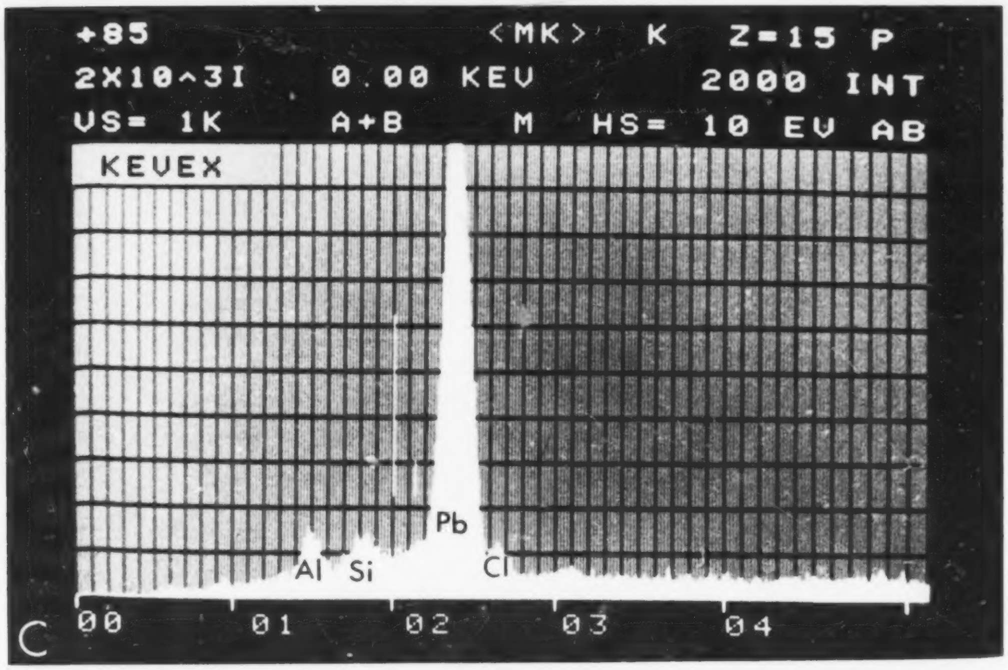
+85
<MK> K Z=15 P
2X10^3I 0.00 KEV 2000 INT
VS= 1K A+B M HS= 10 EV AB
KEVEX
Pb
Al
Si
Cl
00
01
02
03
04
C

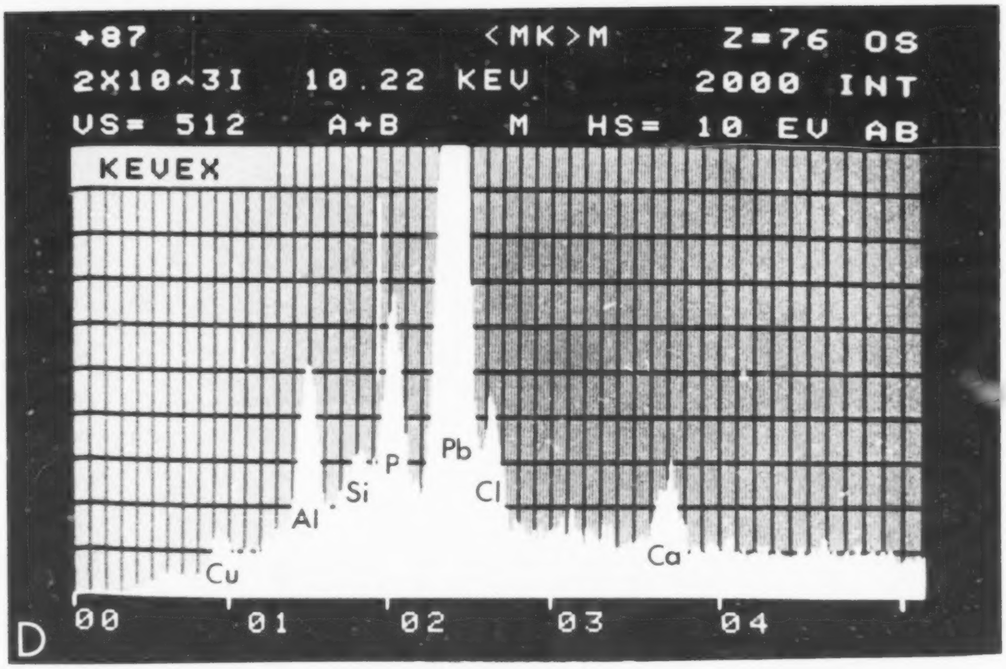
+87
<MK>M Z=76 OS
2X10^3I 10.22 KEV 2000 INT
VS= 512 A+B M HS= 10 EV AB
KEVEX
Pb
P
Si
Cl
Al
Cu
Ca
00
01
02
03
04
D

STUDIES ON NiO TOXICITY

Introduction

Although it is well known that exposure to nickel in either its carbonyl, particulate, or ionic form is toxic and carcinogenic to lung parenchyma regardless of its route of entry (Sunderman, 1977), few reports have appeared in the literature concerning the effects of Ni(II) on the alveolar macrophage. The macrophage is frequently the first cell type to interact intimately with particulate forms, e.g. NiO that might be breathed in occupational settings such as in grinding or catalytic hydrogenation facilities. Bingham et al (1972) have performed light microscopic surveys of the effects of soluble and particulate nickel exposure on the numbers and shapes of alveolar macrophages in laboratory animals in vivo. Yet we are not aware of any published reports on the ultrastructural pathology of macrophages subjected to Ni(II) exposure as determined by electron microscopy.

Therefore, we have designed an in vitro system to culture rabbit alveolar macrophages (RAMs) with and without direct exposure to NiO and NiO coated fly ash, and we have confirmed our findings by exposing RAMs to soluble $NiCl_2$ salts.

Materials and Methods

Rabbit alveolar macrophages were harvested according to Myrvik (1961) and were allowed to attach as monolayers in medium 199 with 10% heat-inactivated fetal calf serum and antibiotics for two hours at 37°. Then the medium was changed, and the RAMs which had attached to the substrate incubated in fresh medium with serum and antibiotics to which were added $NiCl_2$ or particles of NiO coated fly ash.

In the particle experiments, doses of NiO were 10, 30, and 100 ug/ml and the dose of NiO coated fly ash was 1000 ug/ml. RAMs with particles were cultured for 24 hours at 37° in plastic petri dishes or culture flasks. Monolayers were fixed in 3% glutaraldehyde in Na-cacodylate buffer. Pellets were obtained by trypsinizing the cells attached to culture flasks, and spinning them at 10,000 rpm for 10 min. The pellets were then fixed in 3% Na cacodylate buffered glutaraldehyde.

Cells which had been cultured in medium with serum, antibiotics and 0.1, 1.0 and 5.0 mM $NiCl_2$ were harvested as monolayers after 4 hours at 37° and were fixed as described above.

Control RAMs were incubated, harvested, and fixed under identical conditions as for RAMs exposed to soluble Ni or particles, but without exposure to nickel. Some RAMs were incubated in chambers separated from NiO or NiO coated fly ash particles by 0.22 membrane filters, to assess the possible effects of solubilization of the particles. Atomic absorption analysis was performed on the decanted supernatants from the dishes in which the monolayers were cultured (See Chapter IV, V for method).

After glutaraldehyde fixation, pellets and monolayers were post-fixed in OsO_4 or left unosmicated. They were then dehydrated in a graded series of ethanol. Monolayers were stained en bloc with uranyl acetate or were left unstained. Both monolayers and pellets were embedded in Epon 812 and were cut at 0.5 um and stained with toluidine blue for light microscopy. Thin sections were cut at 80-100 nm and were mounted on formvar and carbon-coated grids for transmission electron microscopy. These grids were either left unstained or were stained with uranyl acetate and lead citrate.

Thin sections were examined and photographed on a JEOL 100B electron microscope at 80 KV. Unosmicated, unstained thin sections of NiO and NiO coated fly ash-treated RAMs were visualized by STEM on an ETEC scanning electron microscope, and energy dispersive x-ray microanalysis was performed with a Kevex 5100 analyser with a 30mm Si (Li) detector. STEM images were compared prior to and after microprobe analysis to confirm the location of the probe by beam damage.

Results

By atomic absorption analysis, it was found that nickel did solubilize from the surface of NiO-coated fly ash particles separated from cells by a membrane filter. In cells which had ingested particles of NiO coated fly ash, solubilization of nickel also occurred, and was detectable in the supernatant of the cultured cells (Table 6).

By light and transmission electron microscopy, RAMs exposed to either soluble nickel salt or particles developed similar pathological changes, although the extent of these changes may have depended on the amount of free nickel ion within the cytosol.

By light microscopy, most RAMs exposed to nickel appeared highly vacuolated, and in cells exposed to NiO or NiO coated fly ash, particles could be seen localized to the macrophage. The nuclei often showed signs of cell injury such as prominent margination of the chromatin, karyorrhexis and pyknosis (Figure 22).

With electron microscopy, a greater appreciation could be developed for the diversity of nuclear changes induced by nickel. In many cells cultured with nickel chloride and in some cells exposed to particulate Ni compounds, the nuclei appeared to be relatively normal at low magnification (Figure 29,40,41) compared to control cells (Figure 23). It was not uncommon to find pyknotic nuclei or karyolytic nuclei, however. Separation of the inner and outer membrane of the nucleus was often apparent (Figure 42,46). Nuclear bodies also known as nucleioles of the homogeneous type were seen (Figure 40) as were fibrillar, granular, and complex types (Figure 41, 31a). The nucleoli often appeared intact with characteristic shapes and sizes that are typical for control cells (Figure 40,41). Or they were sometimes enlarged or segregated into dense and less dense areas (Figure 24). Both in control and treated cells, the nucleoli were usually restricted to one or two in number.

The most characteristic change in the nuclei of RAMs exposed to nickel compounds, however, was the development of multilamellar inclusions. These structures varied in appearance from membrane-like (Figure 43) to tubule-like (Figure 27,31) to paracrystalline (Figure 33,34). Some of the inclusions contained within them material resembling the euchromatin matrix of the nucleus (Figure 29, 33, 37) whereas other clearly did not (Figure 34). In many of these bodies, there was an area where the inclusions became diffuse rather than tightly lamellar (Figure 27) suggesting that the inclusions may be forming de novo in the karyoplasm and developing the characteristic osmiophilic periodicity with the time. Some of the inclusions were found in close association with the nuclear membrane, nucleolus, or with nuclear bodies, with the possible exception of the cell in Figure 40b in which lamellae are seen to form around a homogeneous dense body. For comparison, in Figure 40a is a nucleus containing a true homogeneous dense body surrounded by a fibrous halo. Occasionally, RAMs contained both lamellar inclusions and the nuclear bodies of the homogeneous, fibrillar, granular, or mixed types.

The lamellar nuclear inclusions varied in size from ~ .1 um to ~ .7 um and were not readily detectible on light microscopy. In fact, many inclusions were so camouflaged by the nuclear matrix, that even at electron microscopic magnifications, they could easily be overlooked. The most consistent periodicity was about 240 A with a range of from 140 A to 380 A. In some cells exposed to soluble nickel salts, another type of nuclear pathology was seen. Fine fibrous bundles were found in close association with the nuclear envelope (Figure 25,26,28) although some bundles were found in the interior of the nucleus. A nuclear lamellar inclusions can be seen near a bundle of filaments in Figure 28a.

The nuclei of control cells were never found to contain filamentous bundles or lamellar inclusions although nuclear bodies were occasionally observed. The nucleolar material in control cells did not segregate, and there was no intermembrane swelling in the nuclear envelope.

Cytoplasmic changes in cells exposed to nickel compounds varied with the means of exposure to nickel. In cells exposed to soluble nickel chloride, many cells retracted their ruffles (Figure 24a, 25, 30) although a few did not. In some cells dilatation of the ER was prominent (Figure 38) whereas in others it was not (Figure 24). In cells exposed to soluble nickel, whorling of the ER was not as common as it was in cells exposed to particulate NiO (Figure 43, 44). Vacuolation in the cytoplasm was frequently extensive. The mitochondria were found in condensed conformation in many cells, and occasionally, bundles of fine filaments similar to these described above for the nucleus were found in the cytoplasm. Rarely, concentric structures resembling lamellar nuclear inclusions were seen free in the cytosol -- that is, not bound by a single membrane.

In cells exposed to particulate nickel oxides, whether adherent to fly ash or alone, there appeared to be a more prominent effect on the cytoplasm than was found in cells exposed to low dose (1.0 mM or less) $NiCl_2$, possibly due to a higher concentration of solubilized nickel around the ingested particle. Evidence of cytotoxicity was found in the swollen endoplasmic reticulum and cytosegrosomes in a large number of these cells. Many mitochondria also exhibited changes such as swelling, condensation, or disintegration (Figure 46, 47) whereas others evidenced a variety of effects including matrical crystals. A curious phenomenon occurred in the cytoplasm of some cells treated with NiO. Membranes resembling mitochondrial membranes appeared to fuse with each other to produce serpentine lengths of membranes with branching and lamellar patterns (Figure 45). In these cells, mitochondria appear to be fusing with each other and have serpentine membranes.

Particles of NiO exhibited a variety of morphologies. Some particles possessed dense centers bounded by radiating dense fibrous areas and a dense peripheral boundary. The centers of these particles appeared to consist of dense fine granules (Figure 38, 44, 45, 47). Other particles of the same experiment were found to be more dense and homogeneously granular. In different experiments where several different lot numbers of NiO were incubated with RAMs, both the morphology of the particles and the cytotoxicity to RAMs varied widely. However, in all experiments where nickel exerted a cytotoxic effect, the same types of cell pathology were observed as have been described above.

Electron beam microprobe analysis demonstrated the presence of Ni within the phagocytosed particles of NiO and NiO coated fly ash in epon-embedded sections fixed in glutaraldehye and processed for TEM. However, no Ni was detected in the nucleus or the cytoplasm of the treated cells using these glutaraldehyde-fixed preparations.

Discussion

The results of atomic absorption analysis of the supernatant showed that even when separated from cells by a membrane filter, Ni was soluble in the medium from the surface of NiO coated fly ash particles. These findings agree with previously published reports that metallic Ni -- which is also insoluble in cold and hot water -- is soluble in serum enriched medium after incubation at 37° (Weinzierl and Webb 1972). The solubility of Ni is thought to be due to the ligand binding properties of small diffusible molecules in serum. However, RAMs separated from the particles by a membrane filter resembled control RAMs morphologically and ultrastructurally, and therefore it is probable that whatever solubilization of Ni did occur from NiO and NiO coated fly ash particles in the medium did not render available to the RAMs a sufficient quantity of Ni (II) to effect observable changes over the time course studied. However, in RAMs exposed to particulate NiO and soluble $NiCl_2$, evidence of cellular toxicity was observed.

Certain features of the toxic effects of nickel appear to be common to many cell types, e.g. renal tubule cells, lung parenchyma, and fibroblasts. The common ultrastructural findings are swelling of the ER and mitochondria. In lung parenchyma and alveolar macrophages, there may also be evidence of activation and proliferation of cells. Thus Hackett and Sunderman (1968) and Bingham (1972) have shown an increase in cell size attending increases in nuclear and nucleolar volume and also in enhanced development of endoplasmic reticulum and other oranelles. These findings have suggested that Ni many activate cells to proliferative -- which is further supported by the observation that particulate Ni induces blast transformation of lymphocytes in vitro (Sunderman, 1977). In the lymphocyte system the transformation effect is not merely the effect of cell surface to particle interactions, but the detailed relationship between Ni particle and lymphocytes remains to be elucidated.

The present series of experiments using the rabbit alveolar macrophage demonstrated that in RAMs it was common to find enlarged nucleoli in cells which had been exposed to either particulate NiO or soluble $NiCl_2$. In vitro proliferation of alveolar macrophages occurs only under more supportive conditions than were available here, therefore we did not observe any changes in mitotic pattern such as have been described by Hackett and Sunderman (1968) in pulmonary parenchyma following exposure to $Ni(CO)_4$.

Within the cytosol of alveolar macrophages were found not only the more common sublethal changes such as vacuolation and fatty change, but also an unusual phenomenon of formation of extensive networks of membranes. These membranes appear by TEM to be the result of disruption and fusion of mitochondrial membranes, although further work on isolated mitochondria will be required to establish this point. Jasmin (1978) has described mitochondrial intermembrane and matrix crystals induced by nickel, and in many cells we also observed matrical crystals although we were not able to classify them in Jasmin's systems.

Rarely, we observed in the cytosol lamellar and tubule-like inclusions that were not bound by a membrane. Such structures have been noted by Hackett and Sunderman (1968) in membraneous pneumocytes, but it is not yet clear whether these are the same entities that we observed. Nichols (1976) has described lamellar-tubular bodies in the cytoplasm of alveolar macrophages which were thought to consist of "tubular myelin" derived from the surfactant on the alveolar wall which had been ingested and had assumed the configuration of tight coils bounded by a single membrane. We have seen these membrane bound structures too, but since they are more closely akin to residual bodies of phagocytosis, we make the distinction between them and the inclusions that we describe that form free in the cytosol.

Cytoplasmic inclusions of a lamellar form that look superficially like the lamellar nuclear inclusions seen in some metal-poisoned macrophages are seen normally in the visual tracts of the brain. Winfield (1979) and Druger and Maxwell (1969) have reported finding whorled tubular structures in the visual cortex of the cat and monkey and Morales and Duncan (1964), Barron et al (1967), Peters and Palay (1966), Smith et al (1964) and Kalil and Warden (1978) have described the inclusions in the lateral geniculate bodies of cats. The structures are not restricted to the visual tracts, since Morales et al (1964) and Sotelo and Angaut (1973) have found them in the cerebellar cortex and nuclei, and Herman and Ralston (1970) have located them in the cat thalamus.

These authors have found that the cytoplasmic inclusions are constructed from arrays of tubules of rough endoplasmic reticulum separated by an osmiophilic fibrillar or amorphous material. The tubules are packed in concentric lamellae that curve in whorls and fingerprint patterns, with dense line-to-dense line periodicity of about 750A. In certain planes of section, these inclusions look like sheets of membranes; however, in cross section, they are obviously tubular in nature. The inclusions range in size from 0.5 um to 5 um and commonly stain with basophilic dyes. They are found both in the dendrites and soma of the cells, but not in the nucleus. Their functional significance, if any, has not been elucidated.

Again, it is unlikely that these cytoplasmic inclusions are related to those formed in the cytosol of macrophages exposed to Ni (II) because we have not been able to identify in our cells a substructure that corresponds to published photomicrographs of the fine morphology of these inclusions, and the size and periodicity differs distinctly between the two types of inclusions. The inclusions in RAMs do not appear to be associated with the endoplasmic reticulum, but bear an appearance much more similar to the inclusions formed in the nucleus of RAMs on exposure to several different heavy metals.

A word might be said about the similarity between the cytoplasmic lamellar inclusions in RAMs and those seen in the outer segments of frog rod cells (Corless and Costello, in press). These authors have reported finding concentric arrays of lamellae with a periodicity of about 60-120 A associated with lamellar disk membranes. Their inclusions have a regular tubular substructure packed in layers with a hexagonal pattern which are coiled into cylinders visualized by freeze-fracture. These inclusions have not been identified in sections by light or electron microscopy, probably due to a high lipid component which does not survive conventional fixation for TEM.

Since we have not been able to identify a hexagonal substructure in our inclusions, and the inclusions in RAMs do consistently survive aqueous fixation procedures, we believe that the two types of inclusions are not related.

The presence of cytoplamsic inclusions in RAMs is of particular interest because they strongly resemble the lamellar inclusions observed within the nuclei of RAMs treated with Ni (II) and NiO particles. Similar nuclear inclusions have also been described in RAMs exposed to soluble Cd^{++} and Cu^{++} in vitro (Bell et al, 1979, deVries, unpublished). The origin of the Ni, Cd, and Cu induced inclusions has not yet been elucidated, but approaches to investigating their development include in situ histochemical techniques such as digestion by ribonucleases, proteases, lipases, and observation of their effects by electron microscopy. Preliminary attempts at characterizing the inclusions by cytochemical stains and light microscopy in Cd^{++} treated cells have proven unsuccessful due to the small size and subtle qualities of the inclusions. Attempts at locating them within the nucleus by plane polarized light also met with failure, as have attempts at localizing Ni in the inclusions of glutaraldehyde-fixed tissue using electron microprobe analysis.

Since Ni has been shown to localize primarily in the nucleus of cells (Webb et al 1972; Webb and Weinzierl, 1972) and since Bell et al have localized Cd to lamellar nuclear inclusions in freeze-dried, freeze-sectioned RAMs, it seems very likely that in freeze-sectioned RAMs probed by electron microanalysis or by secondary ion mass spectrometry, Ni (II) would be detectable. Further experiments might include isolation and exposure of intact RAM nuclei to ionic nickel and isolation and biochemical characterization of the inclusions themselves.

Conclusion

In experiments where RAMs were exposed to Ni (II) compounds in vitro, we found evidence of both nonspecific effect of cytotoxicity to RAMs and specific effects, i.e., intranuclear lamellar inclusion bodies. The nuclear inclusions formed most readily when the Ni concentration in the medium was moderately higher (greater than or equal to 1.0 nm) or when local concentration within the cytosol was high due to phagocytosis of a particle. Similar inclusions have been reported previously in RAMs exposed to the carcinogenic metal, Cd. The significance of the finding of intranuclear inclusions remains to be determined. We conclude that one effect of Ni on the nucleus is to induce a precipitation of nuclear components in an ordered lamellar array that is possibly due to a specific ligand binding property of the metal causing aberrant lamellar assembly of proteins, phospholipids or tubules.

TABLE 6

Experiment	Exposure Time	Conc. Ni. (AA Data) ± 5%	Results by TEM
Control	4 and 24 hours	< .2 ppm***	Normal
1 mM $NiCl_2$	4 hours	est 59 ppm***	See Text
0.1 mM $NiCl_2$	4 hours	est 5.9 ppm*	Slight sublethal change in cytoplasm
4.2 mM $NiCl_2$	24 hours	est 247 ppm**	Extensive necrosis
5.0 mM $NiCl_2$	4 hours	est 295 ppm*	Similar to 1 mM with more lethal injury
NiO particles	24 hours	------------	Sublethal changes Results variable***
NiO coated fly ash	24 hours	5 ppm*	Lethal and sublethal changes***
Uncoated fly ash	24 hours	------------	Similar to controls***
NiO coated fly ash* with filter (phagocytosis blocked)	24 hours	4.4 ppm*	Similar to controls

---

[*] Results of one experiment

[**] Results of two experiments

[***] Average of three or more experiments

FIGURE 22

Light micrographs of RAMs at 1000 X.

A. Control RAMs. Note the eccentric nuclei and clusters of dense staining granules within the cytoplasm.

B. RAMs exposed to 4.3 mM $NiCl_2$ for 24 hrs. These cells are more vacuolated than controls, and there are many dead cells in the field.

C. RAMs exposed to 1000 ug/ml NiO coated fly ash. The cells have lysed in an explosive pattern, and very few viable cells can be found.

D. RAMs exposed to NiO particles. Cytoplasmic vacuolation is prominent. The nuclear chromatin is more fragmented than in control cells.

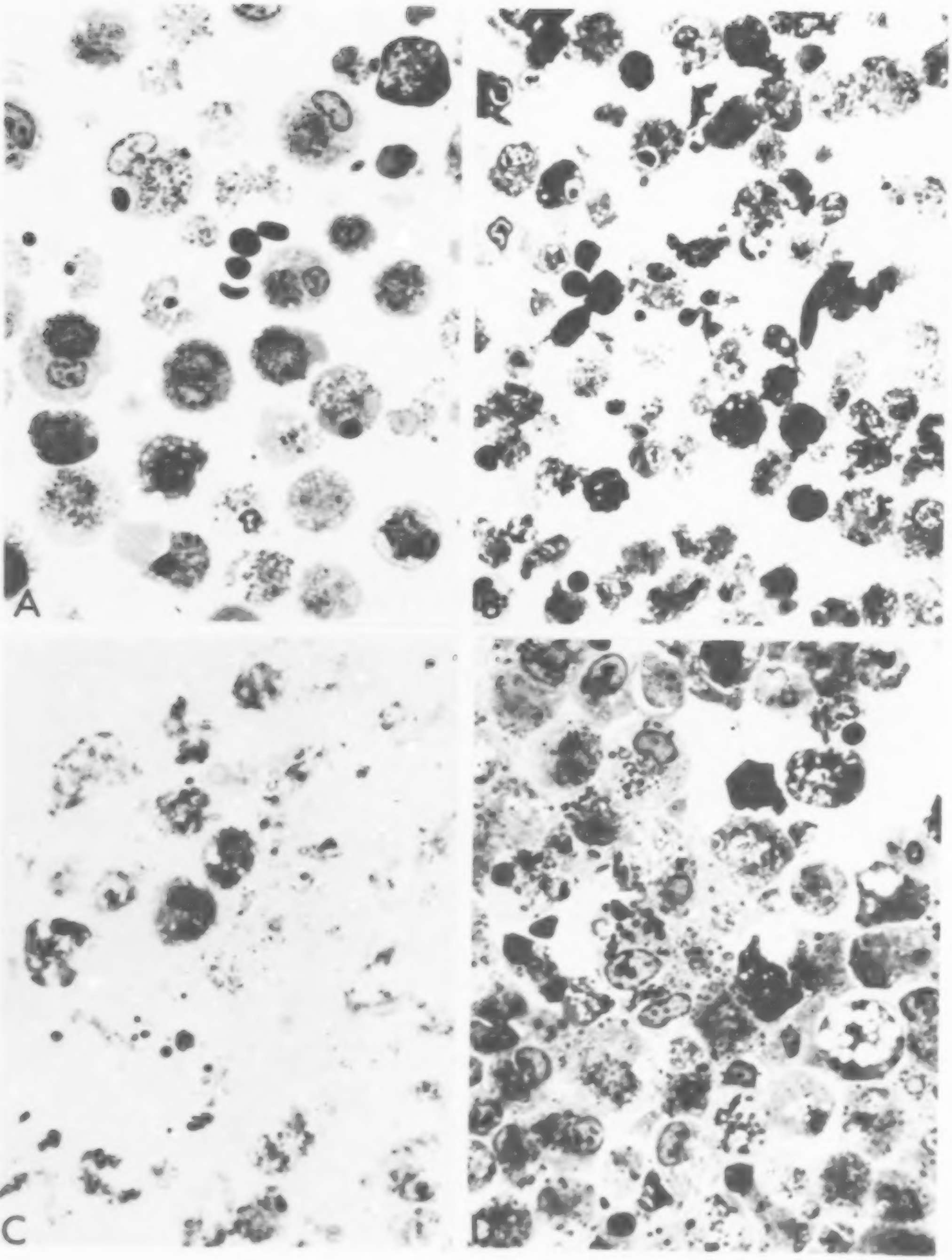
A
B
C
D

FIGURE 23

TEM of a control RAM. The nucleus is eccentric and slightly bean-shaped, and the cytoplasmic dense granules representing lysosomes cluster together near the center of the RAM. At the periphery, the cell exhibits a ruffled border. X 16,000

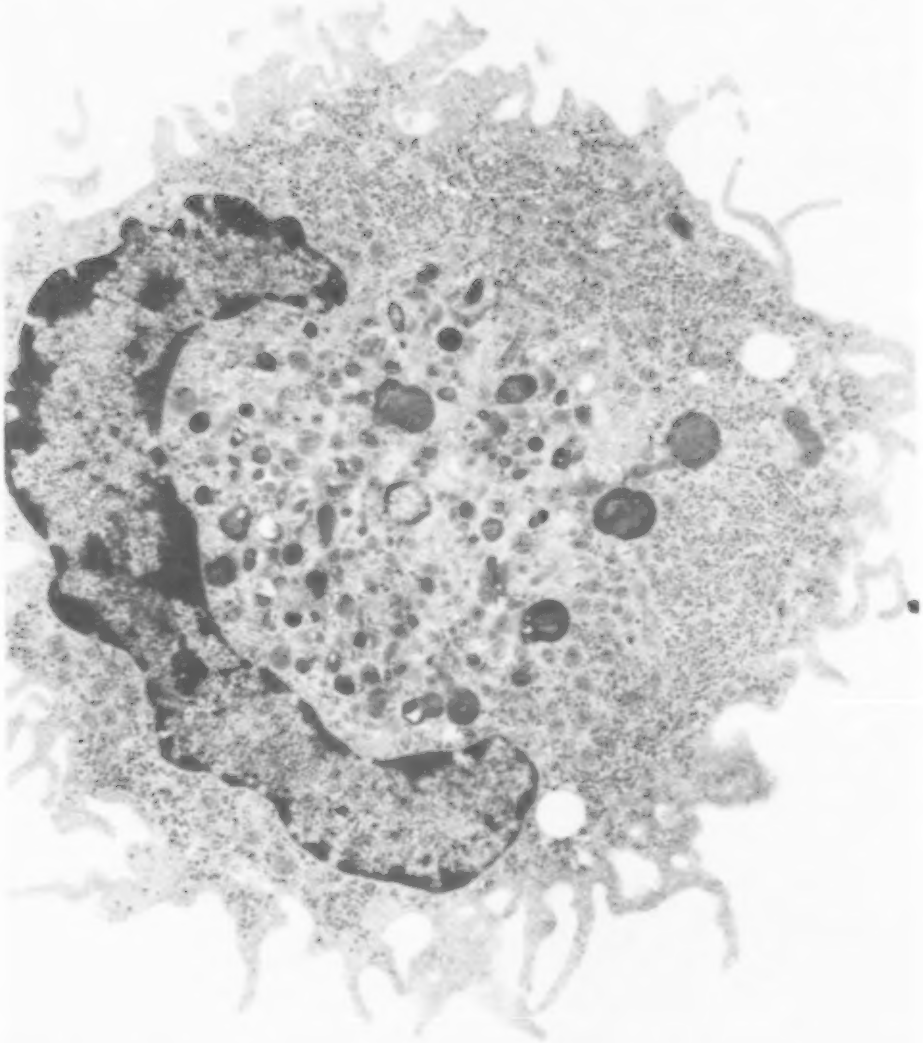

FIGURE 24

A. The RAM seen in this figure was exposed to 1mM $NiCl_2$ for 4 hrs. The cytoplasmic borders are retracted and smooth. The nucleus has an abnormal morphology and the nucleolus is larger than in control RAMs. In the cytoplasm are many swollen mitochondria. The ER and other organelles appear normal. X 12,000

B. In this cell exposed to NiO coated fly ash, note the very large nucleus and the cytoplasmic attenuation forming zeiotic knobs. X 16,000

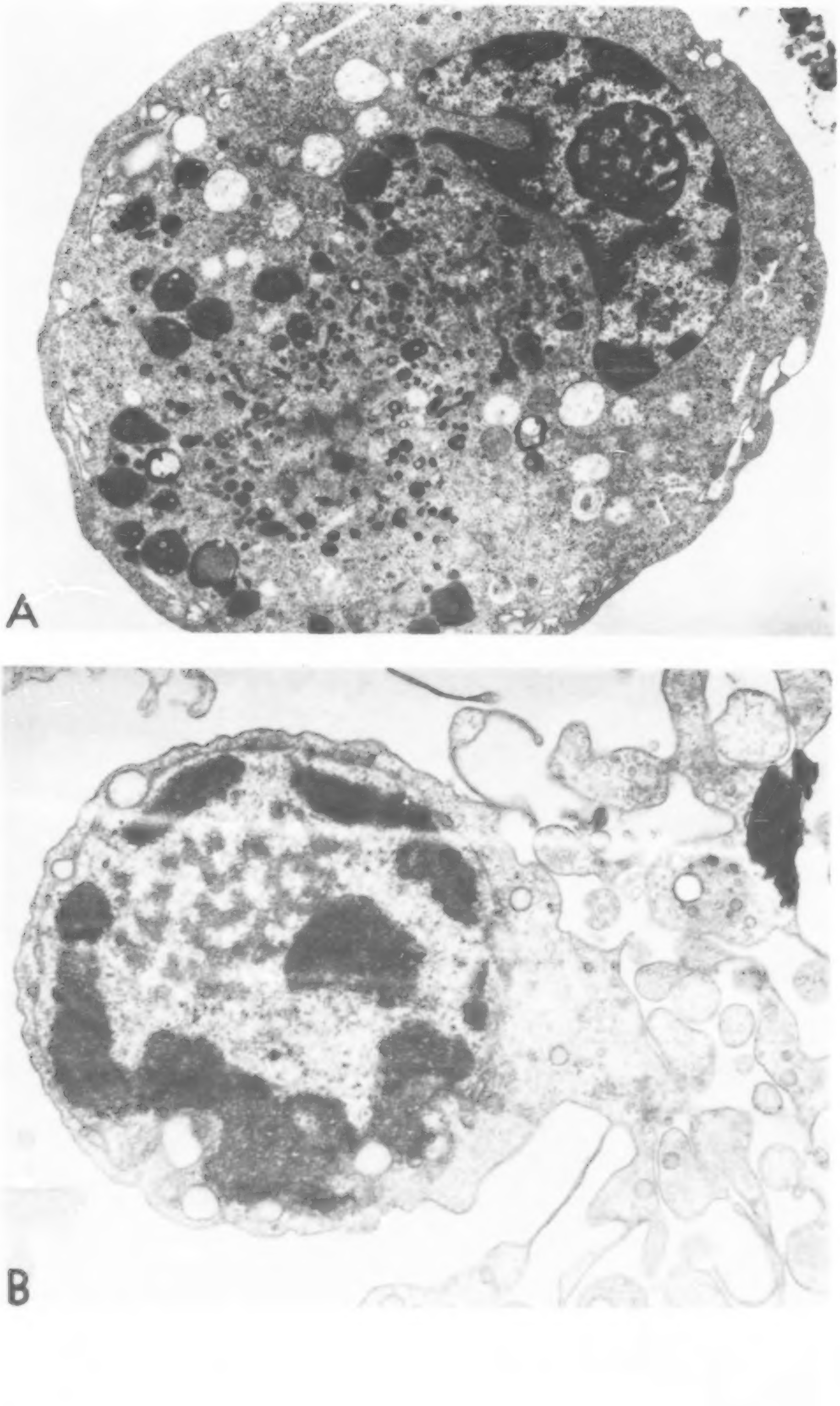
A
B

FIGURE 25

In this RAM, not only has there been a loss of surface ruffles, but within the cytoplasm, long channels corresponding to dilated ER have formed. In the nucleus, fine bundles of filaments have formed and the chromatin has taken on a coarsely granular appearance. X 12,500

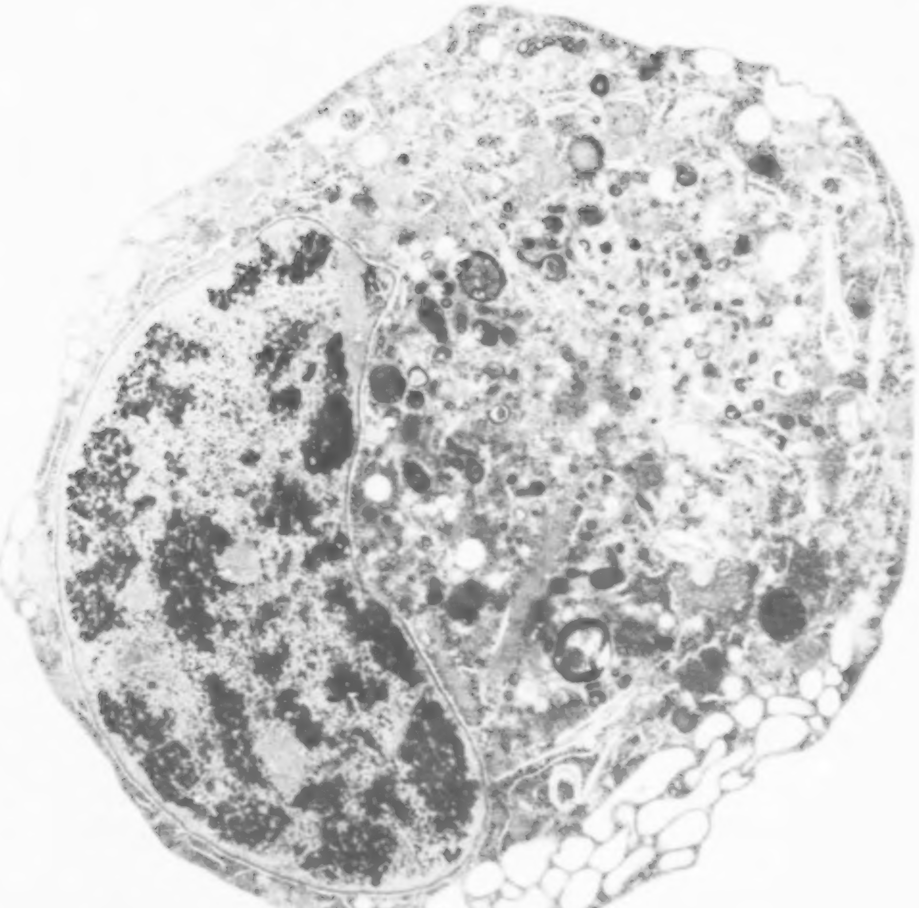

FIGURE 26

In another section of the previous cell, a small nuclear inclusions is seen. This demonstrates that serial sections are often necessary to identify the presence of nuclear inclusions in affected cells. X 12,500

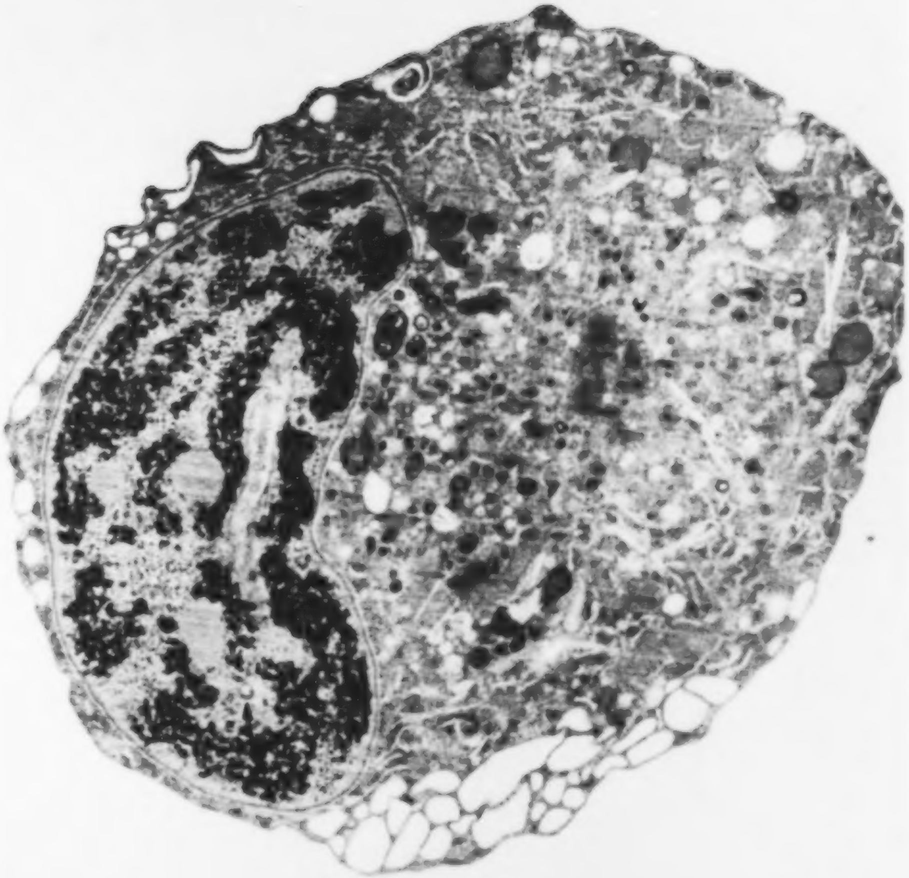

FIGURE 27

A. A nuclear inclusion induced by $NiCl_2$. The structure appears to be forming from the precipitation or assembly of tubular components within the RAM nucleus. The inclusion periodicity is 250 A. X 30,800

B. Similar inclusions may also form in the cytoplasm of RAMs. The inclusions are not membrane-bound and appear to be forming spontaneously within the cytosol. The inclusion periodicity is 350 A. X 31,400

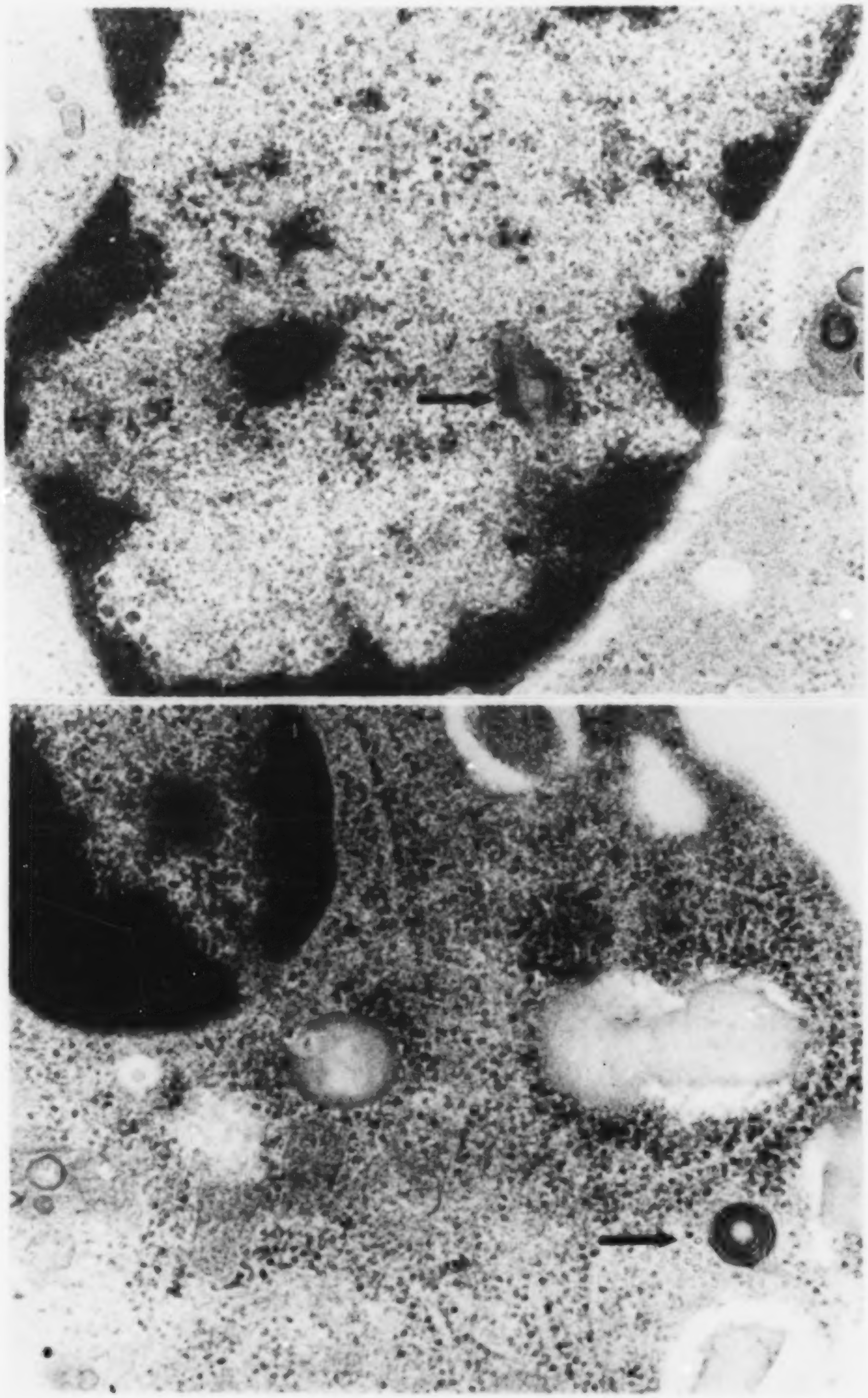

FIGURE 28

A. In this plate is seen at higher magnification the same fibrillar material seen in Plates 25,26. Note the lamellar inclusion in the middle left field. X 24,000

B. Notice that the fibrils are attached to the nuclear membrane. X 40,000

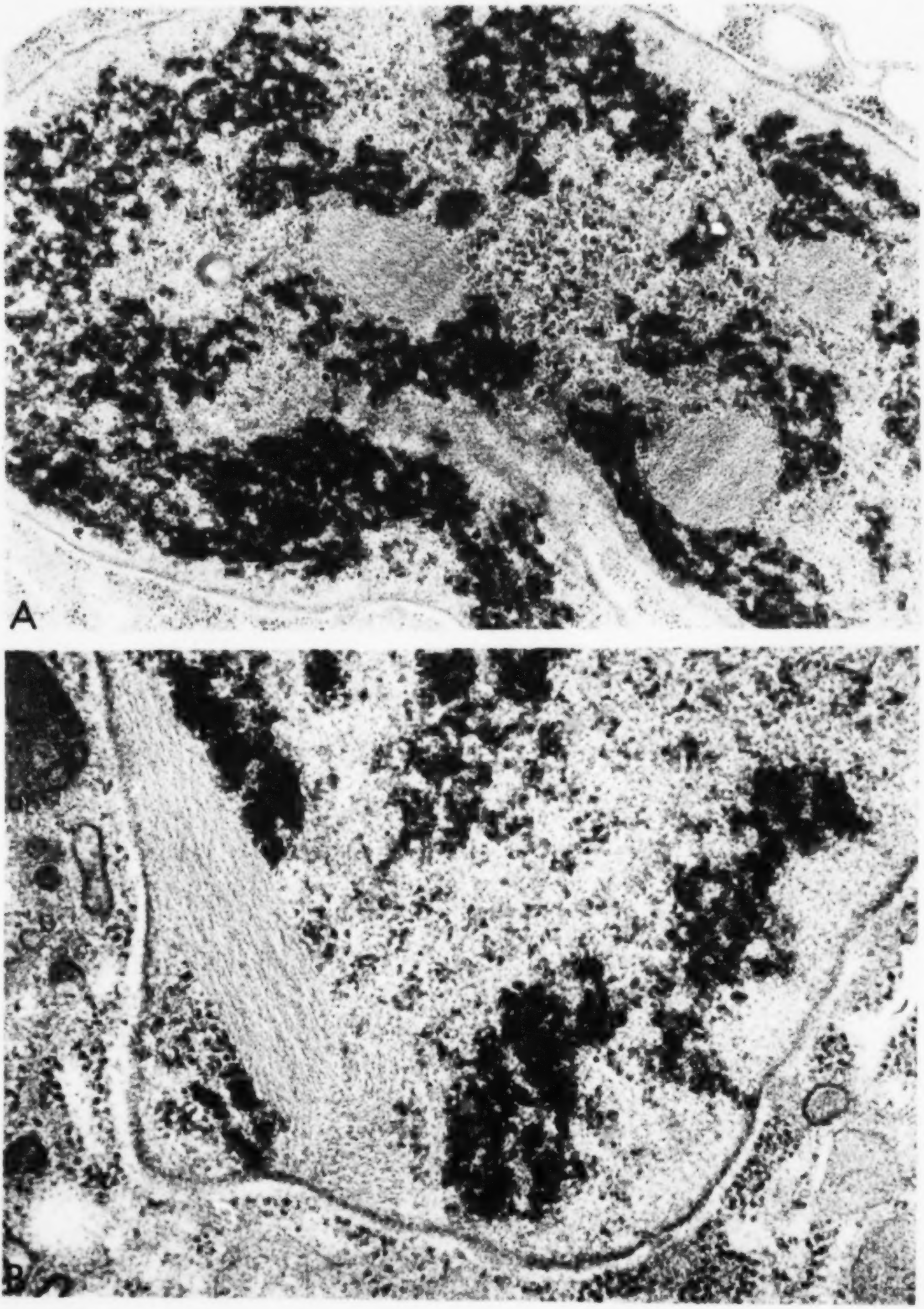
A
B

FIGURE 29

Despite the near normal gross appearance of the nucleus of this cell exposed to lmM $NiCl_2$ for 4 hours, the fine structure is abnormal. Within the nucleus, the nucleolus is slightly enlarged, and there is a concentric ring-like inclusion in the lower right corner (arrow and inset). The inclusion has a periodicity of 380 A and is not dense in the center (compare with Figure 34).

In the cytoplasm are numerous lysosomes which are not oriented at the opposite pole from the nucleus (compare with control RAM Plate 23), suggesting that one effect of nickel toxicity might be to disrupt the normal orientation of organelles within the cytoplasm. Also note the large isolated bundles of fibrils similar to those seen in the cytoplasm and nucleus of the cell in Figures 25,26,28.

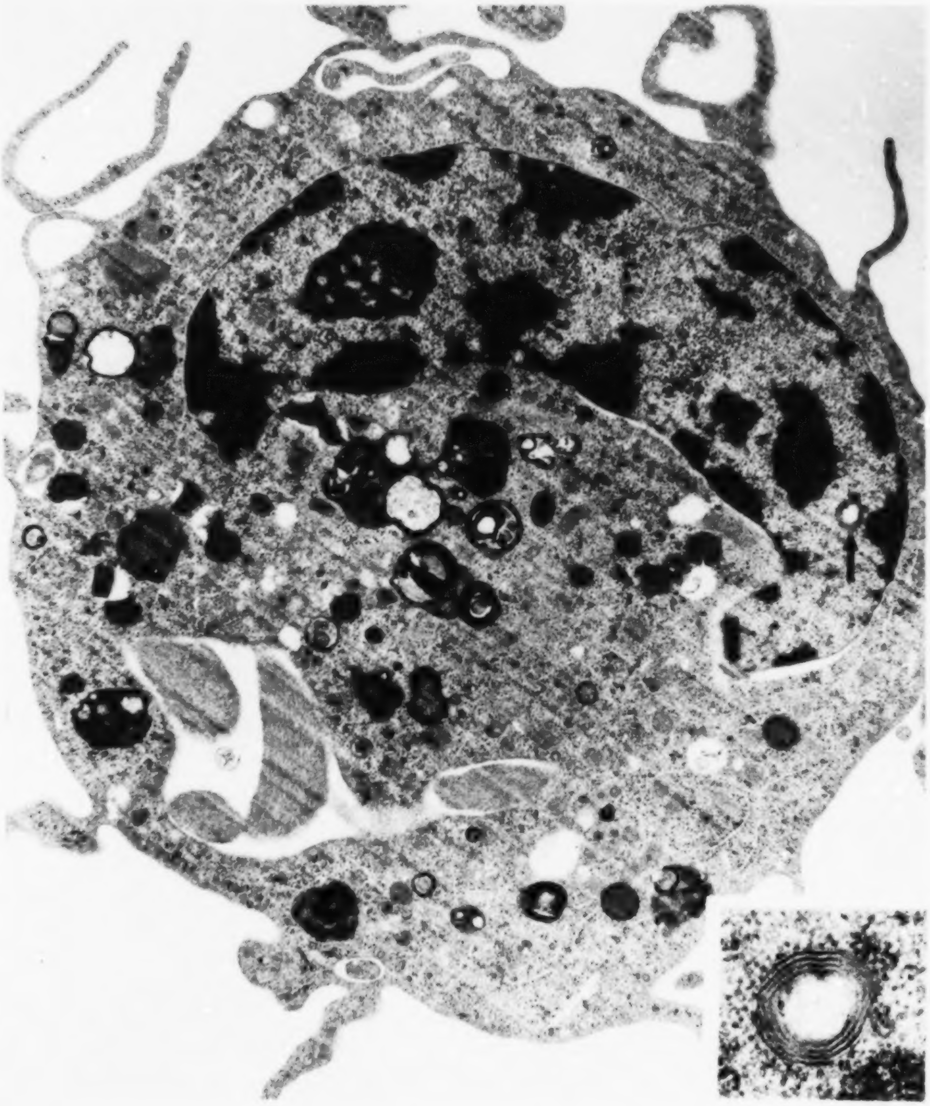

FIGURE 30

Numerous vacuoles can be seen in this cell, and most of them appear to be due to disintegration of the mitochondria. Within several empty spaces, fragments of cristae are still discernable. The cytoplasmic ruffles have retracted enclosing small peripheral vacuoles. The nucleus contains a small multilamellar inclusion which is better seen in 30-b.

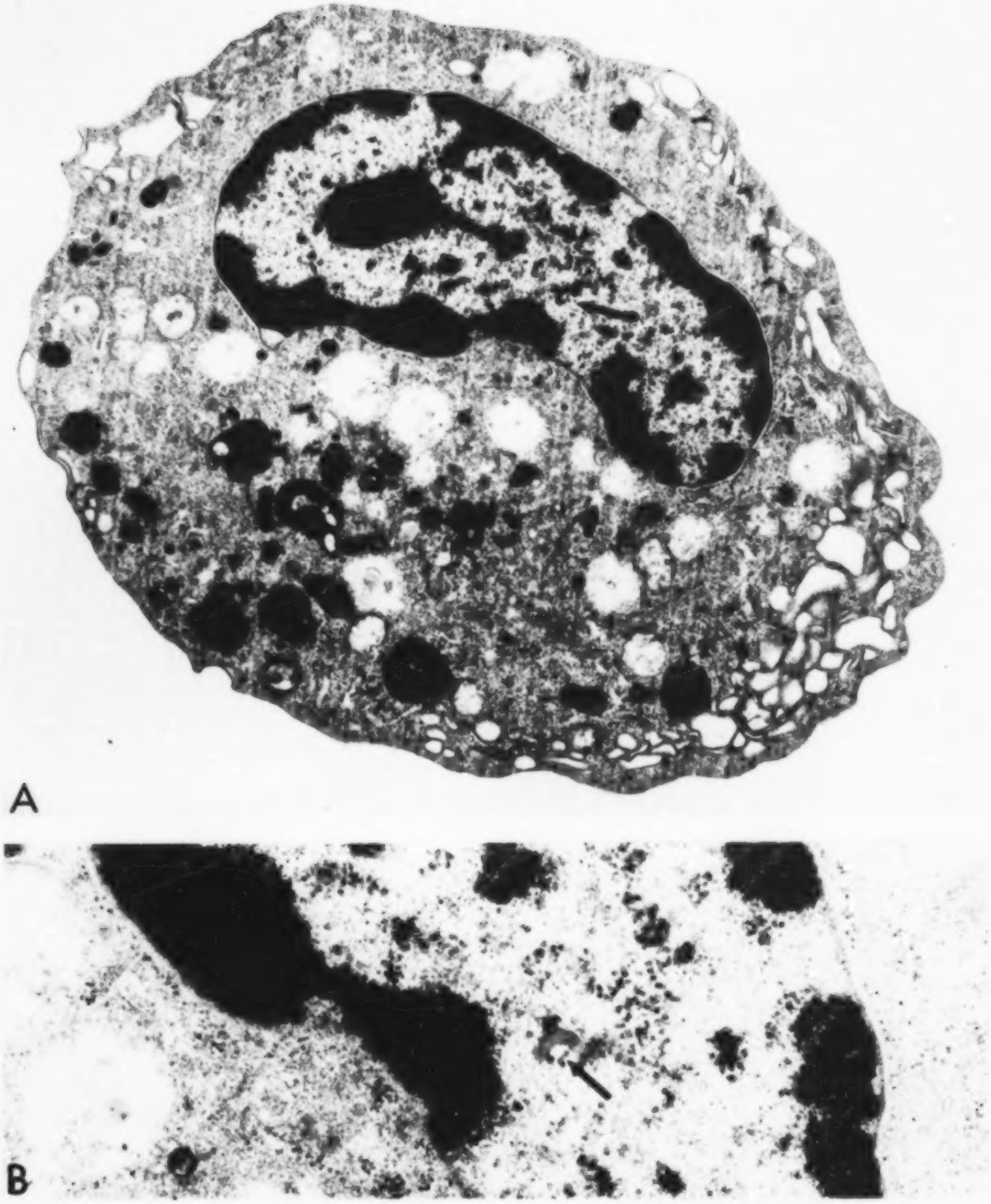
A
B

FIGURE 31

In this cell which has been exposed to $NiCl_2$ for 4 hrs., many pathologic features may be seen. The nucleus to cytoplasm ratio is large; there are few, attenuated ruffles; there is swelling of the nuclear membrane with bridges retained at the nuclear pores, and there is cytoplasmic vacuolation. Few lysosomes are seen, and other cytoplasmic components are barely visible. Within the nucleus, the dense chromatin has assumed a fragmented appearance. One fibrillar nuclear body and two multilamellar nuclear inclusions are seen.

A. X 18,000

B. X 50,000

C. X 50,000

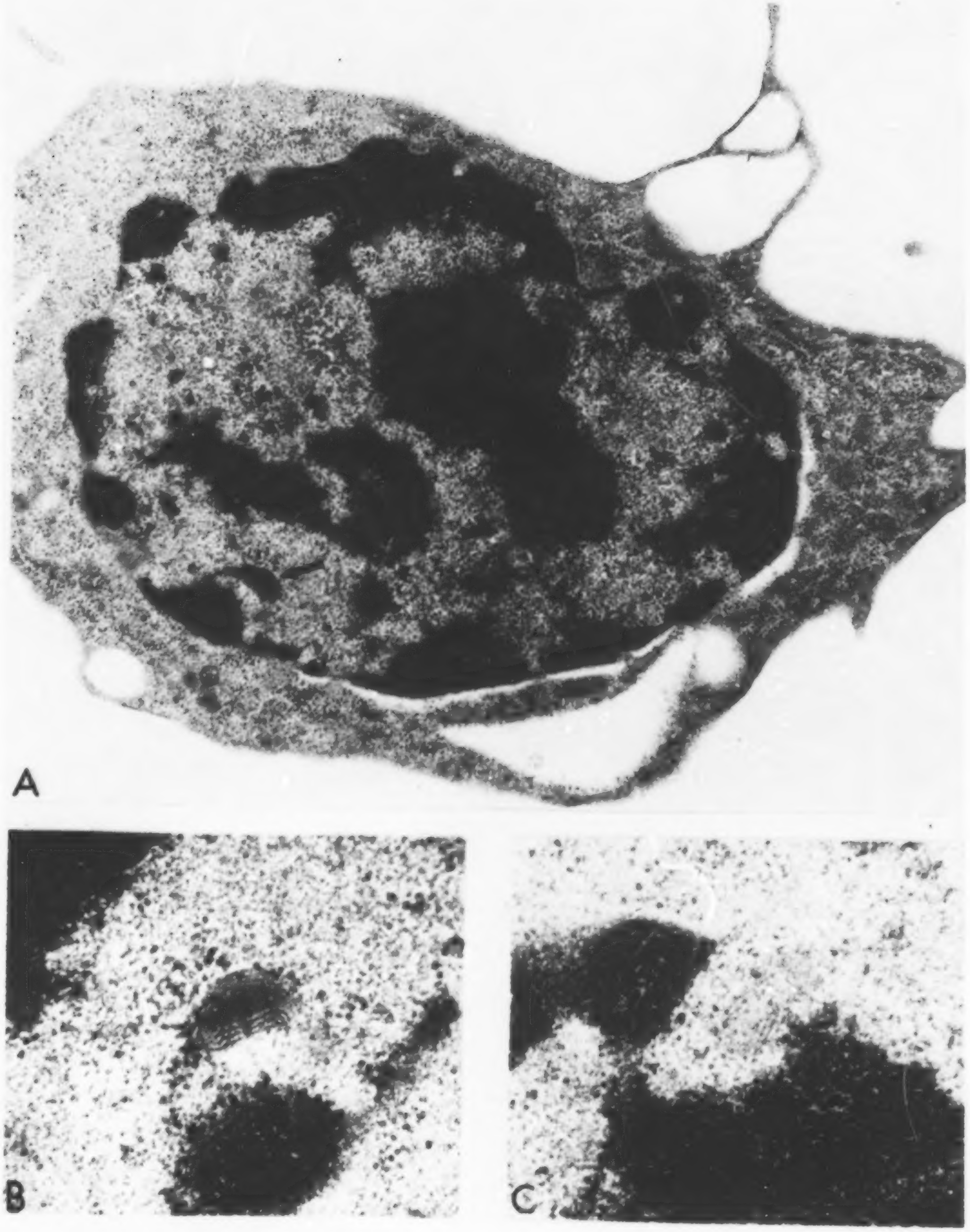
A
B
C

FIGURE 32

This cell exposed to 1mM $NiCl_2$ for 4 hrs. has assumed a smooth contour characteristic of cells exposed to soluble nickel in the medium. The cytoplasmic ruffles have retracted enclosing vacuoles (upper left) and the nucleus has developed a lamellar inclusion (I). Around the periphery of the nucleus, channels of rough ER can be seen.

In the inset, the inclusion can be seen at higher magnification.

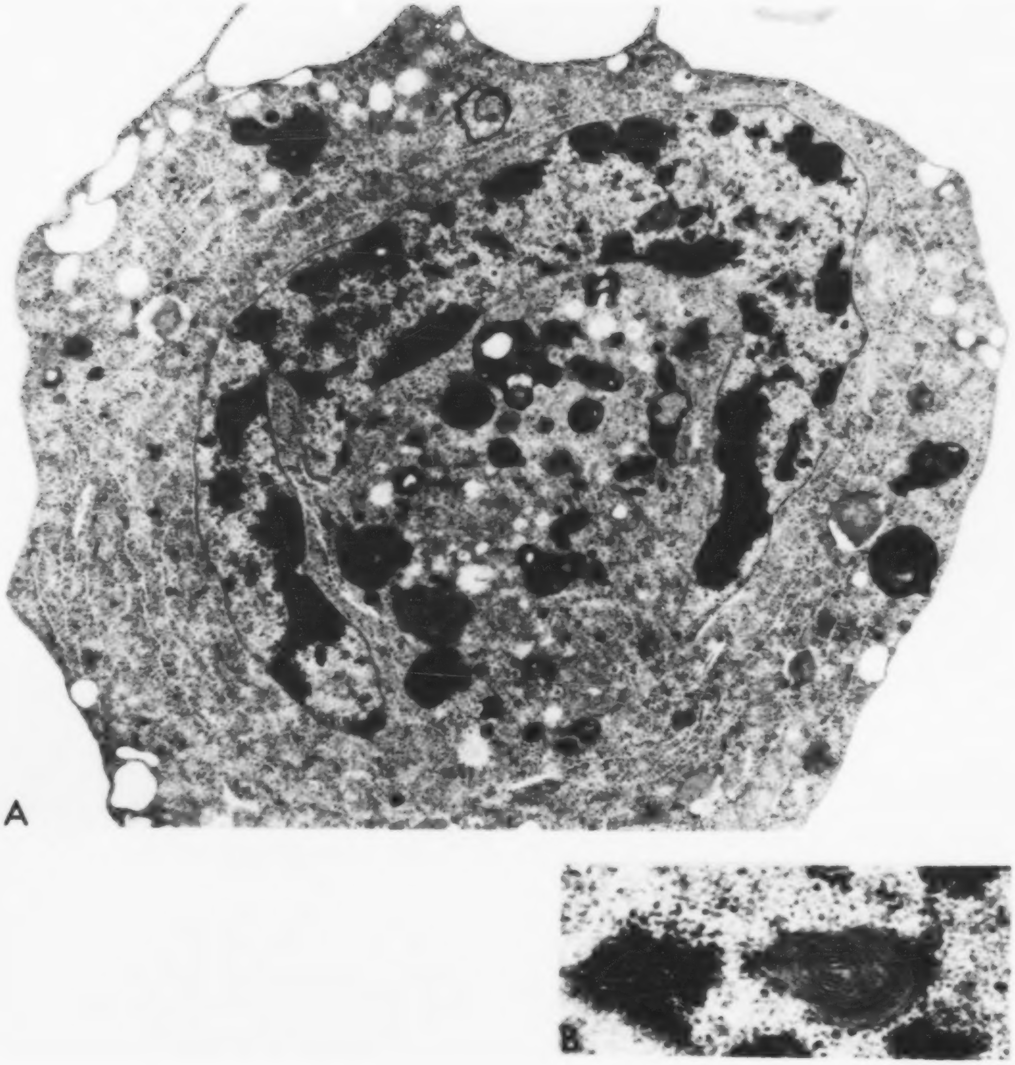
A
B

FIGURE 33

Again, nuclear inclusions are seen in relatively normal looking nuclei. The cells were exposed to 100 ug/ml NiO.

A. The inclusion seen at the right in the large Figure and in the inset is .48 um in diameter and has a periodicity of 300 A. X 50,000 (inset) X 15,000 (large print)

B. In the nucleus illustrated here, two small inclusions are seen (white arrows). The upper inclusion is enlarged in the inset. X 14,900, X 50,000

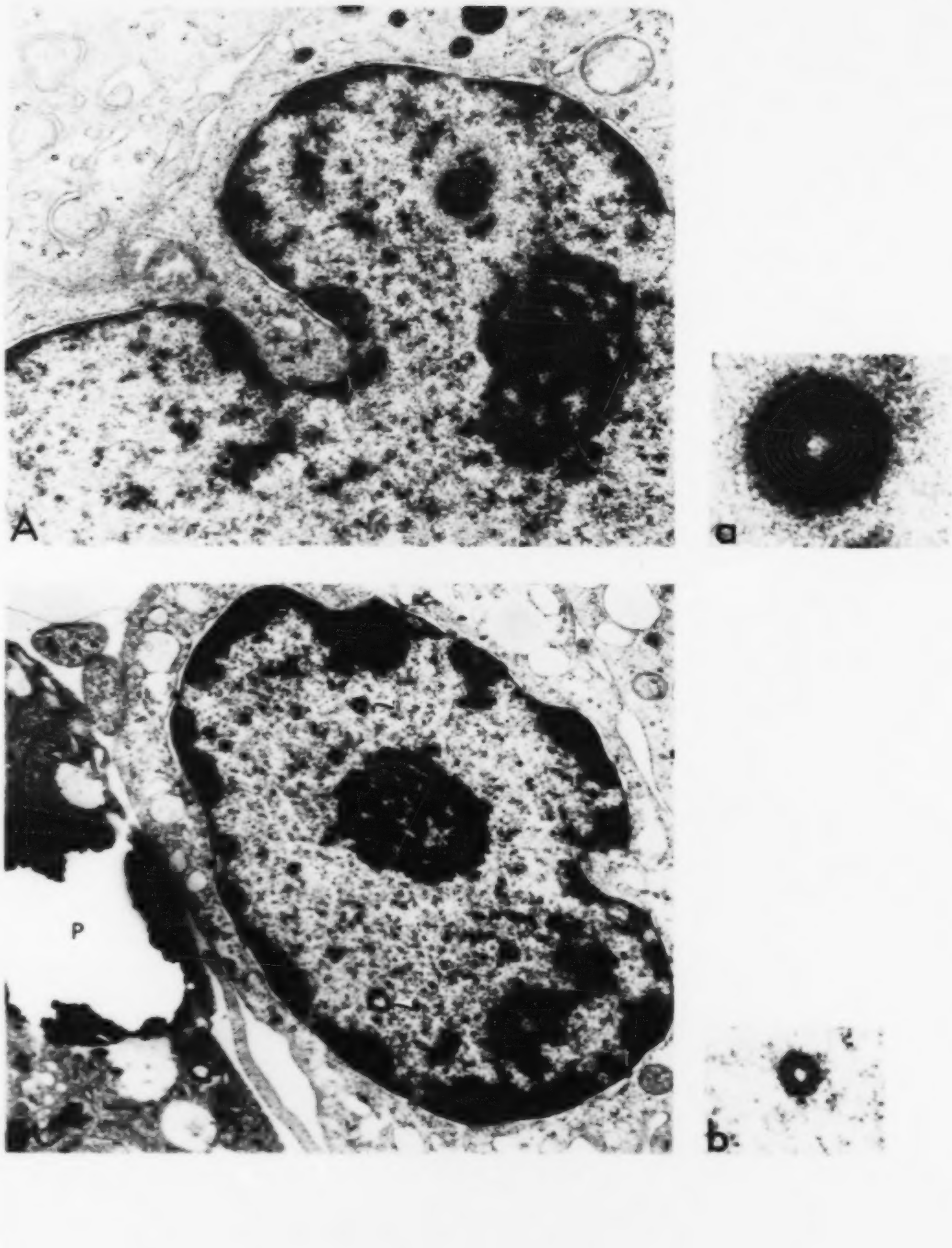
A
a
P
b

FIGURE 34

This figure demonstrates the typical appearance of cells centrifuged to form a pellet. Cell contours are distorted, but the pellet offers the advantage of having many cells available for inspection in a small field. These cells were cultured with 100 ug/ml NiO for 24 hrs. The cell in the 10:00 position displays fragmented dense chromatin in the nucleus and a prominent paracrystalline inclusions seen at higher power in 34-b. Note that the lamellae fade toward to center of the inclusion and that the layers are concentric, not spiral. The dense-to-dense line periodicity at the outer layers is 180 A.

A small nucleolus is present in this cell and a large segregated clump of chromatin is seen occupying the interior of the nucleus. This probably is not of nucleolar origin since an intact nucleolus is present in the same cell and since no other segregation patterns have been seen in other RAMs exposed to nickel. Rather, this probably represents segregation of peripheral heterochromatin. Note the swollen mitochondria at the lower right of 34-b.

A. X 9,100

B. X 39,000

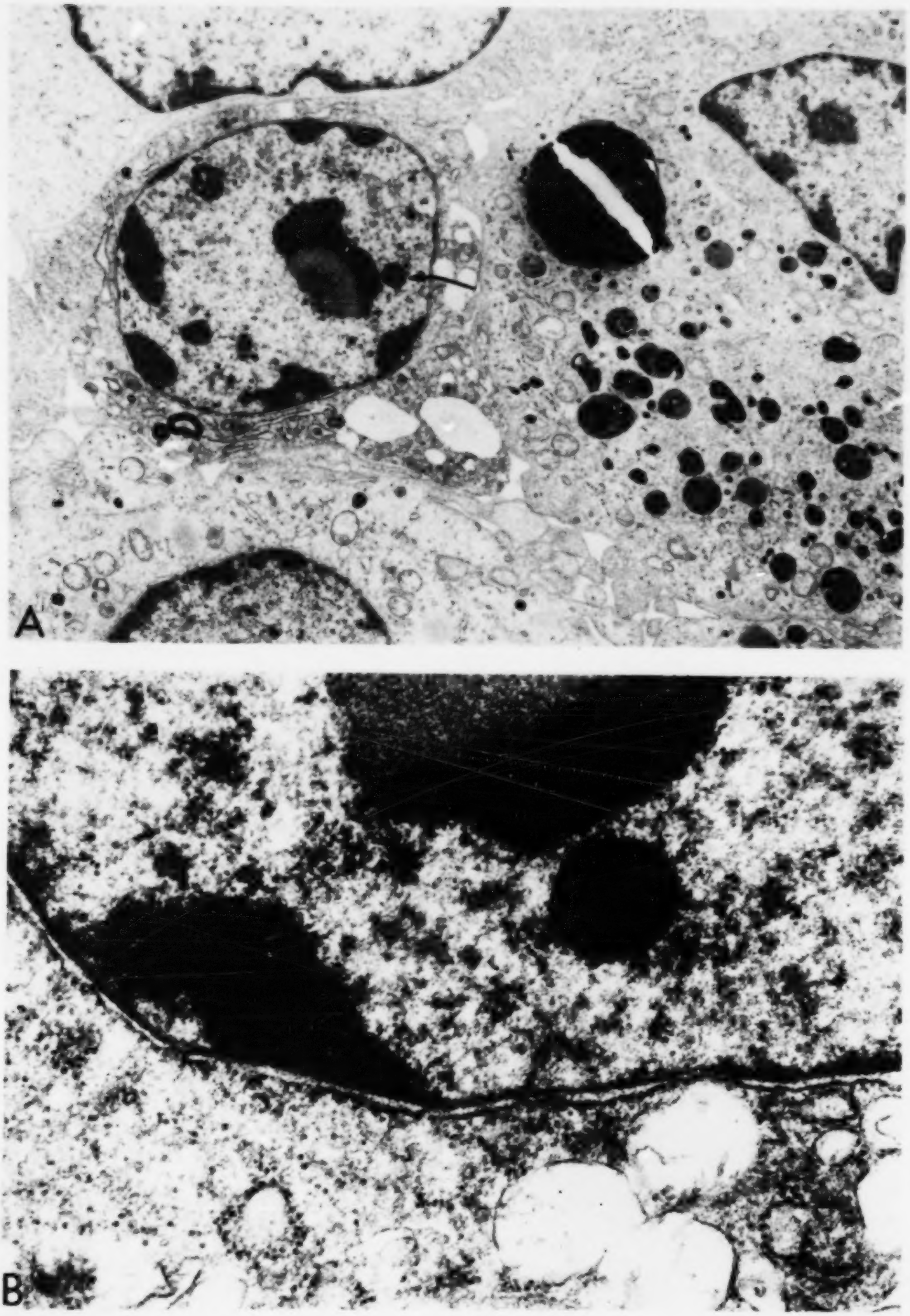
A
B

FIGURE 35

A. That ring-like inclusions commonly develop in RAMs exposed to nickel oxide-coated particles is demonstrated in this cell which was exposed to 1000 ug/ml NiO coated fly ash. The particle has fragmented on sectioning. X 11,800

B. At higher magnification, the inclusions in the same cell are still quite inconspicuous (arrows). In contrast to many other nickel induced inclusions, those in this RAM bear proximity to fragments of heterochromatin. X 28,000

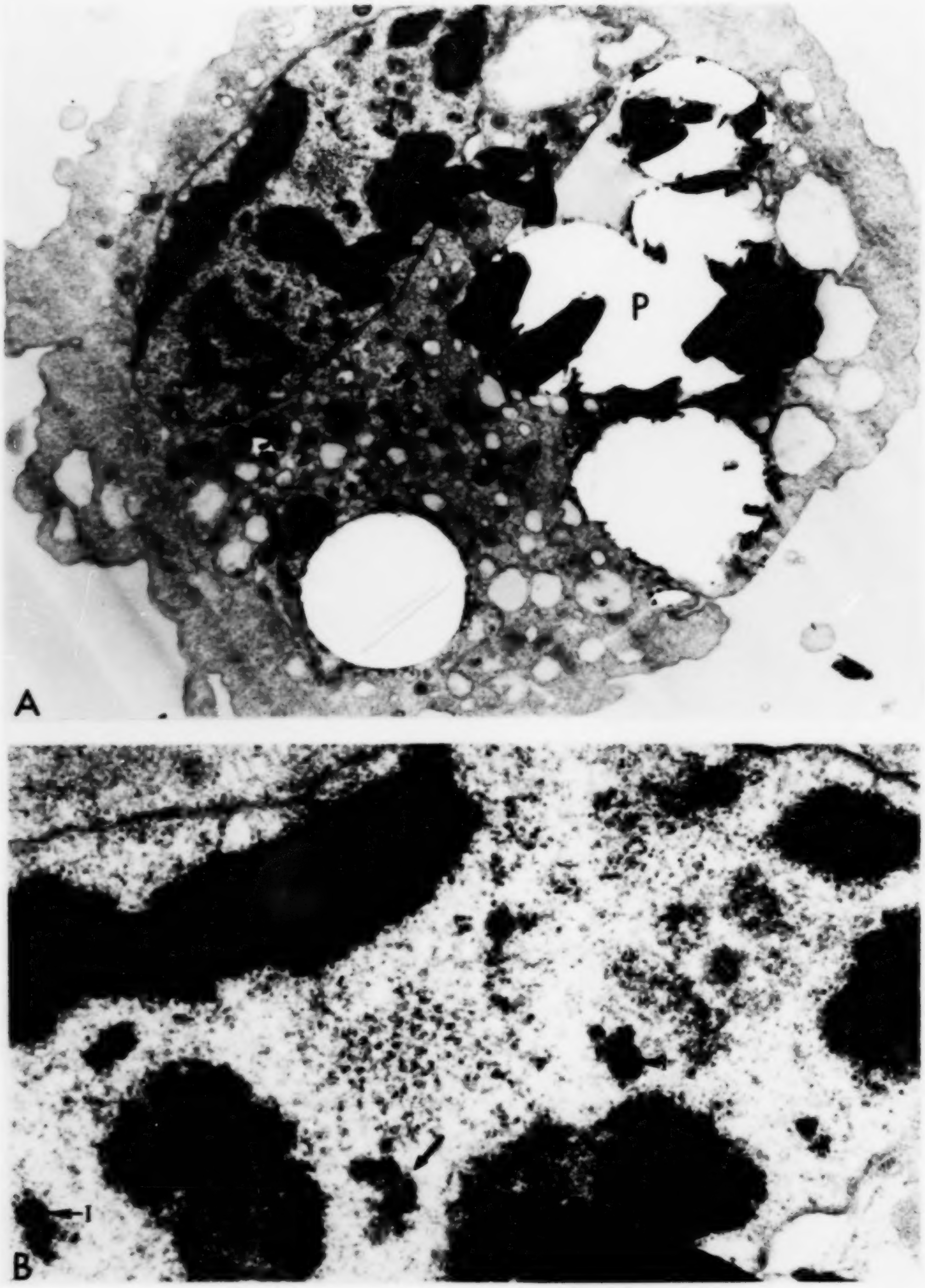
P
A
I
B

FIGURE 36

The familar appearance of RAMs exposed to nickel is seen in this cell with smooth cytoplasmic borders, coarsely granular heterochromatin (see Plates 25,26,27) and an inclusion within an area enclosed by the nucleus.

In the bottom figure, it can be seen that the inclusion is not within the nucleus, but it is not clear whether it originally developed within the nucleus or in the cytosol. It has a periodicity of 230 A and is .53 um in length.

A. X 16,000

B. X 30,000

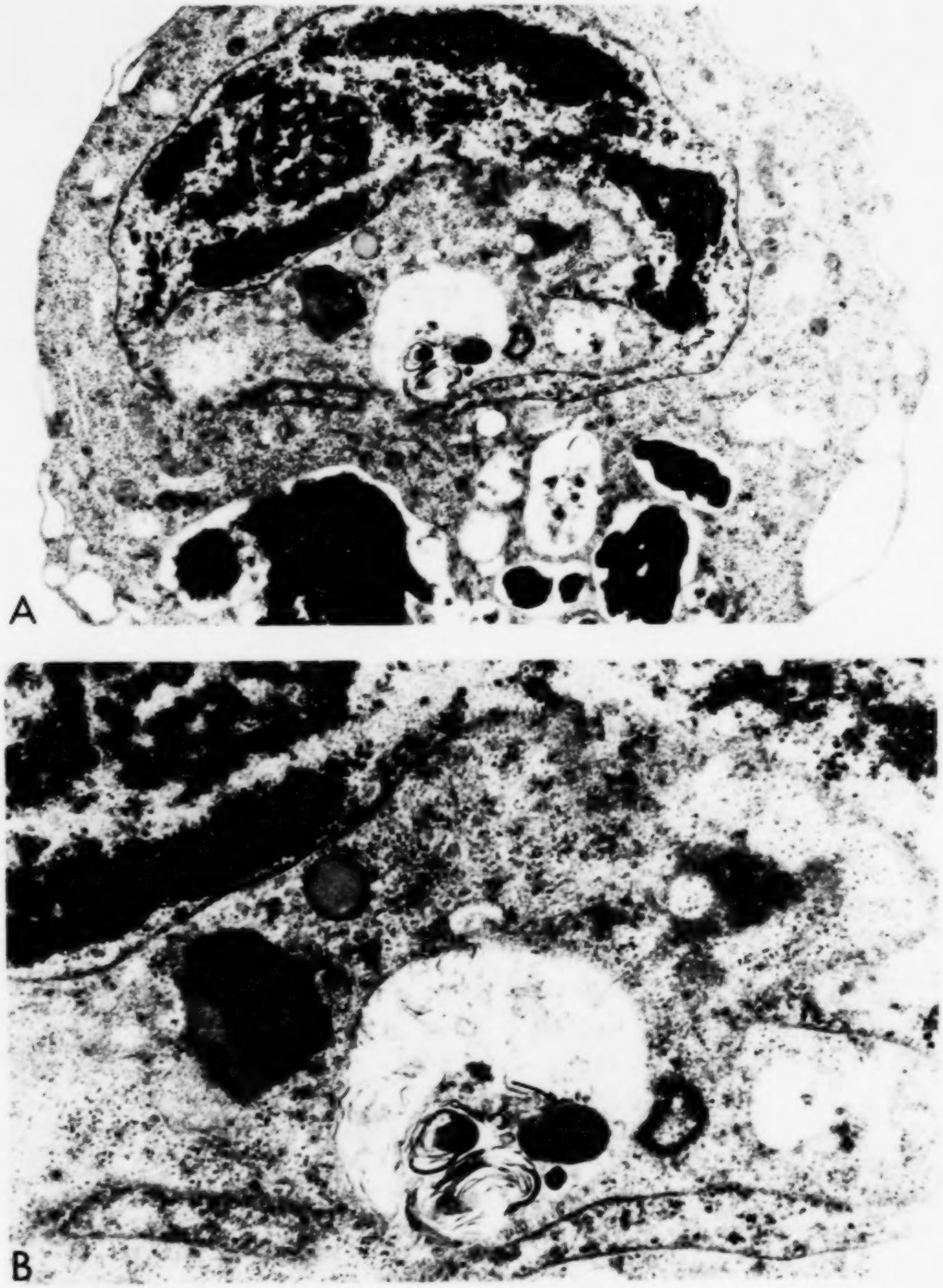
A
B

FIGURE 37

This figure shows the variable nature of nuclear inclusions induced by nickel.

A. In this micrograph, the inclusion peridocity is 250 A and the magnification is 40,000 X.

B. This inclusion has a periodicity of 180 A and is .25 um from the inside to the outside of the band of lamellae. The entire inclusion is .5 um across. X 28,000

C. The inclusion seen here has a periodicity of 140 A. It appears to consist of two bands of lamellae, one within the other. X 43,000

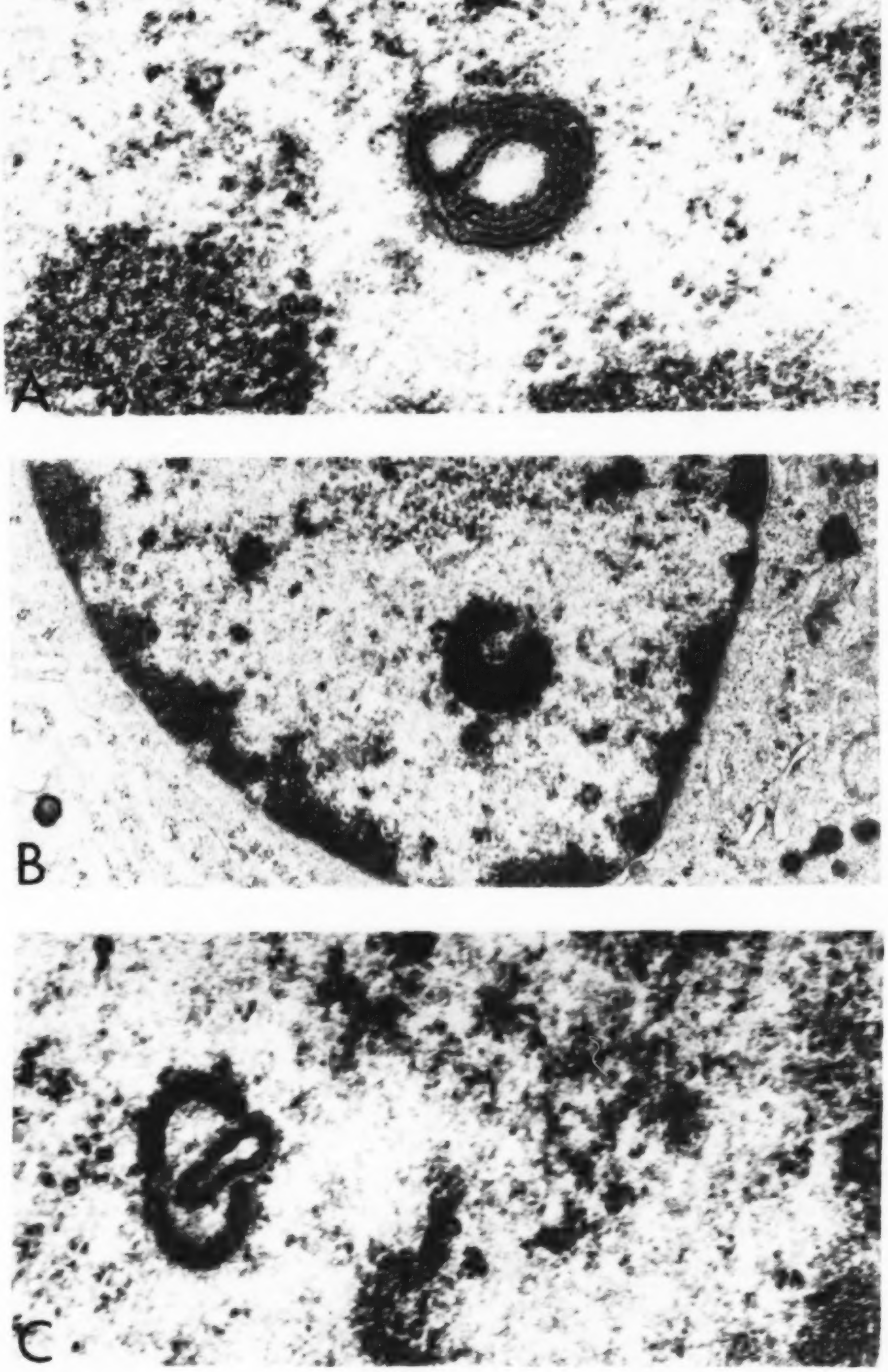
A
B
C

FIGURE 38

A. In this cell which has ingested NiO, note the fine fibrillar particle and the swollen ER and mitochondria. X 25,000

B. In a conspicuously necrotic cell which has also phagocytosed NiO (on fly ash particles) very small lamellar inclusions are seen peripheral to the pyknotic chromatin. The nuclear membrane and ER are swollen, and ribosomes are detaching from their surfaces. X 25,000

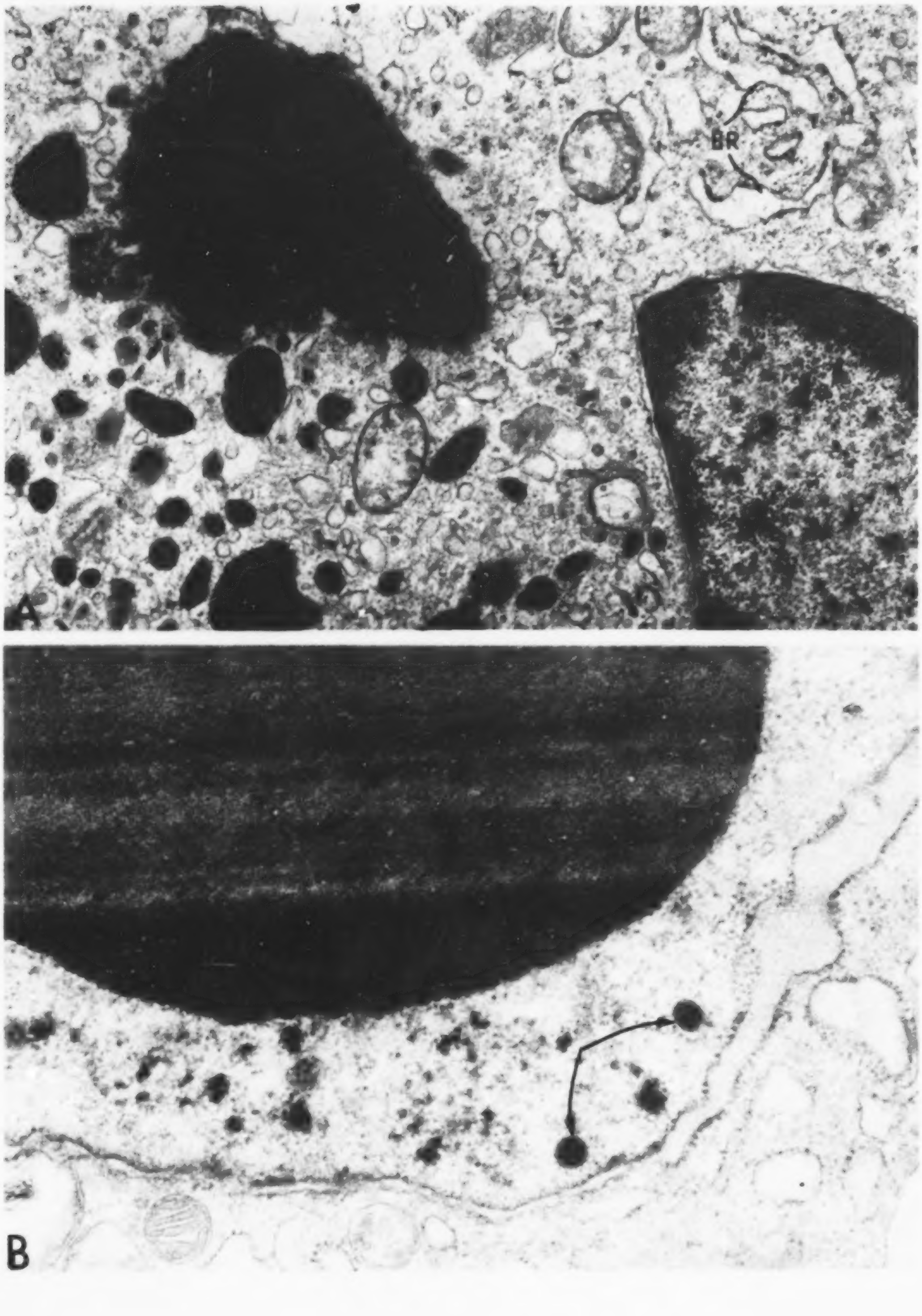
BR
A
B

FIGURE 39

A. In this very necrotic RAM, another nuclear inclusion is seen. At the arrow, a fragment of detached lamellae appears beside a larger, more common type of inclusion. X 33,300

B. This intranuclear inclusion was formed in a cell which had phagocytosed NiO-coated fly ash. It is magnified 112,000 X. The fly ash particle in the upper field lies outside the nuclear space. In this view it is barely possible to distinguish a fine osmiophilic line within the lucent band between the heavier dense lines. The dense line-to-dense line periodicity is 280 A.

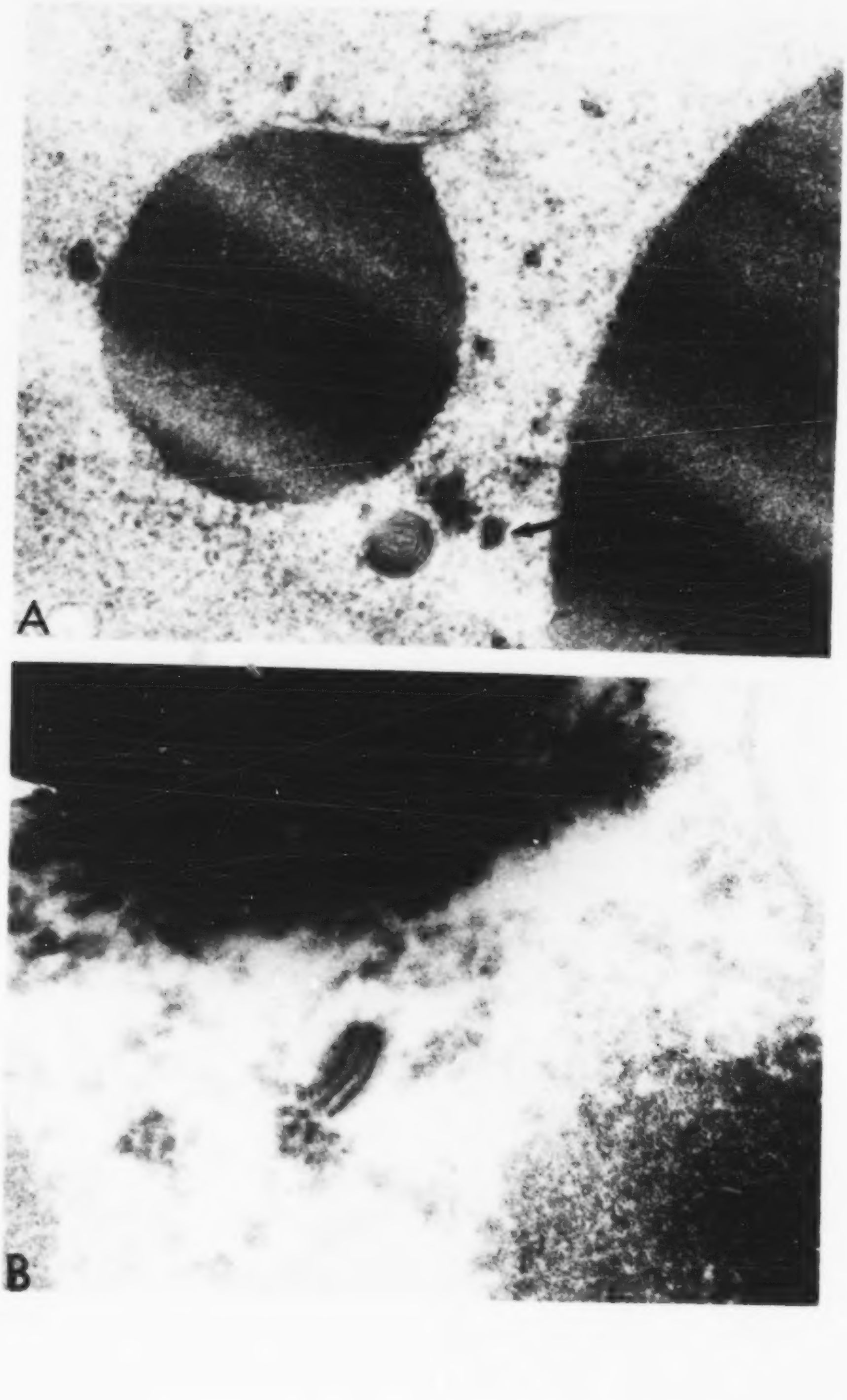
A
B

FIGURE 40

A. In this cell note the nucleolus (N) and a homogenous nuclear body (NB). The cell had been cultured with NiO particles for 24 hours. X 14,000

B. This cell was also exposed to NiO. Around a homogenous osmiophilic area are fine lamellae with a peridicity of 104 A. Compared to the true homogeneous nuclear body seen above, this body has no halo of fibrillar material, and the lamellae adhere directly to the homogenous matrix. Also compare this inclusion /body to the lamellar structure seen in Figure 48. X 38,400.

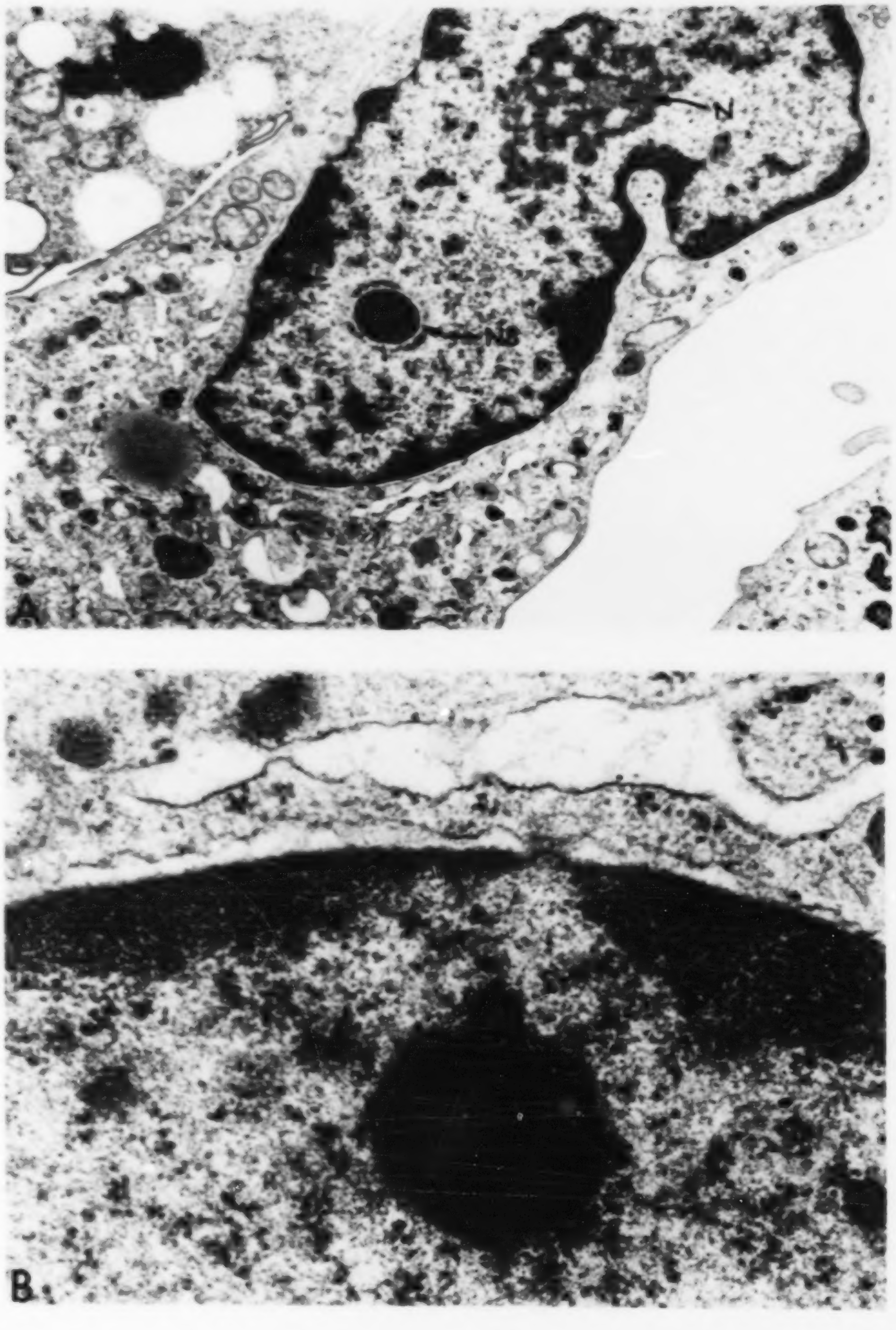
N
NS
A
B

FIGURE 41

A. Note the presence of a heterogenous nuclear body in this RAM exposed to NiO. The nuclear body is composed of homogenous, granular, and fibrillar areas. In the same cell is a good example of a normal nucleolus in a RAM (compare with Figure 22-b). In the nucleolus, are two paler staining fibrillar areas bridged by heterochromatin. X 18,200.

B. This cell was also cultured with 100 ug/ml NiO particles. Within the nucleus are two nuclear bodies; the lower left (N) represents a granular body and the one at the upper left (NB) is a fibrillar body. The origin of these structures remains in debate. They are seen in many normal cells but are thought to increase in number in rapidly proliferating cells. X 38,800

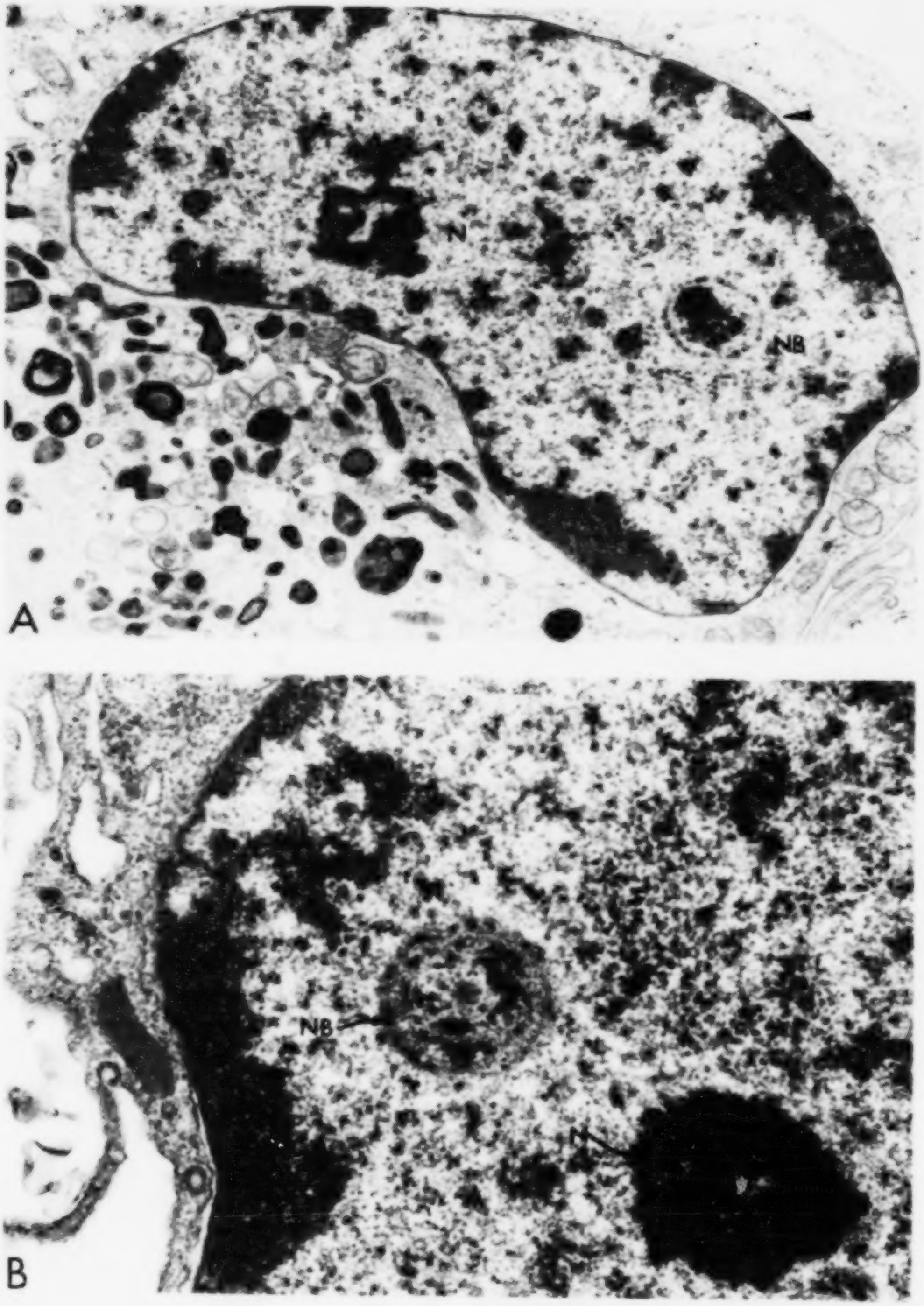
N
NB
A
NB
N
B

FIGURE 42

A. This section is of a pellet of RAMs exposed to 100 ug/ml NiO for 24 hours. It was fixed in glutaraldehyde only, without osmium. Note the large whorl of ER within the cytoplasm of the cell in the center. Such whorls are extremely common in these cells. X 7,000

B. In another cell with whorls of ER, (arrows) is a nuclear inclusion-lower left corner. The whorl at the bottom arrow is partly composed of the nuclear membrane. X 25,000

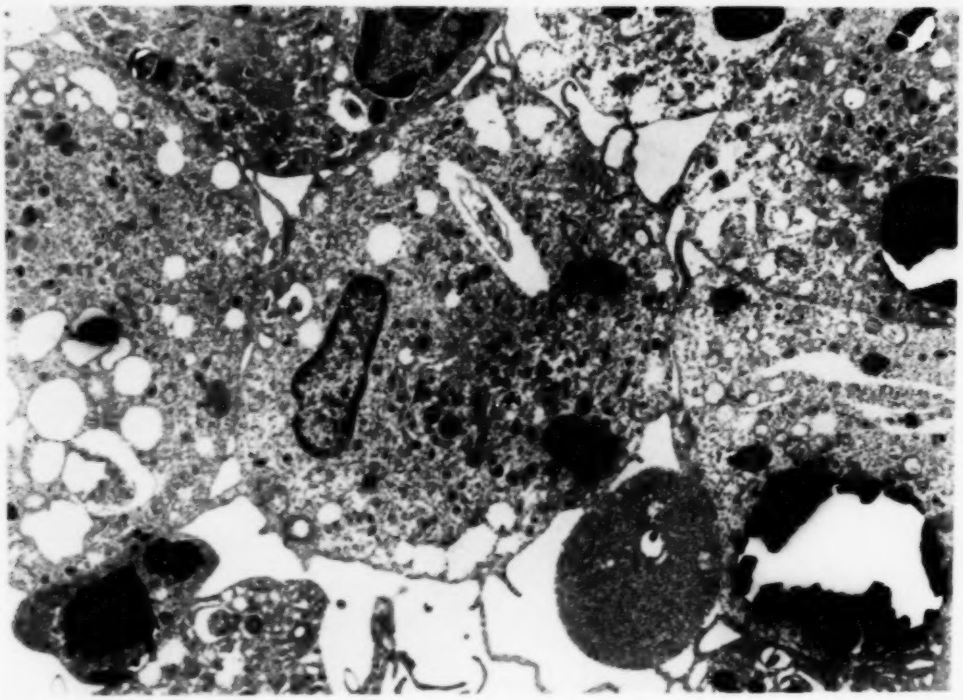

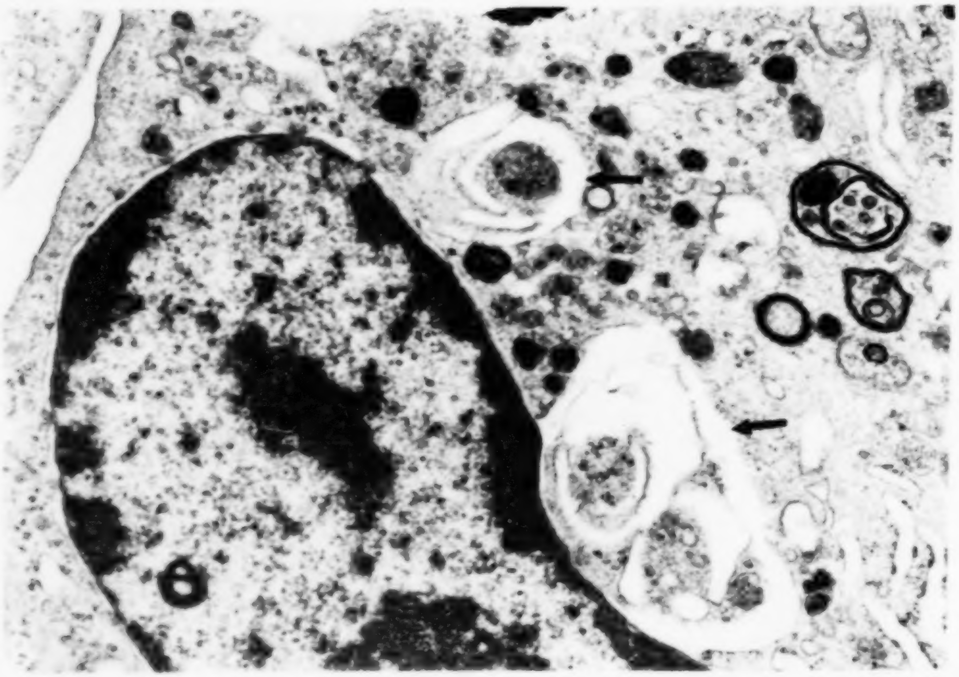

FIGURE 43

A. The nuclear inclusion seen in this nucleus is not, located near the nuclear envelope, nor have similar inclusions induced by nickel developed in close proximity to the nuclear membane. The morphology does appear to be different from the inclusions seen in Figures 27, 33 and 34, but does bear a resemblance to those in Figure 37. X 17,500

B. The nuclear membrane in this plate has expanded imparting a bizarre contour to the nucleus. This is a distinctly abnormal finding in RAMs (compare to control, 23). Note also that the mitochondria are swollen (M) and that the endoplasmic reticulum has formed whorls within the cytosol (arrow). A particle of NiO is also seen in the cytosol (P). X 16,000

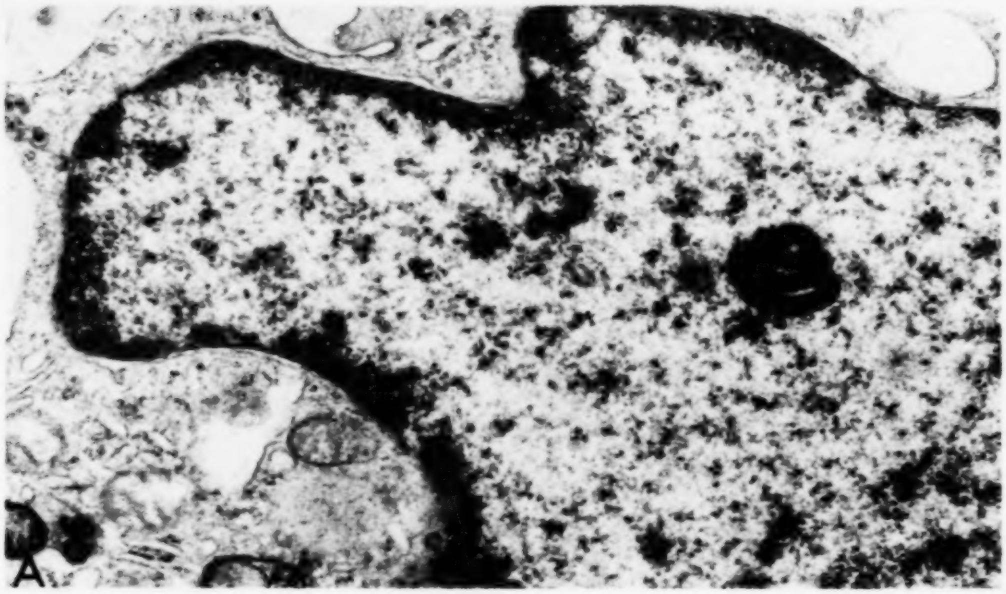
A

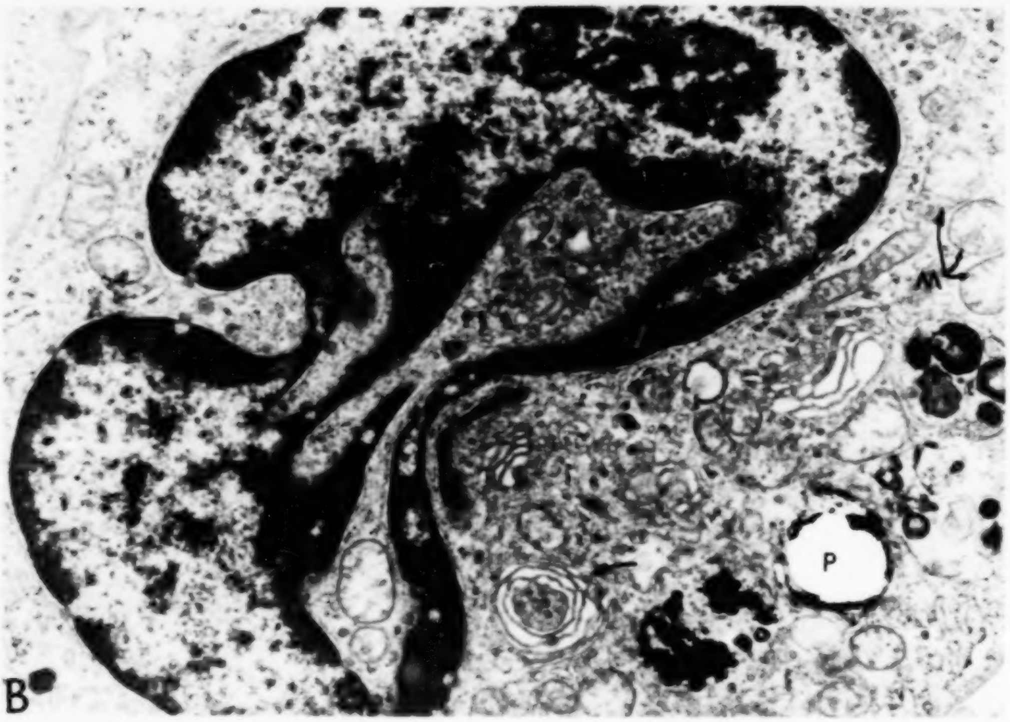
M
P
B

FIGURE 44

This figure illustrated the typical fibrillar appearance of NiO particles in this experiment. The particle is dense and granular near the center, but has a finer mycelia-like border. Whorls of ER (W) and cytoplasmic vacuoles are also seen. X 19,000

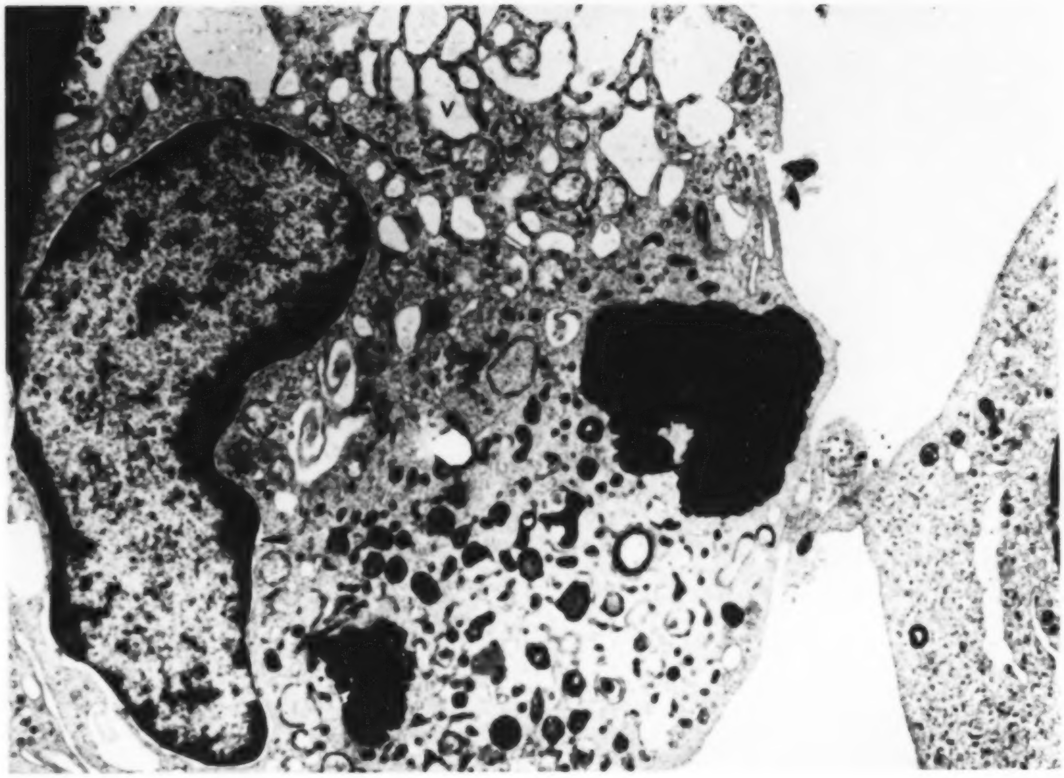
V

FIGURE 45

A.B. The top figure is a higher magnification of the lower. Occasionally in RAMs exposed to NiO particles, there developed within the cytoplasm long serpentine branching membranes. They bear a striking resemblance to the mitochondrial membranes seen in the same field, and sometimes it appears as if cristae fragments remain attached to the fusing membranes.

Within the same cell, the endoplasmic reticulum is swollen (top right) and also forms whorls within the cytoplasm (bottom left).

In the top figure, the membranes also fuse laterally to form double lamellae (small arrows).

A. X 25,000

B. X 18,600

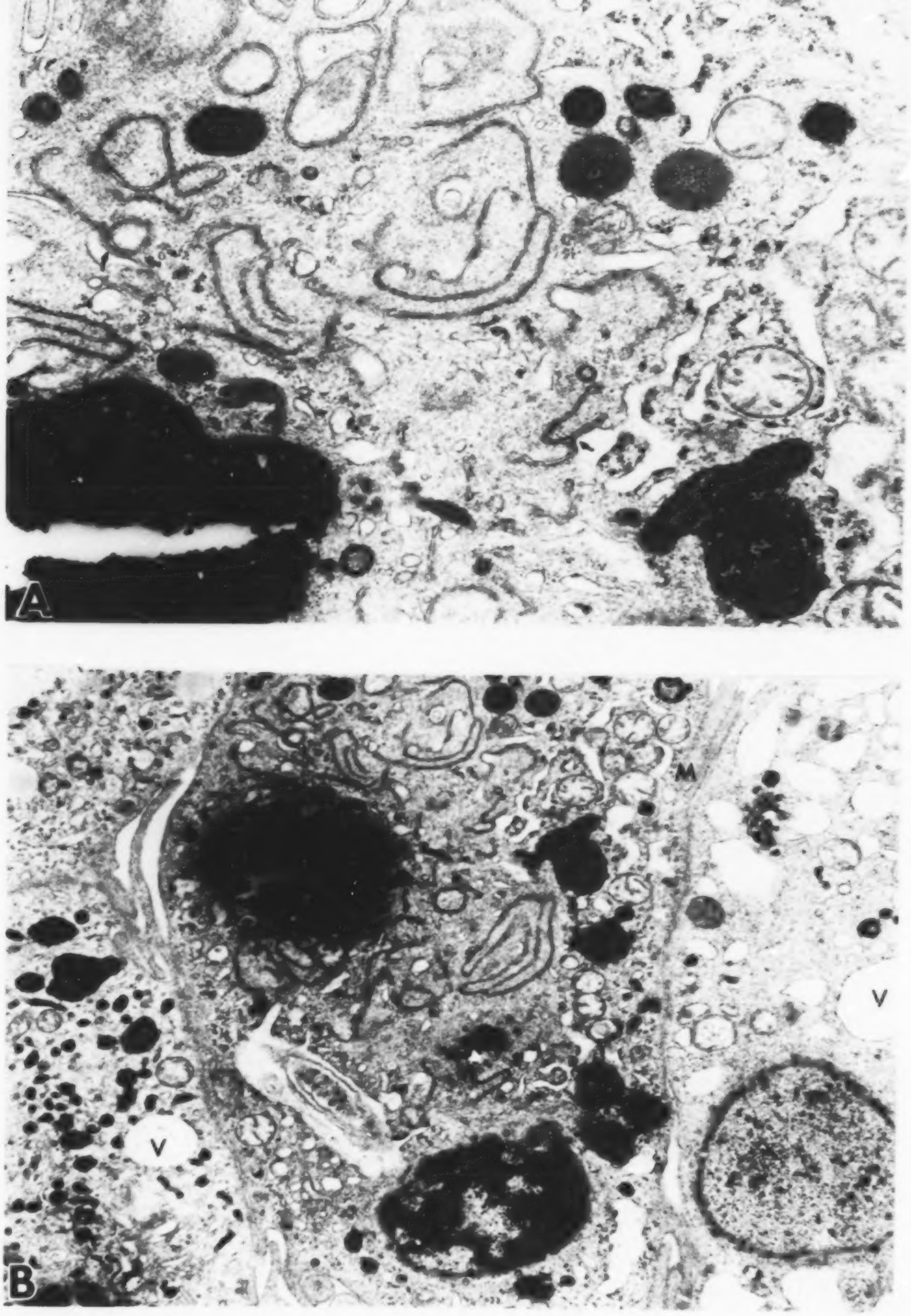
A
M
V
V
B

FIGURE 46

A. The cell was exposed to 100 ug/ml NiO particles. It has developed swelling of the nuclear membrane and RER, and a fragmented nuclear inclusion can be seen near the edge of the pyknotic nucleus. The large mitochondrion in the field is in condensed conformation. X 34,600

B. In another cell, the mitochondria displays a range of pathologic changes. In the top center is a condensed form, and in the bottom left are several swollen mitochondria. X 35,000

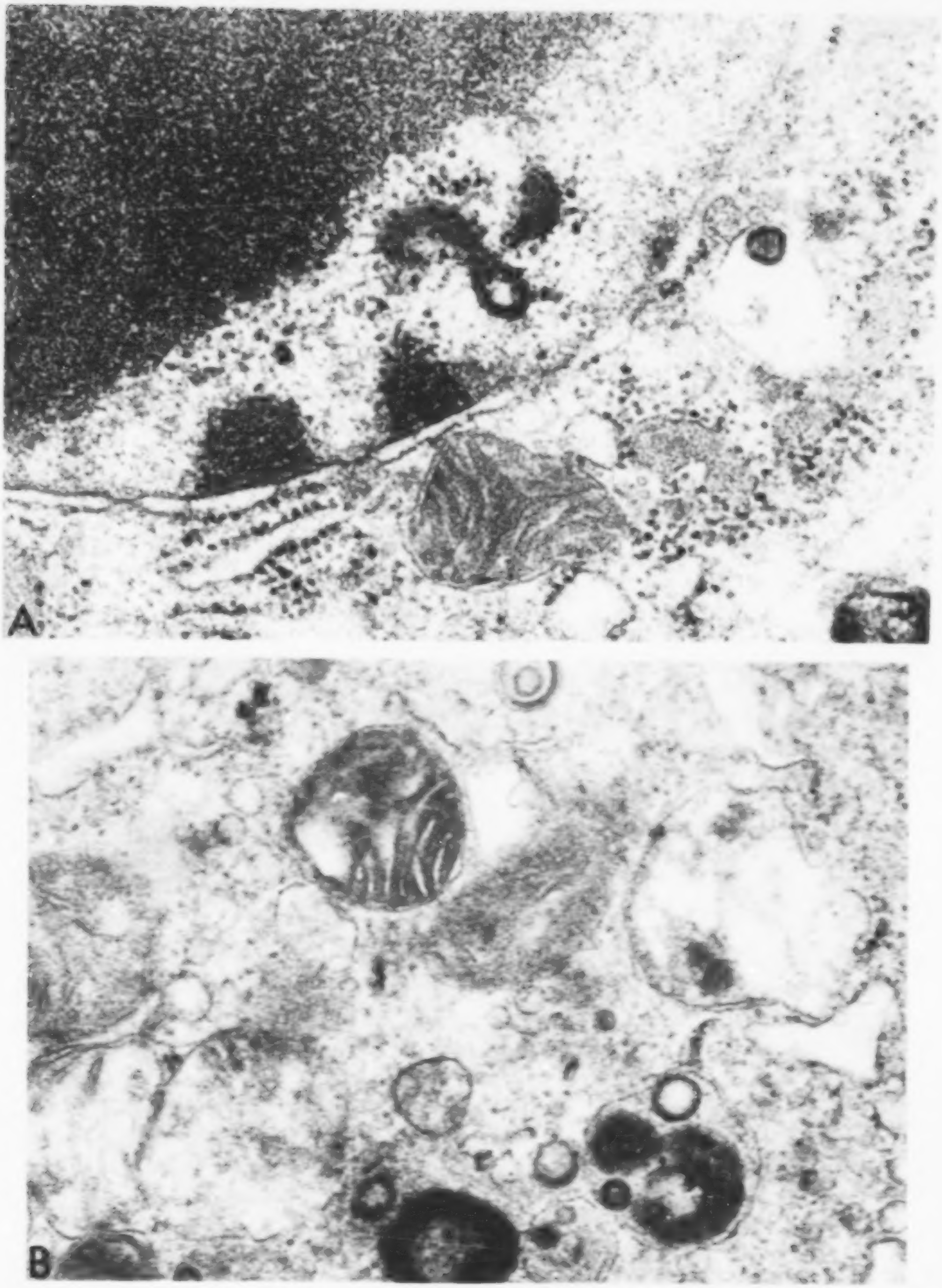
A
B

FIGURE 47

A.,B. Both of these cells were exposed to particles of NiO which can be seen in the cytoplasm. Within the mitochondria of these cells are small crystals (arrow, top). Other mitochondria seen in the same cells are swollen, or occasionally appear normal.

A. X 30,000

B. X 36,000

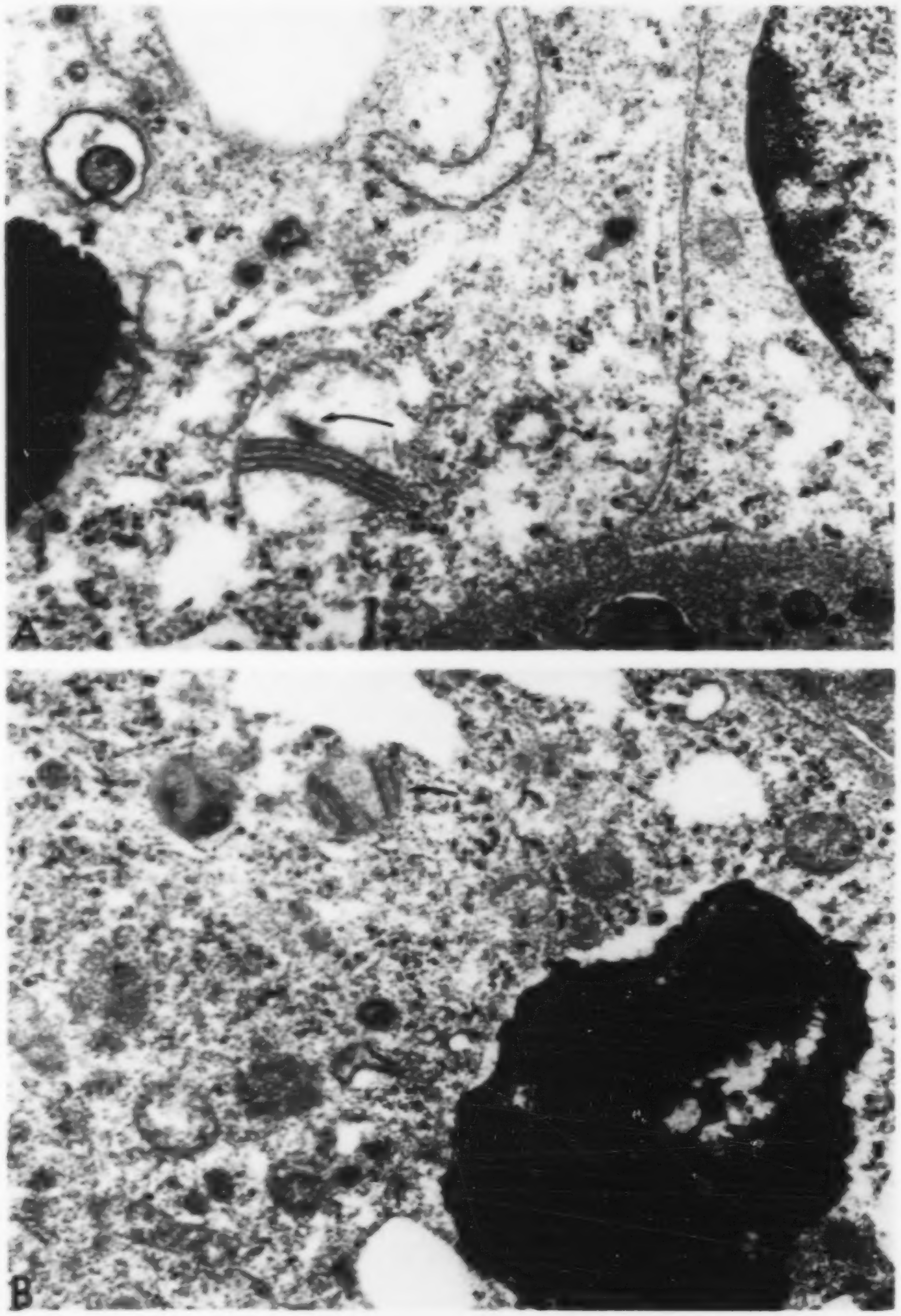
A
B

FIGURE 48

A. This cell has been exposed to 100 ug/ml NiO coated fly ash. Its overall shape is bizarre, and the cytoplasm is vacuolated. In the upper left is a rare cytoplasmic lamellar inclusion. X 15,00

B. At higher magnification it can be appreciated that these lamellae terminate abruptly at the edges of the inclusion and that the structure is attached to a homogenously dense body. Note the fine bundles of fibrils surrounding the fly ash particle at the upper right. The mitochondria in the field are swollen. Inclusion periodicity is 240 A. X 41,700

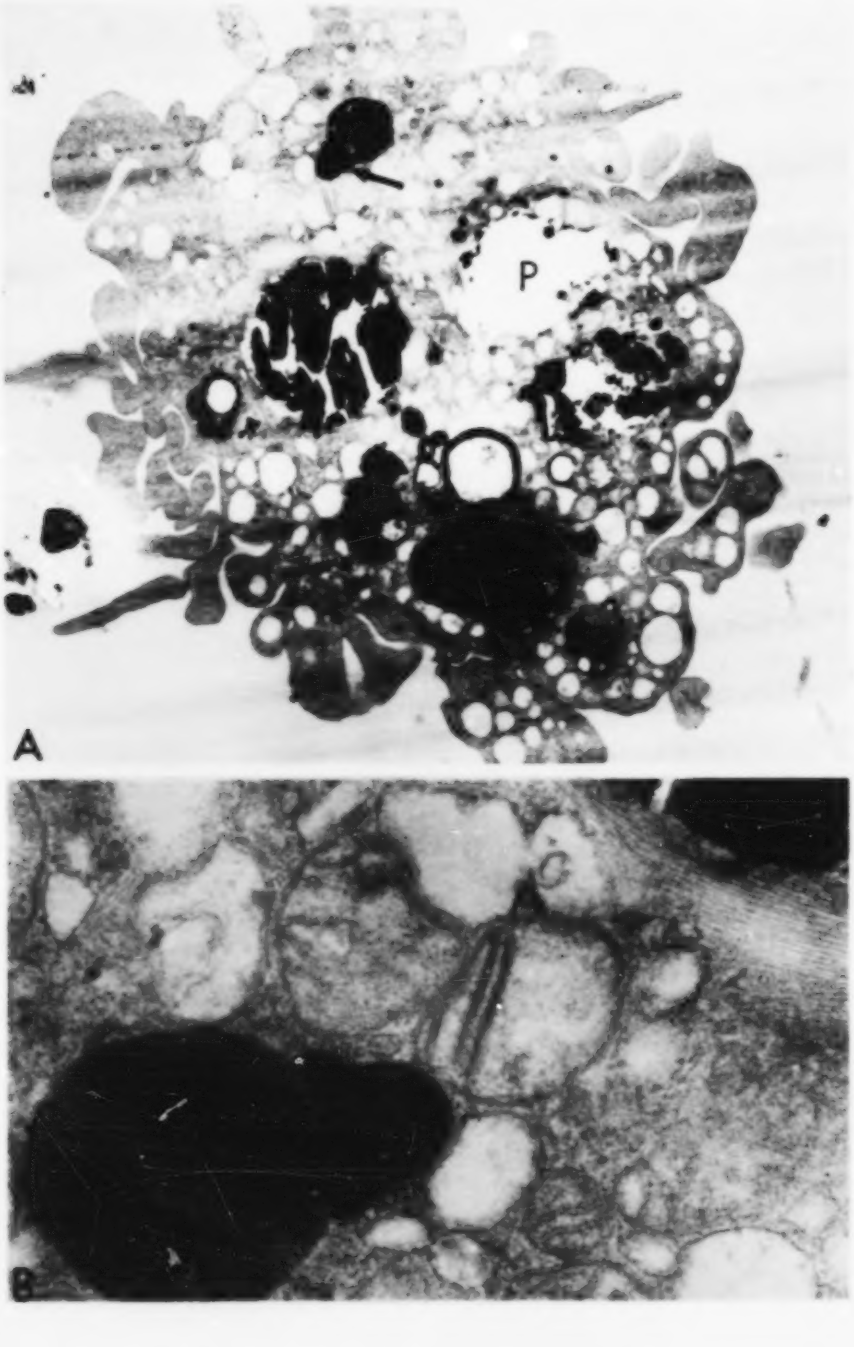
P
A
B

SUMMARY OF EXPERIMENTS ON CELL-PARTICLE INTERACTIONS

Summary: CHO/RAMs exposed to PbO

Two different cell types have been used to determine the relative ultrastructural damage caused by ingestion of particles of lead-oxide-coated fly ash. It was found that in the chinese hamster ovary (CHO) epithelial cell system, extensive phagocytosis of particles did not result in specific or nonspecific pathological changes over the period of 24 hours. However, in rabbit alveolar macrophages (RAMs), phagocytosis of comparable amounts of lead over the same time period produced dramatic damage to the fine structure of the ER, mitochondria, and nucleus, with reprecipitatation of crystals of a lead, phosphorus and calcium-containing compound localized to membrane-bound structures thought to be lysosomes.

Since it is known that lysosomal constitutents and surface membrane properties vary between cell types, it is reasonable to believe that these factors are responsible for the differences observed in ultrastructural manifestations of cytotoxicity. It is likely that the mechanism of particle engulfment follows the same pattern in both cell systems, therefore it is probable that the differences result from differences in lysosomal number, membrane structure, and enzyme constituents.

Summary: RAMs exposed to PbO and Pb_3O_4

Using the rabbit alveolar macrophages (RAM) cell system, experiments were performed to determine whether cells exposed to two different compounds of lead would be subject to identical toxic manifestations and ultrastructural changes. PbO, PbO-coated fly ash, and Pb_3O_4 were introduced to cultures of macrophages in vitro. The cells engulfed particles of all types of lead extensively. Within the cells, both forms of lead oxides interacted with the lysosomal microenvironment to release lead ion into the cytosol, as evidenced by reprecipitation of lead, phosphorus, and calcium-containing crystals within membrane-bound structures at sites distant from the phagolysosome. Therefore it is apparent that despite published reports that PbO is not soluble at acid pH, within the lysosomal microenvironment, some lead ion is released from the particle surface. The factors mediating this solubilization remain to be determined. Pb_3O_4 is a soluble compound in acid environments. Whether ingested lead particles form short distance hydrogen bounds with the inner lysosomal membrane as has been suggested for phagocytosed monosodium urate crystals is unknown, as is whether lysosomal enzymes are also released with the lead. The present study confirms that leakage of lead ion from the phagosome does occur when cells phagocytose different lead oxide compounds and that the reprecipitation of lead containing compounds can be demonstrated by microscopic and microanalytical methods.

Summary: RAMs exposed to NiO, NiO-coated fly ash, and $NiCl_2$

In the rabbit alveolar macrophage (RAM) system the ultrastructural manifestations of cytotoxicity due to ingested particles of NiO and NiO-coated fly ash were assessed. RAMs exposed to both types of particles phagocytosed the material extensively. Subsequently, either cells developed a characteristic set of pathologic changes defined by multilamellar intranuclear inclusion bodies, mitochondrial crystals, and whorling of the ER as well as many nonspecific events, or they evidenced no toxic effects at all except for a slight fatty vacuolation. The changes specific for nickel intoxication of RAMs were reproduced in cells exposed to 1mM $NiCl_2$ $6H_2O$. The toxicity of the particles seems to depend on whether the NiO is heavily coated with an oxide layer or whether metalic Ni is exposed to the lysosomal internal membrane surface. NiO is reported to be insoluble in warm water but soluble at acid pH. However, in our experiments, lysosomal pH did not seem to be the determining factor mediating the toxicity of NiO. More important was the finding that washing previously inert particulate NiO in weak acid and subsequently bringing the pH to 7.0 with distilled H_2O rendered a form wherein particulate Ni had greater access to the lysosomal surface. Under these conditions, previous experiments using "fresh" commercially available NiO were confirmed -- that is, in NiO particle-lysosomal interactions, direct exposure of the metal to the membrane surface appears to be essential to the toxic process.

When active NiO was ingested by the phagocyte, usually autolysis did not occur even when the chracteristic lamellar intranuclear inclusions were present. Two possible mechanisms are suggested to explain this finding. Either 1) Ni interacts with the vacuolar membrane via H-bridges or another physico-chemical interaction mechanism without leakage of the ion or hydrolytic enzymes into the cytosol, and disrupts the nuclear and cytoplasmic contents from a distance via some "carrier" or "messenger" system, or 2) Ni produces membrane changes that allow solubilized Ni or Ni and enzymes out into the cytosol, thereby evoking direct damage. Although the latter scenario seems the more likely, further research will be needed to resolve the dilemma.

SECTION 5

EXPERIMENTS WITH OTHER METALS AND SOLUTIONS

We have also studied the effects of soluble copper, vanadium and cobalt on rabbit alveolar macrophages. While these metals do produce a variety of non-specific changes, only copper produces the dramatic finding of a lamellated nuclear inclusion. We have utilized the techniques of Masters, et. al. (5) involving freeze fixation for RAMs exposed to vanadium. Unfortunately EDX microprobe analysis of RAMs exposed to 1 millimolar vanadium for 4 hours still fails to reveal intracellular vanadium unambiguously (5). We were only able to detect a trace of this metal. Consequently, we feel that SIMS microanalysis will be necessary to continue this work with vanadium.

FIGURE 49

In the nucleus of a RAM exposed to 1 mM $CuCl_2$, small lamellar inclusions developed. The largest inclusion seen was .29 um in diameter, and had a periodicity of 160 A. (X 68,000).

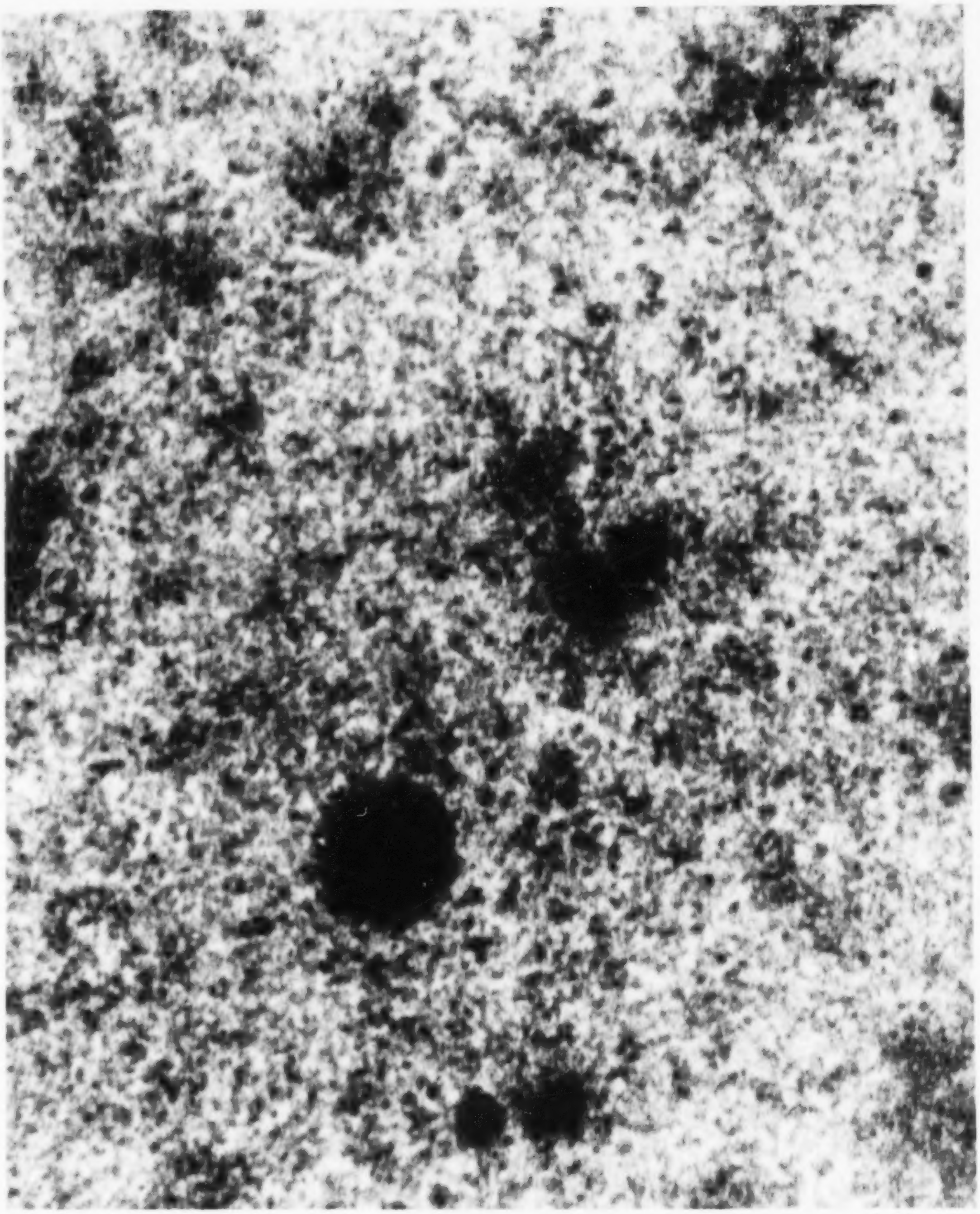

SECTION 6

EXPERIMENTS ON INSTRUMENTATION

SENSITIVITY

The literature on the sensitivity of EDX techniques is confusing since a wide range of different instruments (e.g., TEM, SEM, etc.), units of measurement (e.g., ppm, molarity, etc.) and standards are employed by different laboratories. In addition, the fact that most investigators must analyze dry specimens necessitates extrapolation from measurements made on dry tissues to an estimate of the "wet" concentration in the original tissue.

In the case of calcium, potassium and chloride, (Shuman et al., SEM 1977, p. 663) report that in thin sections of soft tissue, sensitivity limits of about 5 mM or roughly 200 ppm are about the best that can be achieved. Values for sodium are slightly higher. Our results are in agreement with this value, as we have been able to detect in RAMs (see attached reprints by Masters and Bell) normal intracellular sodium (about 16-20 mM), phosphorus (roughly 60 mM), chloride (20 mM), and potassium (150 mM), but not calcium in normal RAMs (approximately 2 mM).

With respect to abnormal cells, we have been able to detect intracellular calcium and cadmium in RAMs exposed to 0.2 mM cadmium for 20 hours and in RAMs exposed to higher, but not lower, concentrations of cadmium. Extrapolating from the work of Failla et al. (B.B. Acta 583:63-72, 1979), we estimate that roughly 1 mM (or roughly 100 ppm) cadmium may have been present in our experiments with RAMs exposed to 10 micromolar cadmium for 30 hours. Nevertheless, we could not detect cadmium in these cells.

Consequently, we decided to check the sensitivity of our instrument by using standards. Using a technique described by Roomans, we dissolved known amounts of phosphorus and potassium in Epon, polymerized the Epon and cut standard sections on E.M. grids. We studied these standard grids both with the original 10 mm^2 EDX window, and with the new 30 mm^2 EDX window purchased with this grant. The results were as follows:

For the case of potassium, we were able to detect 200 ppm with the new detector (500 ppm with the old detector). In a wet tissue, 200 ppm would be roughly equivalent to a 5 mM concentration of potassium.

In the case of phosphorus, a lighter element and thus more difficult to detect, 500 ppm was the best we could do with both the new and the original detector.

In summary, both our findings and that of the literature suggest that roughly 5 mM concentrations of elements of physiologic interest (e.g., K, Cl, P) are about the best that can be achieved. This value corresponds to roughly 200 ppm for these elements. The sensitivity limits will of course be better for xenobiotic elements of high atomic number, but our results to date with cadmium suggest that its detectable limit is close to these same values. We are presently preparing standards of cadmium to determine this limit more precisely.

DISCOVERY OF A NEW IMAGING TECHNIQUE

During the course of our experiments on cell-particle interactions we discovered a new imaging technique which we refer to as "Total Rate Imaging With X-rays" or TRIX. These techniques have proved to be of great value in the visualization of particles "hiding" in an organic matrix. Often it is superior to backscatter imaging, however, we usually use the two together since they yield different information. This technique is fully described in the attached preprint by Ingram and Shelburne (1980) (16).

DISCOVERY OF A NEW DRYING TECHNIQUE

During the course of these experiments we realized that the cost, danger and nuisance of classical critical point drying is not necessary for some tissues. Consequently, we developed a simpler technique using ethanol and argon which does not involve any dangerous high pressures, is inexpensive, and can be used to dry many large specimens simultaneously. This technique is fully described in the paper by Lamb and Ingram (1979) (15).

SECTION 7

PUBLICATIONS SUPPORTED IN PART BY THIS GRANT

1. Shelburne, J.D., Ingram, P., Hawkins, H.K., and Waters, M.D. X-ray mapping of lysosomal inclusions. Scanning Electron Microscopy/1976 (Part III), I.I.T. Research Institute, Chicago, Ill., 485-492.

2. Shelburne, J.D., Ingram, P., and Waters, M.D. Ultrastructure and x-ray microanalysis of rabbit alveolar macrophages after incubation with soluble manganese chloride. Scanning Electron Microscopy/1977 (Vol. II), I.I.T. Research Institute, Chicago, Ill., 137-144.

3. Shelburne, J.D. and Ingram, P. Use of Epon Embedded Tissues for X-Ray Microanalysis. Proceedings of the V.A. Third Diagnostic Electron Microscopy Conference. May 10-11, 1977, Chicago, Ill., p. 41.

4. Feussner, J.R., Cohen, H.J., Bredehoeft, S.B., and Shelburne, J.D. Arsenic-induced bone marrow toxicity: Ultrastructure and electron-probe analysis. Blood 53:820-827, 1979.

5. Masters, S.K., Bell, S.W., Ingram, P., Adams, D.O., and Shelburne, J.D. Preparative techniques for freezing and freeze-sectioning macrophages for energy dispersive X-ray microanalysis. Scanning Electron Microscopy/1979/III, Johari, O., Ed., SEM, Inc., AMF O'Hare, Ill., 60666, pp. 97-110 and 122.

6. Bell, S.W., Masters, S.K., Ingram, P., Waters, M.D., and Shelburne, J.D. Ultrastructure and X-ray microanalysis of macrophages exposed to cadmium chloride. Scanning Electron Microscopy/1979/III, Johari, O., Ed., SEM, Inc., AMF O'Hare, Ill., 60666, pp. 111-121.

7. Pratt, P.C., Vollmer, R.T., Shelburne, J.D., and Crapo, J.D. Pulmonary morphology in a multihospital collaborative extracorporeal membrane oxygenation project. Amer. J. Path. 95:191-214, 1979.

8. Garrett, N.E., Chescheir, G.M., Custer, N.A., Shelburne, J.D., DeVries, C.R., Huisingh, J.L., and Waters, M.D. An evaluation of the cytotoxicity and metagenicity of environmental particulates in the CHO/HGPRT system. Proceedings of the Second Symposium on the Transfer and Utilization of Particulate Control Technology. Denver, Colorado, 1979.

9. Ingram, P. and Shelburne, J.D. X-ray ultrastructural studies in cadmium coated fly ash particles. Poster session at the Symposium on Application of Short-Term Bioassays in the Fractionation and Analysis of Complex Environmental Mixtures. February 21-23, 1978, Williamsburg, Virginia.

10. Shelburne, J.D., Ingram, P., Masters, S.K., and Bell, S.W. Microprobe Studies on particulates in Human Tissues and on Freeze-Dried Frozen Sections of Macrophages Exposed to Pollutants. Keynote address to the Annual Meeting of the Midwest Society of Electron Microscopists, Chicago, Ill., Feb. 16, 1979.

11. Shelburne, J.D., Kinney, J., Ingram, P., and Pratt, P.C. Ultrastructural Studies of Non-Neoplastic Pulmonary Disorders. Fourth Diagnostic Electron Microscopy Conference. May 8, 1979, Tampa, Fla.

12. Shelburne, J.D., Ingram, P., DeVries, C., and Walker, S. Techniques for localization of translocatable ions within cells. Invited participant. *In Vitro* Toxicity Testing of Environmental Agents: Current and Future Possibilities. Monaco, September 22-29, 1979.

13. Bell, S.W., Masters, S.K., Ingram, P., Waters, M.D., and Shelburne, J.D. Ultrastructure and X-ray microanalysis of nuclear inclusions in macrophages exposed to cadmium chloride. Federation Proceedings, 38:1353, 1979.

14. Shelburne, J.D. Ultrastructural Alterations in Pathologic States, in *Pathobiology of Ocular Disease*. Klintworth, G.K. and Garner, A., eds., M. Dekker, in press.

15. Lamb, J.C. and Ingram, P. Drying of biological specimens for scanning electron microscopy directly from ethanol. Scanning Electron Microscopy/1979/III, Johari, O., Ed., SEM, Inc., AMF O'Hare, Ill., pp. 459-464.

16. Ingram, P. and Shelburne, J.D. Total rate imaging with X-rays (TRIX) - A novel form of X-ray microscopy in SEM and its application to biological specimens. Scanning Electron Microscopy 1980, in press.

17. Linton, R., Walker, S.W., DeVries, C.R., Ingram, P., and Shelburne, J.D. Application of SIMS imaging to freeze-fixed, freeze-dried cell monolayers and sections. Scanning Electron Microscopy 1980, in press.

18. DeVries, C.R. Studies of cell-particle interactions. Masters Dissertation, Duke University, for Spring, 1980.

19. DeVries, C.R., Ingram, P., Gutknecht, W.F., Walker, S.R., Linton, R.W., and Shelburne, J.D. Cell-particle interactions: Intracellular redistribution of heavy metals from particle surfaces. Lab. Invest. 42:111-112, 1980.

SECTION 8

GENERAL REFERENCES

Ackerman, N.R., and Beebe, J.R. Release of lysosomal enzymes by alveolar mononuclear cells. Nature 247: 475-478, 1974.

Adler, K.B., Davis, G.S., Woodworth, C.W., and Brody, A.R. The human alveolar macrophage: Two distinct morphological populations. Scanning Electron Microscopy/ 1979/III 921-928.

Alexander, F.W. The uptake of lead by children in differing environments. Environ. Health Perspect. 7: 155-159, 1974.

Allison, A.C. Science Basis of Medicine Annual Reviews. Athelone P[illegible], 1968. Chapter II.

Allison, A.C. Pathogenic effects of inhaled particles and antigens. Ann. New York Acad. Sci. 221: 299-308, 1974.

Allison, A.C., Davies, P. and dePetris, S. Role of contractile microfilaments in macrophage movement and endocytosis. Nature New Biol. 232: 153, 1971.

Altman, H.W.,„and Pfeifer, U. Betrag zur kenntnis der kayosphäridien 'nucler bodies' fetthaltige spharidien nach partieller hepatiktomie. Virchows Arch. Abt. B. Zellpath. 2: 220-228, 1969.

Angevine, J.M., Kappas, A., DeGowin, R.L. and Spargo, B.H. Renal tubular nuclear inclusions of lead poisoning: A clinical and experimental study. Arch. Path. 73: 66-74, 1962.

Aranyi, C., Andres, S., Erlich, R., Fenters, J.D., Gardner, D.E., and Waters, M.D. Proceedings of the Sixteenth Annual Hanford Biology Symposium. Pulmonary macrophage and epithelial cells. Sept. 27029, 1976, Richland, Washington, p. 58-65.

Azevedo, C. Intranuclear membraneous inclusions in oocytes of a viviparous teleost (Xiphophorus Helleri). J. Cell. Sci. 22: 325-334, 1976.

Barron, E.D., Doolin, P.F., and Oldershaw, J.B. Ultrastructural observations on retrograde atrophy of lateral geniculate body." J. Neuropath. Exp. Neurol. 26: 300-326, 1967.

Beaver, D.L. The ultrastructure of the kidney in lead intoxication with particular reference to intranuclear inclusions. Am. J. Path. 39: 195-208, 1961.

Beaver, D.L., and Burr, R.E. Bismuth inclusions in the human kidney. Arch. Path. 76: 89-94, 1963.

Beaver, D.L., and Burr, R.E. Electron microscopy of bismuth inclusions. Amer. J. Path. 42: 609-617, 1963.

Beck, E.G., Manojlovic, N., and Fischer, A.B. Proc. Int. Symp. Environmental Health Effects of Lead Luxembourg 451-461, 1973.

Bell, S.W., Masters, S.K., Ingram, P., Waters, M., and Shelburne, J.D. Ultrastructure and X-ray microanalysis of macrophages exposed to cadmium chloride. Scanning Electron Microscopy/1979/III: 111-122.

Berry, J. P., Henoc, P. and Galle, P. Phagocytosis by cells of the pulmonary alveoli: Transformation of crystalline particles. Am. J. Path. 93: 1, 1978.

Bingham, E., Barkley, W., Zerwas, M., Stemmer, K. and Taylor, P. Responses of alveolar macrophages to metals. I. Inhalation of lead and nickel. Arch. Environ. Health. 25: 406-414, 1972.

Bingham, E., Pfitzer, E.Z., Barkley, W., and Radford, E.P. Alveolar macrophages: Reduced number in rats after prolonged inhalation of lead sesquioxide. Science 162: 1297-1299, 1968.

Birns, M. The localization of acid phosphatase activity in the ameba Chaos Chaos. Exp. Cell Research 20: 202-205, 1960.

Blackman, S.S. Intranuclear inclusion bodies in the kidney and liver caused by lead poisoning. Bull. John Hopkins Hosp. 58: 384-403, 1936.

Booker, D.V., Chamberlain, A.C., and Newton, D. et al. Uptake of radioactive lead following inhalation and injection. Br. J. Radiol. 42: 457-466, 1969.

Bouley, G., Dubreuil, A., Arsac, F., et Boudene, C. Effet du plomb microparticulaire, introduit dans l'appariel respiratoire, sur la sensibilite de la souris a l'infection par aerosol de Pasteurella multicida. Comptes Rendus Hebdomadiares des Senances de L'Academie des Sciences. Series D (Sciences Naturelles) 285: 1153-1156, 1977.

Boulos, B.M. Special problems of lead in women workers. In National Conference on Health Effects of Occup. Pb & As Exposure. B.W. Carrow (ed) U.S. Dept of HEW 39-50, 1976.

Bowden, D.H. The alveolar macrophage. C.T. in Path. 55: 1-35, 1971.

Boxer, L.A., Ismail, G., Allen, J.M., and Baehner, T.L. Oxidative metabolic responses of rabbit pulmonary alveolar macrophages. Blood 53: 486-491, 1979.

Bracken, E.C., Beaver, D.L., and Randall, C.C. Histochemical studies of viral and lead-induced intranuclear bodies. J. Path. Bact. 75: 253-256, 1958.

Brittin, G.M., Tanaka, Y., and Brecher, G. Intranuclear inclusions in multiple myeloma and macroglobulinemia. Blood 21: 335-350, 1963.

Brown, S.S. (ed) Clinical Chemistry and Toxicology of Metals. New York: Elsevier/ North-Holland Biomedical Press, 1977.

Bruaux, P. Metabolisme du plomb chez les animaux: Possibilities d'utilization des resultats pour l'homme. In International Symp. On Eviron. Health Aspects of Lead. Amsterdam, 1973.

Bruch, J., Brochkaus, A., und Dehnen, W. Elektronmikroskopische beobachtungen an rattenlungen nach exposition mit partikelformigem blei. International Symp. on Envir. Health Aspects of Lead. Amsterdam, 1973.

Brun, A. and Brunk, U. Lead induced injury on in vitro cultured rat fibroblasts: A histochemical study. Histochemie 35: 227-234, 1973.

Brun, A. and Brunk, U. Lead induced injury of in vitro cultured rat fibroblasts. Acta Path Microbiol. Scand. Section A 82: 311-318, 1974.

Brunk, U. and Brun, A. Histochemical evidence for lysosomal uptake of lead in tissue cultured fibroblasts. Histochemie. 29: 140-146, 1972.

Burr, R.E., Gotto, A.M., and Beaver, D.L. Isolation and analysis of renal bismuth inclusions. Toxicol. and Appl. Pharm. 7: 588-591, 1965.

Caplan, P.E. Monitoring workplaces for lead and problems involved. In: National Conference of Health Effects of Occupational Lead and Arsenic Exposure. B.W. Carrow (ed.) U.S. Dept. HEW, 1976.

Caprio, R.J., Margules, H.C., Joselow, M.M. Lead absorption in children and its relationship to urban traffic densities. Arch. Envir. Health. 28: 195-197, 1974.

Carroll, K.G., Spineas, F.R., and Goyer, R.A. Electron probe microanalysis localization of lead in kidney tissue of poisoned rats. Nature 337: 1056, 1970.

Chiodi, H., and Cardenza, A.F. Hepatic lesions produced by lead in rats fed a high fat diet. Arch. Path. 48: 395-404, 1949.

Choie, D.D. and Richter, G.W. Cell proliferation in mouse kidney induced by lead. I. Synthesis of deoxyribonucleic acid. Lab Invest. 30: 647-651, 1974.

Choie, D.D. and Richter, G.W. Cell proliferation in mouse kidney induced by lead. II. Synthesis of ribonucleic acid and protein. Lab. Invest. 30: 652-656, 1974.

Choie, D.D. and Richter, G.W. Lead poisoning: Rapid formation of intranuclear inclusions. Science 177: 1194-1195, 1972.

Cohn, Z.A. The structure and function of monocytes and macrophages. Advan. Immunol. 9: 163-214, 1968.

Cohn, Z.A., and Wiener, E. The particulate hydrolases of macrophages. II. Biochemical and morphological response to particle ingestion. J. Exp. Med. 118: 1009-1019, 1963.

Cohn, Z.A., and Wiener, E. The particulate hydrolases of macrophages. I. Comparative enzymology, isolation, and properties. J. Exp. Med. 118: 991-1008, 1963.

Corless, W.M., and Costello, M.J. Paracrystalline inclusions associated with the disk membranes of frog retinal rod outer segments. (In Press) 1980.

Coulston, F., Goldberg, L, Griffin, T.B., and Russell, J.C. The effects of continuous exposure to airborne lead. I. Exposure of rats and monkeys to particulate lead at a level of 21.5 mg/m^3. Final Report to the EPA, 1972.

Cowdry, E.V. The problem of intranuclear inclusions in virus diseases. Arch. Pathol. 18: 527-542, .

Cramer, K., Goyer, R.A., Jagenburg, O.R., and Wilson, M.H. Renal ultrastructure, renal function and parameter of lead toxicity in workers with different lengths of lead exposure. Br. J. Ind. Med. 31: 113-127, 1974.

Dallenbach, F.D. Uptake of radioactive lead by tubularepitholium of the kidney. Verh. Deutsch. Ges. Pathol. 49: 179, 1965.

De Boni, Otvos, U.A., Scott, J.W. and Crapper, D.R. Neurofibrillary degeneration induced by systemic aluminum. Acta Neuropath. 35: 285-294, 1976.

DeDuve, C., and Wattiau, R. Functions of lysosomes. Ann. Rev. Physiol. 8: 435-492.

deVries, C.R., Gutnecht, W., Walker, S.R., Lintonm, R.W., and Shelburne, J.D. Cell-particle interactions: Intracellular redistribution of heavy metals from particle surfaces. Lab Invest. 42: 15, 1980.

Dialdetti, M. and Lewinski, V.H. Original intranuclear inclusions in mycloma cells. Scad. J. Haematol. 20: 200-205, 1978.

Elsbach, P. Phagocytosis. The Inflammatory Process (second edition). Zweifach, B.W., Grant, L. and McCluskey (eds.) New York: Academic Press, 1974.

Endo, H., Takayama, S., Kasuga, T., and Ohashi, M. Histochemical studies on nuclear inclusions in tissue culture cells induced by 4-nitroquinoline N-oxide." Gann. 52: 173-177, 1961.

Ericsson, J.L.E., and Brunk, U.T. Alterations in lysosomal membranes as related to disease processes. Pathobiology of Cell Membranes. Vol. I B.F. Trump and A.U. Ar [illegible] Academic Press, 1975.

Evans, M.J., Cabral, L.J., Stevphens, R.J., and Freeman, G. Cell division of alveolar macrophages in rat lung following exposure to NO$_2$. Am. J. Path. 70: 199-208, 1973.

Fairhall and Sayers (1940). Reported in Waldron, H.A. and Stofen, D. Subclinical Lead Poisoning. London: Academic Press, 1974.

Finner, L.L., and Calvery, H.O. Pathologic changes in rats and in dogs fed diets containing lead and arsenic compounds. Arch. Path. 27: 433-446, 1939.

Fischer, A.B. The effect of lead on cells cultivated in vitro: I. Acute effects. Zbl. Bkt. Hyg., I Abt. Orig. B 161: 26-37, 1975.

Flicker, M., and Ross, J. Mechanism of chemical instability for periodic precipitation phenomena. J. Chem. Phys. 60: 3458, 1974.

Fowler, B.A., and Goyer, R.A. Bismuth localization within nuclear inclusions by X-ray microanalysis: Effects of accelerating voltage micro. J. Histochem. and Cytochem. 23: 722-726, 1975.

Feldman, R.G. Urban lead mining: Lead intoxication among deleaders. New Eng. J. Med. 298: 1143-1145, 1978.

Garrett, N.E., Campbell, J.A., Huisingh, J.L., and Waters, M.D. Symposium on the transfer and utilization of particulate control technology: Vol. 4: Fugitive dusts and sampling analysis and characterization of aerosols. Venditti, F.P., Armstrong, J.A., and Durham, M. (Eds.) EPA-600/7-70-044D. Feb. 1979.

Garrett, N.E., Campbell, J.A., and Stack, H.F. Evaluation of cell systems for cytotoxicity: II. Studies with rabbit alveolar macrophages, chinese hamster ovary, and human neonatal fibroblast cell systems. Quarterly Report, Research Task 9192. Determination of cellular toxicity of compounds from stationary sources and ambient air. April, 1979.

Garrett, N.E., Chescheir, G.M., Custer, N.A. Shelburne, J.D., deVries, C.R., Huisingh, J.L., and Waters, M.D. An evaluation of the cytotoxicity and mutagenicity of environmental particulates in the CHO/HGPRT system. Proc. of the Second Symposium on the Transfer and Utilization of Particulate Control Technology, Denver, 1979.

Ghadially, F.N., and Yong, N.K. Ultrastructural and X-ray analytical studies on intranuclear bismuth inclusions. Virchows Arch. B. Cell Path. 21: 45-55, 1976.

Goldsmith, J.R., and Hexter, A.L. Respiratory exposure to lead: Epidemiological and experimental dose-resoponse relationships. Science 158: 132, 1967.

Goyer, R.A. Lead and the kidney. C.T. in Path. 55: 147-176, 1975.

Goyer, R.A., and Cherian, M.G. Clinical Chemistry and Chemical Toxicology of Metals. Edited by S.S. Brown. Elsevier: North-Holland Biomedical Press, 1977.

Goyer, R.A., and Chisolm, J.J. Metalic Contaminants and Human Health. Edited by Lee. New York: Academic Press, 1972.

Goyer, R.A. and Krall, R. Ultrastructural transformation in mitochondia isolated from kidneys of normal and lead-intoxicated rats. J. Cell Biol. 44: 393-400, 1969.

Goyer, R.A., May, P., Cates, M.M., and Krigman, M.R. Lead and protein content of isolated intranuclear inclusion bodies from kidneys of lead poisoned rats. Lab. Invest. 22: 245-251, 1970.

Goyer, R.A., and Mushak, P. Advances in Modern Toxicology Vol. 12. Edited by R.A. Goyer and M.A. Mehlman. Washington: Hemisphere Publishing Corp., 1977.

Goyer, R.A., and Rhyne, B.C. Pathological effects of lead. Rev. Exp. Path. 12:1-77, 1973.

Goyer, R.A., and Wilson, M. Lead induced inclusion bodies: Results of EDTA treatment. Lab. Invest. 32:149-156, 1975.

Graham, J.A., Gardner, D.E., Waters, M.D., and Coffin, D.L. Effect of trace metals on phagocytosis by alveolar macrophages. Infect. Immun. 11: 1278-1283, 1975.

Groth, D.H., Stottler, L., and Mackay, G. Effects and Dose-Response Relationships of Toxic Metals. Edited by G.F. Nordberg. Amsterdam: Elsevier Scientific Publishing Company, 1976.

Hackett, R.L., and Sunderman, W.F., Jr. Pulmonary alveolar reaction to nickel carbonyl. Arch. Environ. Health. 16:348-362, 1968.

Harington, J.S., Allison, A.C., and Badamie, D.V. Mineral fibers: chemical, physiochemical, and bioproperties." Adv. Pharmacol. Chemother. 12:291, 1975.

Hass, G.M., Brown, D.V.L., Eisenstein, R., and Hemmens, A. Relations between lead poisoning in rabbit and man. Am. J. Path. 45:691-727, 1964.

Herman, M.M., and Ralston, H.J. Laminated cytoplasmic bodies and annulate lamellae in the cat ventrobasal and posterior thalamus. Anat. Rec. 167: 183-196, 1970.

Hirsch, J.C. Phagocytosis. Ann. Rev. Microbiol. 19:339-350, 1965.

Hocking, W.G., and Golde, D.W. The pulmonary alveolar macrophage. New Eng. J. Med. 301:580-587, 1979.

Horn, J. Isolation and examination of inclusion bodies of the rat-kidney after chronic lead poisoning. Virchows Arch Abt. B. Zell Path. 6:313-317, 1970.

Horstmann, E., Richter, R., and Runge, E.R. Zur elektronen microskopie der kerneinschlusse im menschlichen nebenhodenepithel. Zeitschrift fur Zellforschung. 69:69-70, 1966.

Hsie, A.W., O'Neill, P., San Sebastian, J.R., Couch, D.B., Brimer, P.A., Sun, W.N.C., Fuscoe, J.C., Forbes, N.I. Machanoff, R., Riddle, J.C., and Hsie, M.H. Application of Short-Term Bioassays in the Fractionation and Analysis of Complex Environmental Mixtures. Edited by M.D. Waters, S. Nesnow, J.L. Huisingh, S.S.Sandhu, and L. Claxton. New York: Plenum Press, 1978.

Hsu, F.S., Krook, L., Shively, J.N., and Duncan, J.R. Lead inclusion bodies in osteoclasts. Science. 181:447-448, 1973.

Hursh, J.B., and Mercer, T.T. Measurement of ^{212}Pb loss rate from human lungs. J. Appl. Physiol. 28:268-274, 1970.

Ingram, P., and Shelburne, J.D. Total rate imaging with X-rays (TRIX)--a simple method of forming a non-projection X-ray image in the SEM using an energy dispersive detector and its application to biological specimens. Scanning Electron Microscopy/ 1980 (in press).

Itabashi, M., Hruban, Z., Wong, T.W., and Chou, S.F. Concentric nuclear inclusions. Virchows Arch. B. Cell Path. 20:103-111, 1976.

Jacques, Y.V., and Bainton, D.F. Changes in pH within the phagocytic vacuole of human neutrophils and monocytes. Lab. Invest. 39:179-185, 1978.

Jasmin, G. Ultrastructural patterns of Ni-induced crystalline inclusions in mitochondria of renal tubules. Exp. and Molec. Pathol. 20:199-210, 1978.

Johnson, Sheena, M. The inability of macrophages to digest liposomes containing a high proportion of cholesterol. Biochem. Soc. Trans. 3:160-161, 1975.

Jones, K.W. The induction of paracrystalline thread-complexed in the nuclei of amphibian cells by Actinomycin D and other DNA-binding antibiotics. J. Ultrast. Res. 18:71-84, 1967.

Joselow, M.M. Biological monitoring problems of blood lead levels. National Conference on Health Effects of Occupational Lead and Arsenic Exposure. Edited by B.W. Carnow. U.S. Dept. H.E.W. 1976.

Juers, J.A., Rogers, R.M., McCurdy, J.B., and Cook, W.W. Enhancement of bacterial capacity of alveolar macrophages by human alveolar lining material. J. Clin. Invest. 58:271-275, 1976.

Kalil, R., and Worden I. Cytoplasmic laminated bodies in the lateral geniculate nucleus of normal and dark reared cats. J. Comp. Neur. 178:469-486, 1978.

Kerr, R.A. Global pollution: is the arctic haze actually industrial smog? Science. 205:290-293, 1979.

Kilham, L., Low, R.J., Contix, S.F., and Dallenbach, D. Intranuclear inclusions and neoplasms in the kidneys of wild rats. J. Nat. Cancer Inst. 29:863-885, 1962.

Knelson, J.H. The problem of estimation respiratory lead dose in children. Environ. Health Prospect. 7:53-58, 1974.

Knelson, J.H., Johnson, R.J., Coulston, F., Goldberg, L., Griffin, T. Kinetics of respiratory lead uptake in humans. International Symp. on Environ. Health Aspects of Lead. Amsterdam, 1973.

Kruger, L., and Maxwell, D.S. Cytoplasmic laminar bodies in the striate cortex. J. Ultrast. Res. 26:387-390, 1969.

Kusell, M., Lake, L., Anderson, M., and Gerschenson, L.E. Cellular and molecular toxicity of lead. II. Effect of lead on aminolevulinic acid synthetase of cultured cells. J. Toxicol. and Environ. Health. 4:515-523, 1978.

Kusell, M., O'Cheskey, S., and Gerschenson, L.E. Cellular and molecular toxicity of lead. I. Effect of lead on cultured cell proliferation." J. Toxicol. Environ. Health. 4:503-513, 1978.

Lafarga, M., and Hervas, J.P. Intranuclear inclusions in pericytes of the hypothalamus of the rat. Cell Tiss. Res. 193:315-322, 1978.

Lake, L., and Gerschenson, L.E. Cellular and molecular toxicology of lead. III. Effect of lead on heme synthesis. J. of Toxicol. and Environ. Health. 4:527-540, 1978.

Landing, B.H., and Hisayo N. Histochemical properties of renal lead inclusions and their demonstration in urinary sediment. Am. J. Clin. Path. 31: 49-503, 1959.

Landrigan, P.J. The exposure of children to lead from industry: Epidemiology and health consequences. National Conference on Health Effects of Occupational Lead and Arsenic Exposure. Edited by B.W. Carnow. U.S. Dept. of H.E.W., 1976.

Lawther, P.J., Commins, B.T., Ellison, McKay, J., and Biles, B. More observations on airborne lead. National Symp. on Environ. Health Aspects of Lead. Amsterdam, 1972.

Lazarus, S.S., Vethamany, V.G., Shapiro, S.H., and Amsterdam, D. Histochemistry and fine structure of 4-nitroquinoline-N-Oxide induced nuclear inclusions. Cancer Res. 26:2229-2238, 1966.

Lepow, M.L., Bruchman, L., Rubine, R.A., Markowits, K., Gillett, M., and Kapish, I. Role of airborne lead in increased body burden of lead in Hartford children. Environ. Health Perspect. 7:99-102, 1974.

Lilis, R., Fishbein, A., Eisinger, J., Blumberg, W.E., Diamond, S., Anderson, H.A., Rom, W., Rice, G., Sarkosi, L., Kon, S., and Selikoff, I.J. Prevalence of lead disease among secondary smelter workers and biological indicators of lead exposure. Environ. Research. 14:225-285, 1977.

Lin, H.S., Kuhn, C., and Kuo, TT. Clonal growth of hamster free alveolar cells in soft agar. J. Exp. Med. 142:887-886, 1975.

Linton, R.W., Walker, S.R., deVries, C.R., Ingram, P., and Shelburne, J.D. Ion microanalysis of cells. Scanning Electron Microscopy/1980 (in press).

Luchtel, D.L., and Naum, Y. Ultrastructural characteristics of pulmonary alveolar macrophages induced to multiply in vitro. Pulmonary Macrophage and Epithelial Cells. Edited by C.L. Sanders, R.D. Schneider, G.E. Dagle, and D.D. Ragen, ERDA Conf. 760927, 1977.

Maldonado, J.E., Brown, A.L., Bayrd, E.D., and Pease, G.L. Cytoplasmic and intranuclear electron-dense bodies in the myeloma cell. Arch. Path. 81: 484-500, 1966.

Mao, P., and Molnar, J.J. The fine structure and histochemistry of lead-induced renal tumors in rats. Amer. J. Path. 50:571-603, 1967.

Mast, S.O. The hydrogen ion concentration of the content of the food vacuoles and the cytoplasm in amoeba and other phenomena concerning the food vacuoles. Biol. Bull. 20:173-204, 1942.

Masters, S.K., Bell, S.W., Ingram, P., Adams, D.O., and Shelburne, J.D. Preparative techniques for freezing and freeze-sectioning macrophages for energy dispersive X-ray microanalysis. Scanning Electron Microscopy/1979/III:97-111 and 122.

Mehaffey, K.R. Quantities of lead producing health effects in humans: sources and bioavailability." Environ. Health Perspect. 19:285-295, 1977.

Mehani, S. Lead retention by the lungs of lead exposed workers. Ann. Occup. Hygiene. 9:165-171, 1966.

Middlekamp, J.N., Patrizi, G., and Reed, C.A. Light and electron microscopic studies of the guinea pig cytomegalovirus." J. Ultrastruct. Res. 18:85-101, 1967.

Miranda, A.F., and Godman, G.C. The effects of Cytochalasin D on differentiating muscle in culture. Cell and Tissue. 5:1-22, 1973.

Moore, J.F., Goyer, R.A., and Wilson, M. Lead-induced inclusion bodies: solubility, amino acid content, and relationship to residual acidic nuclear proteins. Lab. Invest. 29:488-494, 1973.

Morales, R., and Duncan, D. Multilaminated bodies and other unusual configurations of endoplasmic reticulum in the cerebellum of the cat. An electron microscopic study. J. Ultrast. Res. 15:480-489, 1964.

Morales, R., Duncan, D., and Rehment, R. A distinctive laminated cytoplasmic body in the lateral geniculates body neurons of the cat. J. Ultrast. Res. 10: 116-123, 1964.

Mudd, S., McCutcheon, M., and Lucke, B. Phagocytosis. Physiol. Rev. 14: 210-275, 1934.

Myrvik, Q.N., Leake, E.S., and Fariss, B. Studies on pulmonary alveolar macrophages from the normal rabbit: A technique to procure them in a high state of purity. J. Immunol. 86:133-136, 1961.

Nash, T., Allison, A.C., and Harington, J.S. Physico-chemical properties of silica in relation to its toxicity. Nature. 210:259-261, 1966.

National Academy of Sciences. Lead: Airborne Lead in Perspective. Washington, D.C., 1972.

Nelson, K. Industrial hygiene of Pb production: A brief review. National Conference on Health Effects of Occup. Lead and Arsenic Exposure. Edited by B.W. Carnow. U.S. Dept. of H.E.W. 1976.

Nichols, B.A. Normal rabbit alveolar macrophages. I. The phagocytosis of tubular myelin. J. Exp. Med. 144:906-919, 1976.

Niege, G., Berry, J.P., Galle, P., Ripault, J., Desoille, H., and Philbert, M. Lesions hepatiques d'apparence cytotoxique au cours d'une intoxication experimentale par le cadmium: Etude preliminaire. Archives des Maladies Professionnelles de Medicine du Travail, et de Securite Sociale 35:709-718, 1974.

Olitsky, P.K., and Harford, C.G. Intranuclear inclusion bodies in the tissue reactions produced by injections of certain foreign substances. Am. J. Path. 13: 729-747, 1937.

Panel on Nickel (NAS) National Academy of Sciences, 1975. Committee on Medical and Biologic Effects of Environmental Pollutants, Nickel., Washington, D.C.

Pappenheimer, A.M., and Maechling, E.H. Inclusions in renal epithelial cells following the use of certain bismuth preparations." Am. J. Path. 10:577-588, 1934.

Pejic, S. The nature of the primary renal lesion produced by lead. Ann. Int. Med. 1:577-604, 1928.

Peters, A., and Palay, S.L. The morphology of lamina A and A_1 of the dorsal nucleus of the lateral geniculate body of the cat. J. Anat. 109:451-486, 1966.

Reynolds, R.C., Montgomery, P.O.B., and Hughes, B. Nucleolar 'caps' produced by Actimomycin D." Cancer Res. 24:1269-1277, 1964.

Richter, G.W., Kress, Y., Cornwall, C.C. Another look at lead inclusion bodies. Am. J. Path 53:189-217, 1968.

Robinson, D.G., and Hammerl, I. Intranuclear rodlets in glaucocystis: structure, induction, and inhibition. Cytobiol. 16:199-208, 1978.

Rosenbaum, R.M., and Wittner, M. The activity of intracytoplasmic enzymes associated with feeding and digestion in *Paramecium caudatum*: The possible relationship to neutral red granules. Arch. Protistenk Bd. 106:223-240, 1962.

Roth, L.E. Electron microscopy of pinocytosis and food vacuoles in pelomyxa. J. Protozo. 7:176-185. 1960.

Sayre, J.W., Charney, R., Vostal, J., et al. House and land dust as a potential source of childhood lead exposure. Am. J. Dis. Child. 127:167-170, 1974.

Schlipkoter, H.W., and Pott, F. Die pulmonale resorption von bleistraub. Proc. Int. Symp. Environmental Health Aspects of Land, Luxembourg, 1973.

Silbergeld, E.K., Fales, J.T., and Goldberg, A.M. The effects of inorganic lead on the neuromuscular junction. Neuropharmacol. 13:795-801, 1974.

Silverberg, B.A., Stokes, P.M., and Fertenberg, L.B. Intranuclear complexes in a copper-tolerant green alga. J. Cell. Biol. 69:210-214, 1976.

Simard, Rene. The nucleus: action of chemical and physical agents. Int. Rev. Cytol. 28:169-211, 1970.

Simpson, C.F., Damron, B.L., and Harms, R.H. Abnormalities of orythrocytes and renal tubules of chicks poisoned with lead. Am. J. Vet. Res. 31:515-523, 1979.

Skaar, H. and Ophus, E. Lead accumulation within nuclei of moss leaf cells. Nature 241:215-216, 1973.

Smith, J.M., O'Leary, J.L., Harris, A.D., and Gay, A.J. Ultrastructural features of the lateral geniculate nucleus of the cat. J. Comp. Neur. 123:357-378, 1964.

Soderland, S.C., and Naum, Y. Growth of pulmonary alveolar macrophages in vitro. Nature. 245:150-152, 1973.

Sotelo, L., and Angaut, P. The fine structure of the cerebellar central nuclei in the cat in neurons and neuroglial cells. Exp. Brain Res. 16:410-430, 1973.

Steinbock, R.T. Lead ingestion in history. New Eng. J. Med. 301:277, 1979.

Sunderman, F.W., Jr. A review of the metabolism and toxicology of nickel. Ann. of Clin. and Lab. Sci. 7:377-398, 1977.

Sunderman, F.W., and Sunderman, F.W., Jr. Nickel poisoning. XI. Implication of nickel as a pulmonary carciongen in tobacco smoke. Am. J. Clin. Pathol. 35: 203-209, 1961.

Ter Haar, G., and Aronow, R. New information of lead in dirt and related to childhood lead burdens. Environ. Health Perspect. 7:83-90, 1974.

Ter Haar, G.L., and Bayard, M.A. Composition of airborne lead particles. Nature. 232:533-544, 1971.

Thoenes, W. Fett im nucleolus. J. Ultrast. Res. 10:194-206, 1964.

Tripier, M.D., Berard, M., and Toga, M. 'Membranous nuclear bodies' as possible intermediate structures between nuclear bodies and invaginations of the nuclear envelope. J. Microscopie. 21:21-30, 1974.

Trump, B.F., Berezesky, I.K., Chang, S.H., Pendergrass, R.B., and Mergner, W.J. The role of ion shifts in cell injury. Scanning Electron Microscopy/1979/III:1-14.

Trump, B.F., and Mergener, W.J. The Inflammatory Process, 2nd edition. Edited by B.W. Zweifach, L. Grant, and R.T. Cluskey. New York: Academic Press, 1974.

U.S. Environ. Protection Agency. EPA's position on the health effects of airborne lead. Health Effects Branch, Processes and Effects Division, Office of Research and Monitoring, U.S. Environmental Protection Agency, Washington, D.C. Nov. 29, 1972.

Wachstein, M. Lead poisoning diagnosed by the presence of nuclear acid-fast inclusion bodies in kidney and liver. Arch. Path. 48:442-446, 1949.

Wachstein, M. Studies on inclusion bodies: acid-fastness of nuclear inclusion bodies that are induced by lead and bismuth. Am. J. Clin. Path. 19:608-614, 1949.

Waldron, H.A., and Stofen, D. Subclinical Lead Poisoning. London: Academic Press, 1974.

Walton, J.R. Intranuclear inclusions in the lead-poisoned cultured kidney cell. J. Path. 112:213-215, 1974.

Waters, M.D., Gardner, D.E., Aranyi, C., and Coffin, D.L. Metal toxicity for rabbit alveolar macrophages *in vitro*. Environ. Res. 9:32-47, 1975.

Watrach, A.M. Degeneration of mitochondria in lead poisoning. J. Ultrast. Res. 10:177-181, 1964.

Webb, M., Heath, J.C., and Hopkins, T. Intranuclear distribution of the inducing metal in primary rhabdosarcomata induced in the rat by nickel, cobalt, and cadmium. Br. J. Cancer. 26:274-278, 1972.

Webb, M., and Weinzierl, S.M. Uptake of $^{63}Ni^{++}$ from its complexes with proteins and other ligands by mouse dermal fibroblasts *in vitro*. Br. J. Cancer. 26:292-298, 1972.

Weinzierl, S.M., and Webb, M. Interaction of carcinogenic metals with tissue and body fluids. Br. J. Cancer. 26:279-291, 1972.

Weissmann, G. *Cell Membranes: Biochemistry, Cell Biology and Pathology*. Edited by G. Weissman, and R. Claiborne. New York: H.P. Publishing Co., Inc., 1975.

WHO Task Group on Environmental Health Criteria for Lead. World Health Publication. Geneva, 1975.

Winfield, D.A. Cytoplasmic laminated bodies in the visual cortex of the cat. Brain Res. 161:544-548, 1979.

Wolman, M. On the absence of deoxyribonucleic acid from some chemically-induced cytoplasmic and intranuclear inclusions with reference to a special type of false positive staining by Feulgen's nuclear technique. J. Path. Bact. 68:159-164, 1954.

Yamate, G., and Ashley, H. Preparation and characterization of finely divided particulate environmental contaminants for biological experiment. IIT Research Institute, Chicago, Ill., IITRI Report C6321-5, September, 1975.